Functional study of the intronic enhancer, Eμ, after immunoglobulin heavy chain variable region gene assembly

By
Fubin Li

A dissertation submitted to the Graduate Faculty in Biology in partial fulfillment of the requirements for the degree of Doctor of Philosophy, The City University of New York

2008

This manuscript has been read and accepted for the Graduate Faculty in Biology in satisfaction of the dissertation requirement for the degree of Doctor of Philosophy.

8/21/2008	Dr. Laurel Eckhardt, Hunter College
Date	Chair of Examining Committee
9/10/2008	Dr. Laurel Eckhardt
Date	Executive Officer

Dr. Jill Bargonetti-Chavarria, Hunter College

Dr. Benjamin Ortiz, Hunter College

Dr. Linda Spatz, City College

Dr. Barbara Birshtein, Albert Einstein College of Medicine

Supervising Committee

THE CITY UNIVERSITY OF NEW YORK

Abstract

Functional study of the intronic enhancer, Eμ, after immunoglobulin heavy chain variable region gene assembly

By

Fubin Li

Adviser: Professor Laurel Eckhardt

A series of somatic rearrangement and mutation processes underlie the function of B lymphocytes: V(D)J rearrangement assembles immunoglobulin heavy and light chain (IgH and IgL) variable region (V_H and V_L) genes, and therefore generates a large repertoire of antibody specificity; class switch recombination and somatic hypermutation enable B cells to produce antibodies with different effector functions and high affinity in response to antigens. The intronic enhancer (Eμ) of the *Igh* locus has been shown required for efficient V_H gene assembly previously. In order to study its subsequent function, mice bearing a modified endogenous *Igh* allele with Eμ knockout and V_H knockin were generated and analyzed. In mice homozygous for this Eμ–deficient allele, B cell development was normal and indistinguishable from that of mice with the same V_H knock-in and Eμ intact. In mice heterozygous for the Eμ-deficient allele, however, allelic exclusion was severely compromised. Surprisingly, this was not due to

reduced suppression of V-DJ assembly on the second allele. Rather, the striking breakdown in allelic exclusion took place at the pre-B to immature B cell transition. These findings reveal both an important role for Eμ in influencing the fate of newly-arising B cells and a second “checkpoint” for allelic exclusion. In addition, we detected a substantial decrease in somatic hypermutation frequency on the Eμ-deficient allele, but this was not due to a decrease in transcription, suggesting that Eμ contributes to somatic hypermutation through a transcription-independent mechanism.

Acknowledgements

I gratefully thank all the people who helped or supported me on this project. First, I thank Dr. Laurel Eckhardt, my dedicated mentor, for the training and support. She started this project before I joined the lab, and guided me through thereafter. She showed me how to do research, and she also showed me how to do many other things, such as write and presentation. I thank my committee members, Dr. Jill Bargonetti, Dr. Benjamin Ortiz, Dr. Barbara Birshtein, and Dr. Linda Spatz, for their involvement in my project. I thank everyone in Eckhardt's laboratory, including both previous members and current members who have worked with me, for being great colleague. I especially thank Dr. Yi Yan and Dr. Buyi Zhang for technical assistance and helpful discussion. I also thank Dr. Weigang Qiu for teaching me the bioinformatics tools. I thank Dr. Klaus Rajewsky for providing targeting vector and the B1-8i mice, Dr. Scharff and Dr. Li for help with somatic hypermutation analysis. I thank Hunter Animal facility for taking care of our mice, and Mr. Joon Kim for flow-cytometry sorting. Last but not least, I thank my devoted parents, my sister, and my wife Ling (Tracy) Guo, for their love, concern, and support.

Table of Contents

Lists of Figures and Tables

Chapter 1: Introduction

Overview

Immunoglobulin is a key component of the mammalian immune system protecting the host from foreign pathogens. A large collection of antibodies that can recognize almost any possible pathogen are produced by B cells after they go through a long development process, during which the gene encoding immunoglobulin undergoes somatic rearrangements and mutation processes. These processes are carefully regulated in B cells by cis-control elements so that genome integrity is maintained. In this chapter, after a general introduction, the structure of the immunoglobulin gene and B cell development process will be described, followed by the introduction of known *cis*-control elements in the murine immunoglobulin heavy chain locus and their regulatory function during B cell development. Finally, the research question this project is trying to address, as well as the methodology and significance, will be introduced.

General background

Immunoglobulin, also known as antibody, is one of the major players in the vertebrate immune system. It is able to bind and neutralize toxic pathogens, or target harmful foreign substances for destruction. Each antibody molecule consists of two heavy chains (IgH) and two light chains (IgL) (Figure 1.1). Each chain can be separated into a variable region and a constant region, based on the variability of protein sequences. The variable region is the antigen-binding domain

and determines the specificity of the antibody; the constant region determines the effector function of the antibody, *e.g.*, where the antibody can travel and how the antibody can lead to destruction of antibody bound targets. Since there are many different antigens made by various pathogens, a large collection of antibody with different specificity is necessary for the vertebrate host to be protected.

Immunoglobulins are produced by B lymphocytes. As predicted in clonal selection theory described by Burnet in 1957 (Burnet 1957), and supported by accumulated experimental evidences (Cohn et al. 2007), vertebrate immune systems develop a large pool of B cells, and each one of them makes antibody with a unique specificity. The primary repertoire of antibody specificity is generated by the V(D)J rearrangement process, which assembles the variable region of immunoglobulin heavy chain and light chain genes from discrete gene segments. After B cells are activated by antigen, activated B cells undergo class switch recombination to produce antibody with the same variable region, but different constant region, therefore, conducting different effector functions. Another process, somatic hypermutation, also takes place in activated B cells. It modifies the gene encoding the variable region of immunoglobulin heavy and light chains, and generates B cells making higher affinity antibody.

On one hand, these somatic rearrangement and mutation processes serve the needs to create antibody diversity, generate different effector functions, and perfect binding affinity; on the other hand, these processes involve DNA damage, *e.g.*, single and double strand breaks, and pose a significant threat to the integrity

Figure 1.1: Schematic structure of an antibody molecule

An antibody molecule consists of two identical heavy (H) chains and two identical light (L) chains. Each heavy chain and light chain has an antigen-binding variable (V) region which determines the specificity of the antibody and a constant (C) region which determines the effector function of the antibody. All the chains are held together by disulfide bonds. Some heavy chain constant regions have three CH domains, some have four CH domains.

Figure 1.1 Schematic structure of an antibody molecule

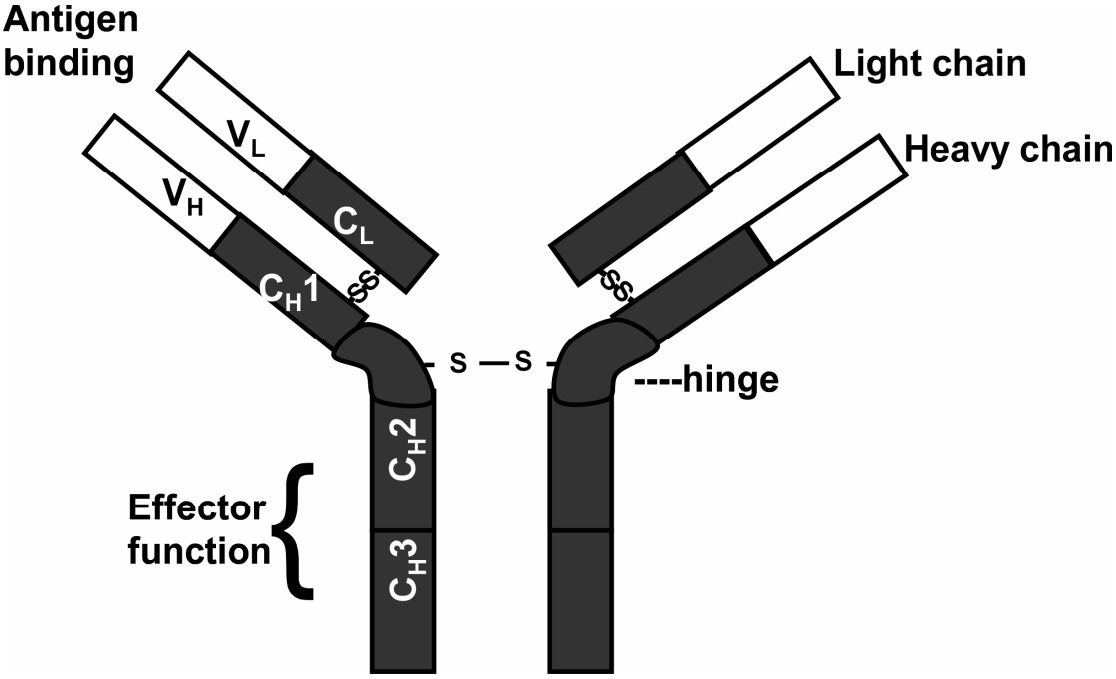

of the B cell genome. Therefore, it is necessary to study mechanisms that regulate these processes since these are still not fully understood.

Structure of antibody

Each antibody molecule consists of of two heavy and two light chains, which are hold together by disulfide bonds (Figure 1.1). Based on the sequence similarity, each heavy and light chain can be divided into two regions, the variable region and the constant region. The variable region is highly polymorphic, which is not surprising since the variable region is the antigen binding domain. The specificity of each antibody is determined by the combination of heavy chain and light chain variable regions. The variable region can be further divided into four framework regions (FR) and three complementarity determining regions (CDR). The CDRs are hypervariable, FRs form a beta-sheet structure which serves as a scaffold to hold CDRs in positions to contact antigens. The constant region determines the mechanisms used to destroy antigens. Murine and human antibodies are divided into 5 classes, IgM, IgG, IgA, IgE, IgD, based on their structure and immune function. (Immunology (Fifth edition, Freeman), by Goldsky, Kindt, Osborne and Kuby).

Structure of the IgH and IgL loci

The loci encoding IgH and IgL are among the largest known. The murine *Igh* locus is located on chromosome 12 and spans about 3 megabase pairs (Zhou et al. 2002; Retter et al. 2007). The IgH genes are composed of four major gene

clusters, variable (V_H) genes, diversity (D_H) genes, joining (J_H) genes, and constant (C_H) genes (Figure 1.2). There are 110 functional V_H and 85 V_H pseudogenes in the V_H cluster, which can be classified into 14 V_H families based on similarity. The largest V_H family, J558 family, lies at the 5' end of the *Igh* locus close to the telomere, and V_H genes at this end are referred to as distal V_H genes; V_H genes of the 7183 family and Q52 family lie at the most 3' end, and they are referred to as proximal V_H genes. Each functional V_H gene has a lymphoid-specific promoter, followed by a leader sequence, leader intron, V_H coding sequences, and recombination signal sequence (RSS). The length of the V_H gene cluster has been estimated to be about 1.5 megabase pairs. Downstream of the V_H cluster is the D_H gene cluster consisting of 11-15 D_H genes, which can be classified into 4 D_H families, DSP2, DFL16, DST4, and DQ52. Each functional D_H gene is flanking by one RSS at each end. Farther downstream, 4 functional J_H genes can be found in a J_H gene cluster, each of which contains an RSS at the 5' end. At the end of the locus, there are 8 constant (C_H) genes, including Cμ, Cδ, Cγ3, Cγ1, Cγ2b, Cγ2a, Cε, and Cα. These gene segments encode three (α, δ and γ) or four (μ and ε) domains (CH1-3 or CH1-4) and are separated by large introns. For Igα, Igδ and Igγ chains, a proline-rich hinge region is present between the CH1 and CH2 domains, and this region can provide some structural flexibility that helps the binding of an antibody to an antigen. With the exception of Cδ, each constant region gene has its own intronic promoter (P_I) (Figure 1.2, *bottom panel*). Transcripts initiated from these promoters are unable to be translated into proteins (the products are also known as "sterile transcripts") and correlate with CSR.

Figure 1.2: Schematic view of murine IgH locus and its somatic modification events.

Upper panel: Schematic view of murine IgH locus and its somatic modification events. IgH locus is organized into four gene clusters: Variable genes (V_H), D_H genes, J_H genes and constant genes (C_H) genes. During the early stages of B cell development, the variable region undergoes VDJ joining and the locus expresses Igμ chain. At later B cell stages, class switching (CSR) happens through the switch regions upstream of each constant region upon certain antigen and/or cytokine stimulation, which results in a different constant chain with the same Ag specificity. After CSR, this locus will produce a different IgH chain (Igγ1 in this diagram). Another change in activated B cells is somatic hypermutation, which can increase antigen binding affinity by making mutations within the V region.

Lower panel: Cis-control elements in murine IgH locus. Murine IgH locus consists of several cis-control elements, including the intronic enhancer Eμ and the 3' regulatory region (3'RR). Eμ is composed of two matrix attachment regions (MAR) and a core enhancer (cEμ). 3'RR contains of 7 DNaseI hypersensitive sites, hs3a, hs1,2, hs3b, hs4, hs5, hs6, hs7There is a promoter at the 5' of each V_H, D_H, and C_H gene except Cδ, i.e., P_{VH}, P_{DH}, and P_I, respectively. The μ0 transcript initiated from the promoter of the last D gene segment is shown as a dashed line with arrow.

Figure 1.2 Schematic view of murine germline IgH locus and its somatic modification events

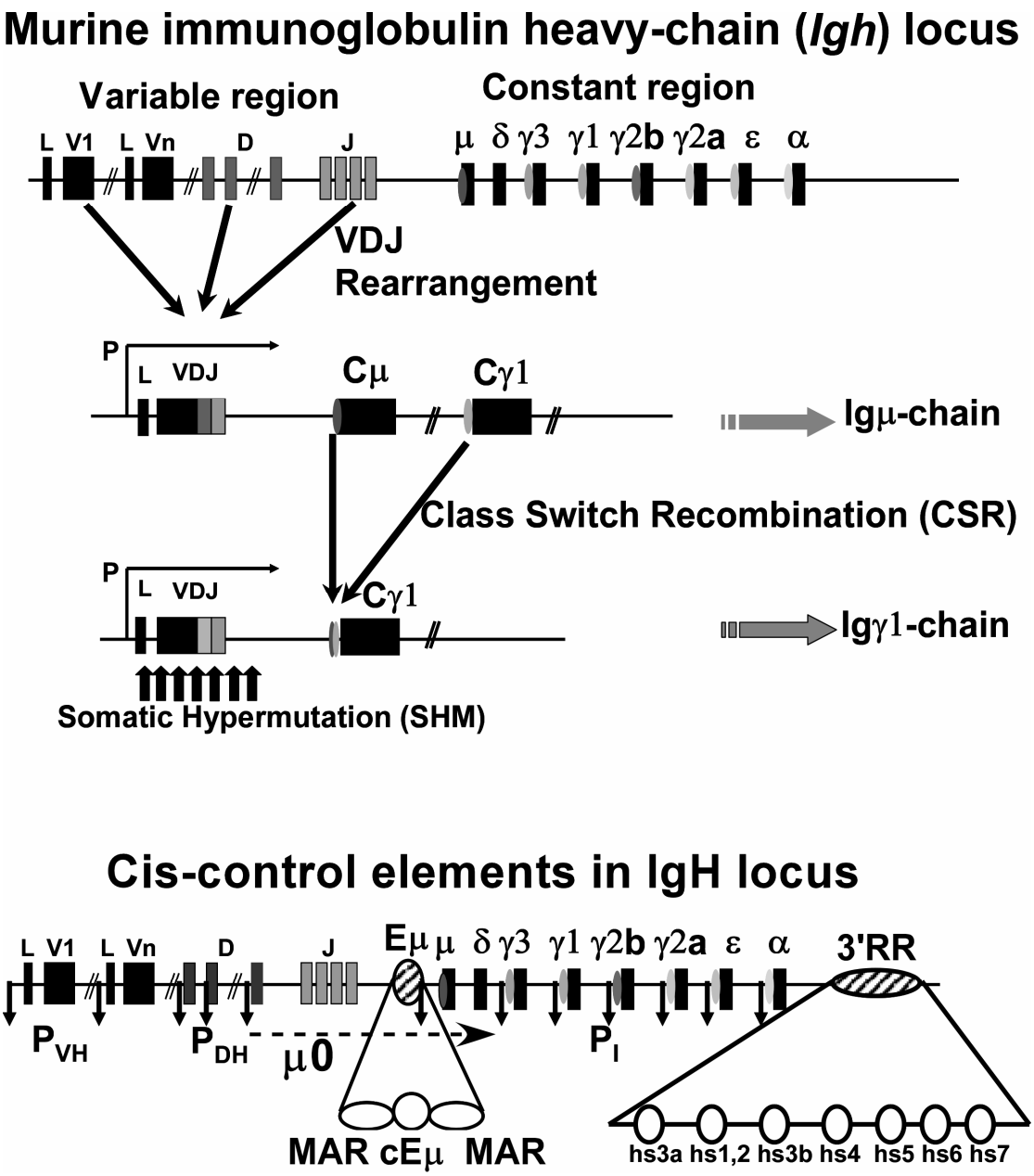

Mouse has two IgL loci, the Igκ and Igλ loci. The overall structure of Igκ locus is similar to IgH, except that there is neither a D gene cluster nor multiple constant region genes. It spans about 1.25 megabases and contains about 140 variable region genes (Vκ), 5 joining genes (Jκ), and 1 constant region gene (Cκ), and the Cκ region is encoded by only one C_L domain. The mouse Igλ locus is the smallest immunoglobulin locus. It contains 2 variable region genes (Vλ), 3 functional joining genes (Jλ), and 3 functional constant region genes (Cλ).

The immunoglobulin loci of humans are very similar to those of mice. The human *Igh* locus also contains V_H, D_H, J_H, C_H clusters, but the number of genes in each cluster is different. Humans also have two IgL loci, human Igκ and Igλ, but the human Igλ locus contains more Vλ and Jλ than murine Igλ locus.

B cell development in bone marrow and rearrangement of immunoglobulin genes

B cells develop from adult bone marrow-derived hematopoietic stem cells (reviewed in: Busslinger 2004; Hardy et al. 2007).The pluripotent hematopoietic stem cell (HSC) has extensive self-renewal potential and regenerates all blood cell types throughout life by differentiating into progenitor cells with gradually restricted developmental potential. One early step in the process of B cell development from the HSC is the commitment of multipotent progenitors (MPP) to either the erythro-myeloid lineage or the lymphoid lineage, resulting in the formation of

common myeloid progenitors (CMP) or common lymphoid progenitors (CLP). The development from HSC to CLP requires expression of the transcription factors Ikaros PU.1, E2A, and EBF1 cells (reviewed in: Busslinger 2004; Hardy et al. 2007). CLP cells express recombinase activating genes (Rag1 and Rag2), and terminal deoxynucleotidyl transferase (TdT), which are enzymes involved in the assembly of immunoglobulin genes and T cell receptors, and D_H-J_H rearrangement is common in CLP cells. During this process, long-term self-renewal potential and the potential to become myeloid lineage cells are gradually lost. CLP cells are able to develop into four cell types: B lymphocytes, T lymphocytes, natural killer (NK) cells, or dendritic cells (DC). A subpopulation of CLP cells differentiate into B220+ cells, constituting a subset of cells that are committed to the B cell pathway. This commitment depends on Pax5, also known as B-cell-specific activator protein (BSAP), which suppresses alternate cell fates in developing B lineage cells and activates B-cell-specific genes such as CD19, Igα, and BLINK (Nutt et al. 1999). Recently, Pax5 has been shown to promote V_H-D_HJ_H rearrangements by inducing large scale of contraction of the *Igh* locus therefore promoting V_H-D_HJ_H recombination by juxtaposition of distal V_H genes and the proximal D_HJ_H-rearranged gene segments (Fuxa et al. 2004; Roldan et al. 2005). Cells committed to the B cell lineage continue to assemble an IgL gene and develop, within the bone marrow, all the way to immature B cells that express surface B cell receptors.

B lineage cells (B220+) undergo $V_HD_HJ_H$ recombination (Figure 1.2 and Figure 1.3). During this process, 1 V_H, 1 D_H, and 1 J_H are picked in a random

Figure 1.3: A flow chart of B cell development.

Newly committed immature B cells develop from the pro-B cell stage in the bone marrow through immature B cell stage and then exit the bone marrow and enter the periphery, where they mature and, upon activation, differentiate into the antibody-secreting plasma cells or memory B cells. B cells at each stage have unique combination of surface markers that can be used in FACS analysis to identify them.

Figure 1.3: A flow chart of B cell development.

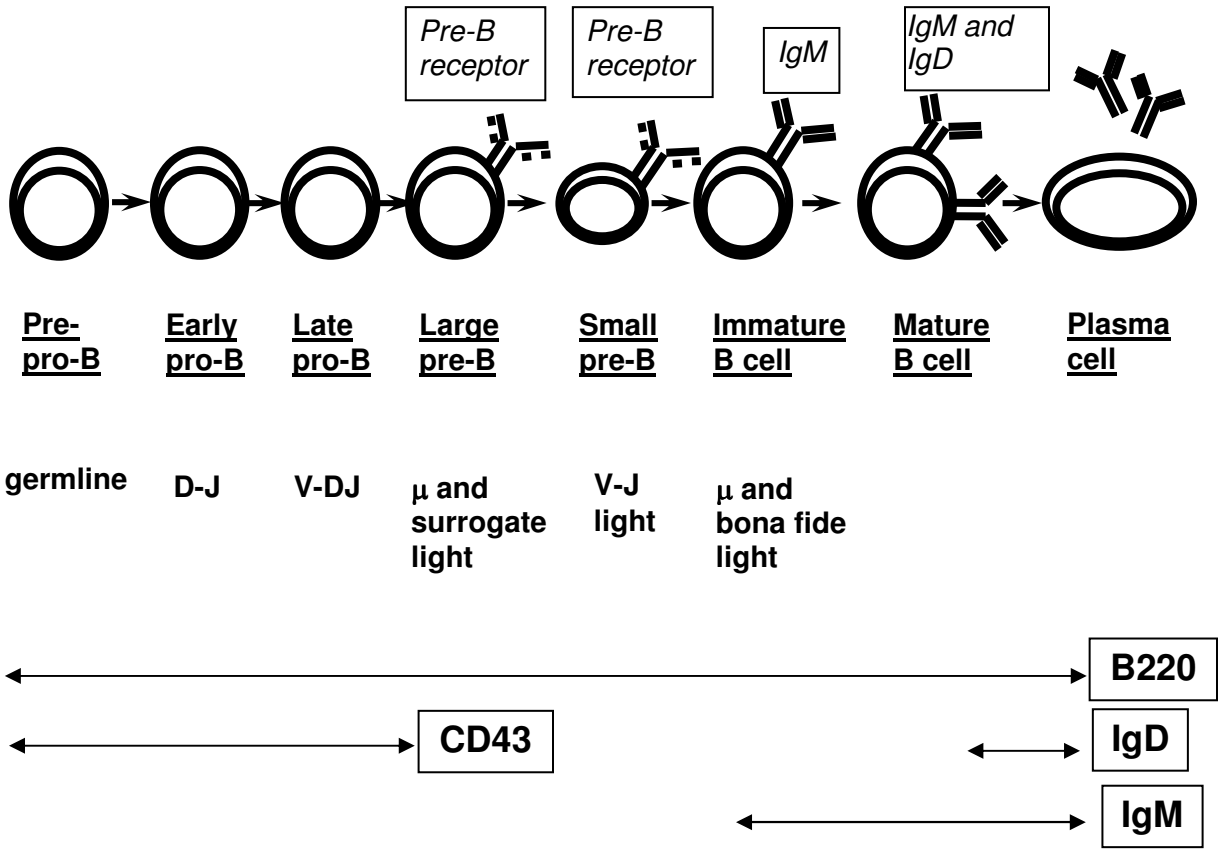

manner to assemble the complete IgH variable region gene. Successful rearrangements lead to the expression of μ heavy chain, which can form a pre-B cell receptor (pre-BCR) with surrogate light chain (λ5 and VpreB) and signaling molecules (Igα and Igβ) (Clark et al. 2005; Martensson et al. 2007). The pre-BCR has been proposed to provide a signal to shut down additional $V_HD_HJ_H$ recombination within the *Igh* loci, therefore only one functional $V_HD_HJ_H$ rearrangement can be achieved in each B lineage cells, a phenomenon termed allelic exclusion (reviewed in Jung et al. 2006). Pre-BCR signaling also promotes cell proliferation and differentiation into pre-B cells (Martensson et al. 2007). The V-J recombination of IgL genes occurs at the pre-B cell stage. Once IgL is expressed from a productively rearranged IgL locus, it replaces surrogate light chain to form a B cell receptor (BCR) with μ. Thus, surface IgM is expressed and the cell enters the immature B cell stage. At the transition of pre-B/immature B, the B cell receptors are assessed for autoreactivity, and autoreactive BCRs can be replaced by non-autoreactive BCRs through receptor editing that replaces the expressed light chain with a different one. Immature B cells can go to the periphery and differentiate into mature B cells that serve various functions.

B cell development in periphery

Three kinds of phenotypically and functionally distinct B cell populations have been described in both mice and people: follicular B cells (also known as conventional B cells or B-2 B cells), marginal zone B cells, and B-1 B cells (reviewed inAllman and Pillai 2008). Follicular and marginal zone B cells, as their

names imply, occupy distinct regions in the spleen. Follicular B cells make up the majority of B cells recirculating in blood, lymph nodes, and spleen. They mediate T-dependent immune responses to protein antigens. Marginal B cells primarily reside in the vicinity of the marginal sinus of the spleen, and they appear to mediate T-independent responses to antigens in blood-borne pathogens. The peritoneal cavity, on the other hand, is largely populated by B-1 B cells, although B-1 B cells are also found in small numbers elsewhere. B-1 B cells are subdivided into those that do (B1a) and those that do not (B1b) express CD5. B-1 B cells can contribute to the generation of IgM responses to T-independent antigens such as phosphorylcholine, an antigen present on many pathogenic bacteria (reviewed inAllman and Pillai 2008).The process by which immature B cells are selected into different subsets of B cells remains to be determined.

In the periphery, mature B cells migrate to secondary lymphoid tissues, in which a small number of B cells are activated by T helper cells, antigens and cytokines. Different stimuli will lead to different outcomes. Activated B cells may undergo class switch recombination, juxtaposing the rearranged VDJ fragment with one of the six C_H classes downstream of Cδ, and generating IgG3, IgG2a, IgG2b, IgG1, IgE or IgA antibodies. Meanwhile, mutations will occur with high frequency in the rearranged variable region gene segments, a process known as somatic hypermutation. As a result of somatic hypermutation and antigen-driven selection, only B cells with enhanced affinity to the antigen will be selected, clonally expanded, and differentiate into plasma cells or memory B cells. Plasma cells can secret antibodies to eliminate the invading antigens, and memory cells

are reserved as a pool of B cells that will efficiently eliminate the same antigen when they invade again.

Class switch recombination

Heavy chain class switch recombination (CSR) is a process in which the intervening sequences between two switch (S) regions upstream of constant (C) region coding sequence are deleted in response to certain cytokine stimulation, juxtaposing the assembled V_H gene with a new downstream C-region without changing the antigen-specificity (Figure 1.2). Therefore, a new antibody with the same antigen binding capability but with a different effector function can be produced. The cytokines inducing CSR are generated by helper T lymphocytes (T_H).

Class switch recombination is initiated by activation-induced cytidine deaminase (AID), which targets the S region and converts C to U, and the repairs of G:U lesions leads to double strand breaks (DSB), and therefore, to class switch recombination (Muramatsu M 2000). Studies using a construct without S region (Kinoshita et al. 1998) or S-region-knockout mice (Jung et al. 1993), have clearly shown that S regions are essential for CSR. Furthermore, knockout mice for the core Sμ region showed decreased levels of CSR to all isotypes (Luby et al. 2001). However, in a recent study when donor Sμ and receptor Sγ1 regions were replaced with yeast I-SceI endonuclease sites, class switching from IgM to IgG1 was induced by site-specific I-SceI DSBs without S regions or AID, suggesting that the contribution of AID and S region is to generate DSBs (Zarrin et al. 2007).

Somatic hypermutation

Somatic hypermutation introduces point mutations into immunoglobulin genes in germinal center B cells during an immune response at a rate one million fold higher than random mutations (reviewed in: Odegard and Schatz 2006; Peled et al. 2008). It was originally proposed as a mechanism to generate the repertoire diversity of immunoglobulin genes (Brenner and Milstein 1966), which is now known to be primarily created by the V(D)J rearrangement process in mice and humans (reviewed in Jung *et al*., 2006). Instead, somatic hypermutation contributes to affinity maturation in the antibody response, by providing substrates for antigen-driven selection for B cells that produce antibodies with higher affinity to antigen. Another proposed function of somatic hypermutation is to help a host to track down fast evolving pathogens (Longo and Lipsky 2006).

The biochemical mechanism of somatic hypermutation has been subjected to intensive study in the last ten years, and the discovery of activation-induced cytidine deaminase (AID) and other important players in somatic hypermutation has greatly improved our understating of this process (reviewed in (Odegard and Schatz 2006; Di Noia and Neuberger 2007; Peled et al. 2008)). Somatic hypermutation is initiated by AID through an enzymatic process that converts cytosine (C) to uracil (U), which might be removed by uracil N-glycosylase (UNG) or recognized by the mis-match repair proteins MSH2/6 to initiate error-prone repair (Rada et al. 1998; Muramatsu et al. 1999; Muramatsu M 2000; Wiesendanger et al. 2000; Rada et al. 2002; Martomo et al. 2004; Shen et al. 2006). DNA replication over U bases or abasic sites (after U removal can result in

mutations at G/C bases, while the exonuclease Exo1, together with error-prone DNA polymerases, such as polη and polθ, can introduce mutations in neighboring DNA nucleotides including A/T bases during DNA repair (Zeng et al. 2001; Zan et al. 2005; Delbos et al. 2007). AID is also required for the class switch recombination process, in which the processing of U lesions leads to the generation of DNA double strand breaks required for class switch recombination (Muramatsu M 2000).

Cis-control elements in the *Igh* locus and their regulatory functions

The multiple somatic recombination and mutation processes are required to produce an efficient immune system, but at same time, these processes pose a great threat to the integrity of the host genome. Therefore, they must be carefully regulated. A number of cis-control elements have been identified, including V_H promoters (P_{VH}), D_H promoters (P_{DH}), intronic promoter for constant regions (P_I), and two major enhancers, the intronic enhancer μ (Eμ) and 3' regulatory region (3'RR) (Figure 1.2). While transcription initiated from promoters is an indication of accessible chromatin and is involved in VDJ or class switch recombination processes, the regulatory function of the enhancers has been a focus of study with the immunoglobulin heavy chain locus.

Intronic enhancer Eμ

Eμ is a 1kb XbaI fragment lying in an intron sequence between J_H4 and Cμ. Eμ consists of both a "core region" (cEμ) with enhancer activity (as defined in transient transfection assays) and two flanking nuclear matrix-attachment regions (MARS) (Cockerill et al. 1987). It was initially discovered as a transcriptional enhancer (Banerji et al. 1983; Gilles and Tonegawa 1983; Neuberger 1983). Similar to conventional enhancers, it can drive the expression of immunoglobulin or other transgenes in an orientation and position independent manner, but it is active only in lymphoid cell lines. Eμ deletion studies within the murine *Igh* locus subsequently demonstrated that this regulatory element was essential for promoting efficient V-D-J recombination, as well (Chen et al. 1993a; Serwe and Sablitzky 1993; Sakai et al. 1999b; Perlot et al. 2005; Afshar et al. 2006).

cEμ and Igμ transcription and VDJ rearrangement

Eμ was the first identified transcriptional enhancer to be identified in the *Igh* locus (Banerji et al. 1983; Gilles and Tonegawa 1983; Neuberger 1983). Similar to conventional enhancers, it can drive the expression of transgenes encoding immunoglobulin, β-globin, and SV40 T antigen in an orientation and position independent manner, but it is active only in lymphoid cell lines. Soon, Eμ was shown to be able to drive the expression of μ transgenes in μ transgenic mice by a number of groups (Grosschedl et al. 1984; Rusconi and Kohler 1985; Weaver et al. 1985; Storb et al. 1986; Nussenzweig et al. 1987). The μ transgene is only expressed in lymphocytes, but not exclusively in B lineage cells (Grosschedl et al.

1984). After the discovery of two MARs in Eμ (Cockerill et al. 1987), the MARs and cEμ were studied for their individual contribution to enhancer activity. MARs were found to be dispensable for the expression of a μ transgene after it was stably transfected into a B cell line (M12), but it was necessary for the expression of the same μ transgene in developing pre-B cells in transgenic animals (as described in more details in next section). cEμ is essential for the expression of the same μ transgene in both systems (stably transfected B cells and developing B cells in transgenic mice). These data demonstrated that cEμ possesses the enhancer activity of Eμ, and this activity seems to be regulated by MARs in developing pre-B cells (Forrester et al. 1994; Fernandez et al. 2001).

Subsequently, analysis of B cells with targeted deletion of all or part of Eμ in the endogenous *Igh* locus demonstrated that cEμ, but not MARs, was essential for promoting efficient V-D-J recombination, as well (Chen et al. 1993a; Serwe and Sablitzky 1993; Sakai et al. 1999b; Perlot et al. 2005; Afshar et al. 2006). In one of two early studies, an embryonic stem cell (ES) line made heterozygous for Eμ deletion was used to generate chimeric mice. Abelson virus-transformed pre-B cell lines were generated from the chimeric animals, allowing for analysis of the Eμ-deficient and wild-type alleles in individual pre-B cells (Chen et al. 1993a). In the other of these early studies, mature B cells heterozygous for Eμ deletion were isolated from chimeric animals on the basis of IgD allotype (Serwe and Sablitzky 1993). Both studies led to the important discovery that Eμ was required for efficient *Igh* variable region gene assembly, with some controversy as to whether this was

due to a block only to V-DJ or to both this and D-J joining. In both of these studies, Eμ deletion involved deletion of both cEμ and the flanking MARs. Follow-up studies showed that deletion of the MARS had no adverse effect on V-D-J assembly, demonstrating that cEμ was both necessary and sufficient for this process (Sakai et al. 1999b). More recently, mice with germline deletions of core Eμ have been generated and studied (Perlot et al. 2005; Afshar et al. 2006). In these mice, B cell development was greatly impaired such that pre-B, immature B, and mature B cell populations in the bone marrow were reduced to less than 10% wild-type levels. There appeared to be some expansion of B cells in the periphery, but spleens were ~1/2 normal size and the proportion of B cells in these small spleens was considerably reduced (1/3-1/2 wild-type). This developmental defect turned out to be attributable to an impairment not only of V-DJ joining but also of D-J joining, resolving the earlier controversy concerning Eμ's effect on D-J joining (Perlot et al. 2005; Afshar et al. 2006).

The Eμ-deletion-caused defects in $V_HD_HJ_H$ recombination correlate with the reduced germline transcript μ_0, which is initiated from the promoter of the last D gene segment (DQ52) (shown in Figure 1.2, lower panel) The replacing of Eμ or cEμ with the Neo^R gene leads to essentially a complete loss of μ0 transcripts, resulting largely impaired $V_HD_HJ_H$ recombination and loss of mature B cells (Chen et al. 1993a; Perlot et al. 2005; Afshar et al. 2006). In contrast, a clean deletion of cEμ does not lead to complete loss of μ0 transcripts, and cEμ-deficient pro-B cells express approximately 10-20 fold less μ0 transcripts compared with wild-type

mice, correlating with the observation that rare B cells undergo Eμ-independent $V_HD_HJ_H$ recombination (Perlot et al. 2005; Afshar et al. 2006).

MARs and *Igμ* transcrption

While cEμ is a positive regulator for transcription, MARs have been reported to have a negative regulatory effect on transcription in non-lymphoid tissue but not in myeloma cells (Imler et al. 1987). The negative regulatory effect correlates with binding to a nuclear protein, NF-μNR, which is expressed in non-B lineage cells (such as, T cells, macrophages, and fibroblasts) and cells representing early stages (μ^- pro-B cells), but not later stages of B cell development (pre-B, mature B and plasma cells) (Scheuermann and Chen 1989). On the other hand, a positive regulatory role for MARs on μ expression has also been reported. In one study, hybridoma cell lines derived from the same parental line but with differently modified endogenous IgH genes were analyzed for μ expression, and deletion of MARs was found to further reduce the expression of μ from 1/2 wild-type levels in cells with only cEμ deletion to 1/50 of wild-type levels (Oancea et al. 1997). Notably, in this study, a transcription unit (*gpt* gene) was inserted downstream of Cμ, which might have had un-expected effects and/or disrupted the interaction of the V_H promoter and the 3' regulatory region. In addition, in a more recent study using this system, after deleting cEμ or Eμ(MARs + cEμ), both stable cell lines with sustained or ceased μ expression were established (Ronai et al. 2005). The latter finding suggests that there is no strong correlation between the integrity of Eμ with μ expression in this experimental

system. And the reported effect of MARs on μ expression in the early study (Oancea et al. 1997) could be due to some other factors.

While these data need to be interpreted with caution, additional evidences for a positive regulatory role of MARs in μ transcription come from the study of transgenic mice bearing a μ transgene without MARs. In this study, an analysis of Abelson-murine leukemia virus (A-MuLV) transformed pre-B cells demonstrated that the cEμ-mediated transcription of μ transgene depended on MARs; perhaps due to their capacity to facilitate cEμ in antagonizing methylation-dependent repression and establishing long range of accessibility of transgenes, as indicated by DNase I sensitivity, and histone acetylation. In the same study, however, cEμ-mediated transcription of the μ transgene did not depend on MARs in stably transfected tissue culture cells as long as the transfected DNA was not pre-methylated (Forrester et al. 1994; Forrester et al. 1999; Fernandez et al. 2001). Therefore, it seems that MARs themselves have no enhancer activity, but they might contribute the enhancer activity of cEμ by helping to open the chromatin structure.

3' Regulatory Region

In addition to Eμ, a series of cis-elements located at the 3' end of the *Igh* locus, known as 3' regulatory region (3'RR), has been identified and shown to be essential to high level expression of IgH genes during late stages of B cell development and class switch recombination (reviewed in Khamlichi et al. 2000). Hs1,2, the first identified 3' enhancer, was discovered in rat by scanning a 3' Cα

region-containing cosmid for the ability to confer tissue-specific transcriptional enhancement activity (Pettersson et al. 1990). Soon after, murine hs1,2 was also found in the *Igh* locus, based on its high homology (82%) with the rat hs1,2 and its enhancer activity in transient assays (Dariavach et al. 1991; Lieberson et al. 1991). A second element, hs3a, was identified by its ability to bind to transcription factors in electrophoretic mobility shift assay (EMSA) (Matthias and Baltimore 1993). Hs3b and hs4 were later found by DNaseI hypersensitivity assay (Madisen and Groudine 1994; Michaelson et al. 1995). More recently, another 3 DNase I hypersensitivity sites were discovered at the further downstream of hs4, presumably at the end of the *Igh* locus (Garrett et al. 2005).

The 3'RR enhances IgH promoter activity over a long distance (Figure 1.2). The nearest enhancer with the 3'RR, hs3a, is about 4.5kb downstream of Cα membrane form exon (Cαm), which is the last exon of the murine heacy chain constant regions. The next enhancer element, hs1,2 lies 15kb downstream of Cαm. It is located at the center of the hs3a-hs1,2-hs3b region and is flanked by several pairs of inverted repeats (IRs) including two other enhancers (hs3a and hs3b) (reviewed in Arulampalam et al. 1997). Hs3a and hs3b are virtually identical (97%) in sequence but oriented opposite to each other (reviewed in Arulampalam V1997). Hs3b and hs4 are about 26kb and 30kb 3' from Cαm, respectively. Hs5, 6 and 7 are located downstream of hs4 and are speculated to act as insulators of the locus (Garrett et al. 2005). Together, all 3' enhancers are over 200 kb away from the rearranged V_H gene and associated IgH promoter.

3' RR and IgH transcription

Several observations led to the search for additional cis-elements at the 3' end of the *Igh* locus. These observations include the sustained IgH transcription level without Eμ in Ig-secreting cells, and the deregulated expression the oncogene *c-myc* when translocated next to the 3' region of the Igh locus (Neuberger and Calabi 1983; Wabl et al. 1984; Eckhardt and Birshtein 1985).

The enhancer activity of hs3a, hs1,2, hs3b and hs4, the four enhancers first identified in the 3'RR, have been analyzed both in cell lines and in animal models. In pre-B cells, hs3a, hs1,2 and hs3b are inert individually, whereas hs4 is active as detected by DNaseI hypersensitivity (reviewed in Arulampalam et al. 1997). In transient assays in pre-B cell lines (18-81 and 18-8), the four enhancers showed almost no enhancer activity individually except hs4. There was little or no synergy among them in driving transcription from a V_H promoter; when the four enhancers were combined together, their enhancer activity was no greater activity than Eμ alone. However, in pre-B cell lines, addition of all four 3' enhancers could boost the enhancer activity of Eμ (Chauveau et al. 1998; Ong et al. 1998). Recently, a human *c-myc* gene driven by hs3a-hs1,2-hs3b-hs4 was shown to be expressed only at low levels in pro/pre-B cells, but highly expressed in immature B cells and mature B cells (Yan et al. 2007). Therefore, in pro/pre-B cells, the 3'RR has either no enhancer activity, or only weak enhancer activity. It appears that Eμ is the essential regulatory element of IgH transcription in early B cell development based on the weak enhancer activity of the 3'RR, Eμ's regulatory function in $V_HD_HJ_H$

recombination, μ0 transcription, and transcription of a μ transgene. It cannot be ruled out that 3'RR is also operational at these early stages, and facilitates Eμ's function in driving IgH transcription. Notably, the low transcription level of μ in late pro-B and early pre-B cells correlates with low 3'RR enhancer activity. Also supporting this hypothesis it the finding that a clean cEμ deletion does not completely block $V_HD_HJ_H$ recombination, while the replacement of cEμ with Neo^R does so (Perlot et al. 2005). This could be explained this way: perhaps, the potential low 3'RR enhancer activity in pro-B cells that might be driving the low level of μ^0 transcripts and $V_HD_HJ_H$ recombination in the absence of cEμ is inhibited by the insertion of NeoR, which has been shown to block the interaction between 3'RR and the V_H promoters of assembled V_H genes (Ju et al. 2007).

In cell lines representing later stages of B cell development, surface Ig+ and Ig-secreting cells, 3'RR enhancers showed much higher enhancer activities. In surface Ig+ cell lines (A20, Raji, Namalwa, M12.4.1), although hs3a, hs1,2, hs3b, and hs4 had almost no or very weak enhancer activity, their combination was strongly active (much stronger or at least equivalent to Eμ alone) through synergistic interactions. In several Ig-secreting cell lines (S194, P3X63Ag8), 3'RR enhancers were strong individually, and were not synergistic while strong synergistic interactions persisted in one plasma cell line (SP2/0). In all Ig-secreting and plasma cell line analyzed, both Eμ and the combination of 3'RR enhancers have strong enhancer activities (Chauveau et al. 1998; Ong et al. 1998). These data, accompanying the observation that the human *c-myc* gene driven by

hs3a-hs1,2-hs3b-hs4 was highly expressed only after the pro/pre-B cell stage, provided evidence that the 3'RR was most effective in late-stage B cells.

Additional evidence for the contribution of 3'RR to IgH expression comes from the analysis of B cell lines containing naturally occurring or engineered mutations in Eμ and/or 3' RR, and from analysis of B cells with IgH transgenes. These data include: i) sustained IgH expression in plasma cell lines (9921) with Eμ deletion (Eckhardt and Birshtein 1985); ii) dramatic reduction in IgH expression to ~1/7 wild-type levels in a IgA-secreting plasma cell line (LP1.2) with a deletion from hs3a through hs4 (Gregor and Morrison 1986; Michaelson et al. 1995); iii) deregulated expression of translocated *c-myc* that is juxtaposed to the 3' end of the *Igh* locus (Neuberger and Calabi 1983); iiii) complete loss of IgH expression in a plasma cell line (B48) with a deletion of Eμ and substitution of the hs1,2 enhancer by neomycin resistant (Neo^R) gene (Lieberson et al. 1995); iiiii) deletion of hs3b and hs4 from a γ2b transgene mini-locus (hs3b-hs4-hs3a-hs1,3-P_{VH}-V_H-Cg2b) in Ig secreting cell line (9921) leads to almost complete loss of Ig-expression (Shi and Eckhardt 2001).

However, neither individual deletion of hs3a or hs1,2, nor pairwise deletion of hs3b and hs4, nor insertion of Neo^R (which was shown to disrupt the interactions between V_H promoter and 3'RR(Ju Z2007)) led to a dramatic reduction in IgH expression when assayed within the endogenous *Igh* locus (Cogne et al. 1994; Manis et al. 1998; Pinaud et al. 2001). After stimulation by LPS and cytokines, B cells with Neo^R replacing hs1,2 or hs3a in the endogenous *Igh* locus seemed to

secret IgM, IgG1, and IgA at levels comparable with those produced by wild-type B cells, and a “clean” deletion of hs1,2 or hs3a alone had no effect on IgH expression (Cogne et al. 1994; Manis et al. 1998). In the case of hs3b and hs4, endogenous deletion led to only a modest effect – surface IgM and μ mRNA level were reduced in splenic B cells to about 49~63% wild-type levels (Pinaud et al. 2001). In another study, bacterial artificial chromosome (BAC) transgenes containing an assembled V_H gene, Eμ, all the constant genes, but no 3’ RR, expressed normal levels of μ expression (Dunnick et al. 2005). More recently, deletion of hs4 in a BAC *Igα* transgene already lacking Eμ was shown not to affect *Igα* expression (Zhang et al. 2007).

Collectively, it seems that, in late-stage B cells, both Eμ and 3’RR contribute to IgH expression, and functional redundancy (for promoting IgH expression) not only exists between Eμ and the 3’RR, but also within the 3’RR. Recently, chromosome conformation capture assay provided evidence of physical interaction between V_H promoter and 3’RR. Ju *et al* (2007) showed that 3’RR physically interacts with the V_H promoter in plasma cell lines, and this interaction was not affected by the loss of Eμ; but in another cell line (B48) with a deletion of Eμ and a replacement of hs1,2 with neomycin resistant gene, the interaction between the downstream elements (hs3b, hs4) and V_H promoter was disrupted, correlating with a complete loss of transcription from the V_H promoter. Interactions between the *c-myc* promoter and 3’RR were also detected in a plasmacytomas cell line containing a reciprocal translocation between the *c-myc* and *Igh* loci.

Regulation of class switch recombination

The isotype-specific germline transcription from intronic promoters (P_I) stimulated by a given cytokine has a close association with the recombination target of S regions, which has led to the accessibility model of CSR (Kinoshita and Honjo 2001). This model proposes that recombination requires opening the chromatin structure to allow access by the recombination machinery. P_I-directed transcription either reflects or induces that change in chromatin structure. Consistent with this notion, several gene-targeting deletions of P_Is have led to abrogation of CSR to the corresponding isotype (Zhang et al. 1993; Seidl et al. 1998). Cis-control elements might dictate class switch recombination by regulating the accessibility, such as promoting germline transcription.

Neo^r replacement of core Eμ and associated MARs in hybridomas decreased, but did not abolish, class switching at the μ locus (Bottaro et al. 1998). Controversially, deletion studies in mice showed that cEμ was necessary and sufficient to promote efficient CSR at the *Igh* locus in the absence of MARs (Sakai et al. 1999a; Perlot et al. 2005).

The 3' RR has been demonstrated to play an important role in regulating class switch recombination. The replace of hs3a or hs1,2 with Neo^R affected class switch recombination to most isotypes, *i.e.*, IgG2a, IgG2b, IgG3 and IgE, but not IgG1 and IgA (Cogne et al. 1994; Manis et al. 1998). However, analysis of B cells with a "clean" deletion of hs3a or hs1,2 showed normal class switch recombination (Manis et al. 1998); in addition, when 70Z/3 cells (a pre-B cell line) with a natural

deletion of hs3a and hs1,2 was fused to plasmacytoma cells (NSO), CSR was not disturbed in the hybrids (Saleque et al. 1999). These data indicate that hs3a and hs1,2, individually or in combination, are not essential for CSR, and the impaired CSR in B cells with Neo^R replacing hs3a or hs1,2 is most likely due to the perturbation of other 3'RR elements' function by Neo^R insertion. In fact, pairwise deletion of hs3b and hs4 affected class switch recombination to all isotype except IgG1 (Pinaud et al. 2001), while complete deletion of the 3' RR in BAC transgenes affected all isotypes (Dunnick et al. 2005), demonstrating 3'RR's essential role in promoting CSR. Mechanistically, 3' RR might promote CSR by inducing germline transcription from I promoters upon cytokine stimulation, and reduced class switch recombination accompanied the reduced germline transcription (Pinaud et al. 2001; Dunnick et al. 2005). Recently, by chromosome conformation capture assay, Wuerffel et al (2007) showed that 3'RR physically interacted with Eμ in resting B cells, and cytokine-mediated activation of B cells leads to recruitment of germline transcription promoters to the Eμ:3'RR complex. These authors also showed that the interaction between Eμ, 3'RR, and germline transcription promoters did not require cEμ (the core enhancer of Eμ) or Sμ (the switch region of μ), but did depend on the integrity of 3'RR (for instance, the Eμ:3'RR interaction was disrupted without hs3b,4), and surprisingly, AID (Wuerffel et al. 2007). It was proposed that the association of germline transcription promoters with Eμ:3'RR creates an architectural scaffold that promotes the synapsis of switch regions during CSR, and that these interactions are stabilized by AID.

Cis-elements regulating SHM targeting

While somatic hypermutation is an important process that contributes to an effective immune response, mis-targeting of somatic hypermutation poses a serious threat to the integrity of the host genome. In fact, the key enzyme, AID, has been suggested to be involved in tumorigenesis and disease progression in a wide variety of cell types (Kotani et al. 2007; Okazaki et al. 2007). Therefore, somatic hypermutation must be carefully regulated. Very recently, Liu *et al* (2008) reported two levels of protection for the B cell genome during somatic hypermutation: selective targeting of AID and gene-specific, high-fidelity repair of AID-generated uracils (Liu et al. 2008). The variable region of immunoglobulin genes is the primary, although not exclusive, target of somatic hypermutation, since all known non-Ig genes targeted by somatic hypermutation are mutated at much lower frequencies. For example, *Bcl6*, the most extensively mutated non-Ig gene reported so far, is mutated at a level 20-50 times lower relative to immunoglobulin genes (Shen et al. 1998; Liu et al. 2008). Although it has been under extensive study, the mechanism directing somatic hypermutation machinery to the immunoglobulin gene loci remains to be determined (reviewed in: Odegard and Schatz 2006; Di Noia and Neuberger 2007; Peled et al. 2008).

Somatic hypermutation preferentially targets RGYW/WRCY hot spots, but these hotspots are present in almost any gene. A correlation between transcription and somatic hypermutation has been established, but the V gene promoter appears to be replaceable (Fukita et al. 1998). Since V_H primary sequences can be replaced with other DNA sequences without affecting somatic

hypermutation, the element(s) responsible for targeting must fall within other cis-control elements in immunoglobulin gene loci. However, deletion of hs3b and hs4 from the endogenous *Igh* locus had no effect on somatic hypermutation, and $cE\mu^{\Delta/\Delta}$ mice seemed to have normal somatic hypermutation although the number of B cells in these mice were rare (Morvan et al. 2003; Perlot et al. 2005). The mechanism that specifically recruits somatic hypermutation machinery to the *Igh* locus is still a fundamental question to be addressed.

What is the function of Eμ after V_H gene assembly – the question addressed in this study

Previous mouse models have demonstrated Eμ's vital role in V_H gene assembly, but the $V_HD_HJ_H$ recombination problem on an Eμ-deficient Igh allele has made study of the function of Eμ thereafter difficult. In this study, in an attempt to address the question "what is the function of Eμ after V_H gene assembly", we developed a V_H knock-in, Eμ knock-out mouse model to circumvent the $V_HD_HJ_H$ recombination problem. We were then able to study the effect of Eμ deletion in several processes subsequent to V_H assembly, such as somatic hypermutation.

As discussed earlier, Eμ is required for efficient $V_HD_HJ_H$ assembly. In early knock-out studies, deletion of Eμ so dramatically impeded V-DJ on the mutant allele that heterozygous mutant B cells almost entirely rearranged and expressed only the wild-type allele (Chen et al. 1993b; Serwe and Sablitzky 1993; Sakai et al. 1999b). This made these models unsuitable for analyzing functions of Eμ after V_H

gene assembly was complete. In more recently generated mice with germline deletions of cEμ, B cell development was greatly impaired such that pre-B, immature B, and mature B cell populations in the bone marrow were reduced to less than 10% wild-type levels. Despite the profound impairment in V_H gene assembly and the subsequent deficiency in B cells in these animals, some cells did undergo full V_H gene assembly and eventually gave rise to mature B cells. There appeared to be some expansion of B cells in the periphery, but spleens were ~1/2 normal size and the proportion of B cells in these small spleens was considerably reduced (1/3-1/2 wild-type) (Perlot et al. 2005; Afshar et al. 2006). While analysis of these B cells might provide some information about Eμ's function in late stages of B cell development, there is the concern that the rare B cells able to circumvent the block to V_H gene assembly might have suffered a compensatory mutation(s) that allowed for both cEμ-independent V_H gene assembly and cEμ-independent B cell development. In addition, the scarcity of B lineage cells with successfully assembled V_H gene in bone marrow and periphery, accompanying the lack of wild-type allele in these B cells, greatly limited the analysis of various events following V_H assembly, such as allelic exclusion. Consequently, Eμ's function in B cell after V_H gene assembly remains to be elucidated.

In the present study, we generated mice bearing a modified *Igh* allele that lacked Eμ but contained a fully-assembled V_H upstream of the constant region (C_H) gene cluster (Figure 1.4, B1-8iΔEμ^a allele). When this study was initially proposed, it was not clear whether and when this modified *Igh* allele would be expressed in developing B cells. But based on the previous reported activity of 3'RR in mature B

Figure 1.4 V_H knockin Eμ knockout experimental system

Igh$^{a/b}$ = the germline configuration of the wild-type *Igh* allele (a or b allotype)

B1-8iΔEμ^{a} = a modified *Igh* allele after V_H knockin and Eμ knockout (derived from a allotype *Igh* allele)

B1-8i^{a} = another modified *Igh* allele with the same V_H knockin as in the B1-8iΔEμ^{a} allele, but Eμ is retained (also derived from a allotype *Igh* allele)

Figure 1.4 V_H knockin Eμ knockout experimental system

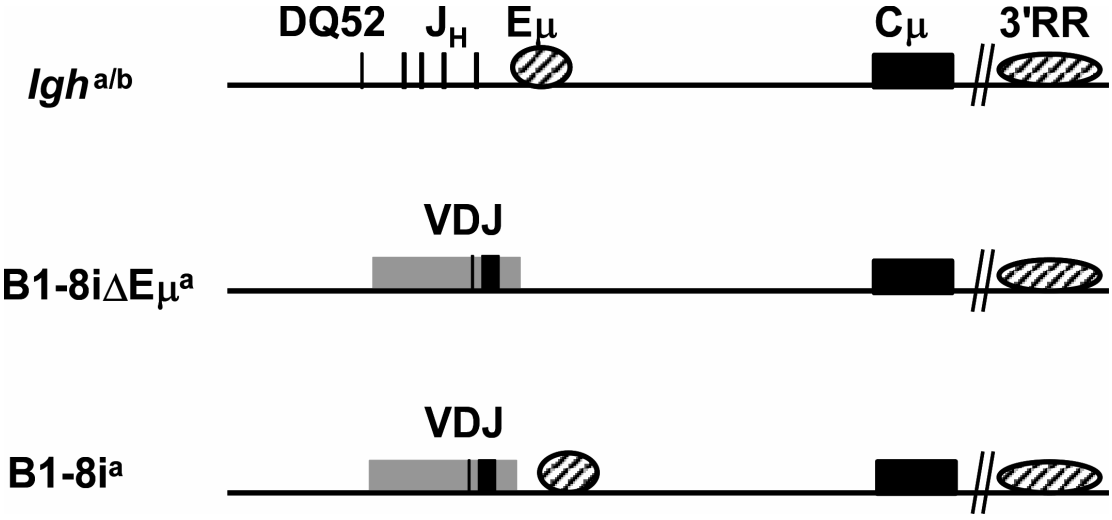

cells and expression of the Eμ-deficient *Igh* allele in a plasma cell line (9921), it seemed likely that this Eμ-deficient allele would be expressed at least in late stages of B cell development. Therefore, our initial plans were to focus on the effect of Eμ deletion on the SHM process which takes place after B cell activation. However, if this modified *Igh* allele were active early, the study of an expressed, Eμ-deficient *Igh* allele in developing B cells could be achieved for the first time, which would provide new information about Eμ's function during B cell development.

Chapter 2: Materials and Methods

I. Generating B1-8iΔEμ mice

The targeting vector used in these experiments was derived from the B1-8iVDJ targeting vector used by others (Sonoda et al. 1997). An ~0.8 kb NotI-ClaI fragment that served as the 3' homology arm for the B1-8iVDJ targeting vector (to generate B1-8i mice) was replaced with a 1.4kb sequence that lies between Eμ and Sμ (Nucleotides 3880-5295, Genbank sequence J00440). A ClaI-NotI fragment containing this sequence was generated by polymerase chain reaction (PCR), using DNA from the 129P2/OlaHsd-derived ES (E14.1) cell line as template. Primers used were:

5'CTCATCGATTCGGTTGAACATGCTGGTTG3' (ClaI site underlined) and

5'CTCGCGGCCGCAGTGTAGGCAGTAGAGTTTA3' (NotI site underlined).

Like the original B1-8iVDJ targeting vector (kindly provided by Werner Muller, University of Koln), the assembled B1-8V_H gene in the B1-8VDJΔEμ vector included ~2kb natural, 5' flanking DNA, and the 5' homology arm was comprised of 9kb of DNA lying immediately upstream of D_HQ52 in the murine *Igh* locus (Reth et al. 1978; Bothwell et al. 1981). The B1-8V_H gene carried a TGT to TGC silent mutation at codon 92 to prevent V_H replacement events (Sonoda et al. 1997).

The B1-8VDJΔEμ targeting vector was used to transfect embryonic stem cell line E14.1, and three clones were isolated that carried the expected

insertion/deletion (Gene Targeting Facility, The Rockefeller University). Cell clones were screened by genomic Southern blot to identify those that had undergone the expected homologous recombination event. As diagrammed in the maps of Figure 3.1, the expected result was insertion of ~3.4 kb (neo^R gene and B1-8V_H) and deletion of ~3.7 kb (including D_HQ52, all of the J_H gene segments and Eμ.

Appropriately targeted E14.1 clones were used to generate chimeric mice (Transgenic Service Laboratory, The Rockefeller University) and these were then mated to the C57BL/6J mouse strain. Successful germline-transmission was achieved in chimeric mice made from one of the targeted ES cell lines. Positive offspring (heterozygous for the *neo*^{R}-B1-8iΔEμ allele) were mated to EIIa-cre mice (C57BL/6J background) (Lakso et al. 1996) to induce deletion of the neomycin resistance gene (EIIa-cre mice were kindly provided by Heiner Westphal, National Institute of Child Health and Human Development, NIH). The resulting mouse line was designated B1-8iΔEμ.

II. Southern Blots

Genomic Southern blot analyses were carried out as previously described (Zhang et al. 2007). Briefly, ~20μg restriction enzyme-digested genomic DNAs were size-fractionated on 0.8% agarose gels and the DNA transferred to nylon membrane (Cat no. 10415296, Schleicher and Schuell BioScience, Inc., Keene, NH). Blots were hybridized with ^{32}P-labeled probes generated by the random

priming method (MegaPrime™, cat no. RPN 1605, Amersham, Arlington Heights, IL).

Probe A (Figure 3.1): A 1.2kb XhoI-HindIII fragment cloned from the B1-8iVDJ targeting (nucleotides 25622029-25623228, GenBank NT_166318.

Probe B (pBS-CμBamHI): 724bp sequence that begins upstream of Cμ and covers C_H1 and ~1/2 of C_H2 (nucl. 1214283-1215005, 129/SvJ Contig NT_114985). Probe was generated by PCR, using E14.1 ES cell DNA as template. Primers used were:

CμU1: 5'CAA GGA AAT AGC AGG GTG TAG3'

CμD1: 5'CTT TGT TCT CGA TGG TCA CC3'

Probe C (V-D interval) (Figure 3.9): A 1056 bp sequence that lies ~ 73 kb upstream of the most distal D gene fragment DFL16.1, and ~ 25 kb downstream of the most proximal V gene fragment V_H81X (nucl.7471-8526, GenBank AC073553). Probe generated by PCR from C57BL/6 mouse genomic DNA using the following primers:

E1f: 5'CATCCAGATACAGCACTCCCTTGTGTC3'

E1r: 5'GAAGGCCAGGACCAAGGATTGAATAC3'

Probe D (Figure 3.9): 1550 bp sequence derived from a region ~70 kb 3' of the hs4 element within the *Igh* 3' Regulatory Region (3'RR) (nucl. 25343803-25345356, C57BL/6 Contig., NT_166318). Probe generated by PCR from C57BL/6J mouse genomic DNA with the following primers:

Df: 5'CTGAAGTTGGATGTAGGCCTGAAACTG3'

Dr: 5'CCTCCCAATGCTAAGTAGAAACAGACG3'

J_H4-probe (Figure 3.10): 156 bp probe for J_H4 (nucl. 134365-134520, GenBank Acc. #AC073553), used to detect DJ and VDJ rearrangements on the *Igh*^{b} allele. Probe was generated by PCR with the following primers:

JH4f: 5'CTATGGACTACTGGGGTCAAGGAAC3'

JH4r: 5'CAACTTCTCTCAGCCGGCTC3'

hs4 probe: 601 bp probe for the hs4 element of the *Igh* 3'RR (nucl. 25418984-25419584, C57BL/6J Contig., NT_166318). Generated by PCR, using C57BL/6J genomic DNA as template. Primers described below under *polymerase chain reaction*.

III. Flow-cytometry

Single-cell suspensions prepared from bone marrow and spleen were treated with ACK lysis buffer (0.15 M NH_4Cl, 10 mM $KHCO_3$, 0.1 mM EDTA, pH 7.3) to lyse erythrocytes before use. Cells from the peritoneal cavity were recovered by flushing the cavity with cold RPMI-1640 media (Mediatech, Inc., Herndon, VA, Cat#10-040-CV), containing 5% bovine calf serum (Hyclone, http://www.hyclone.com, Cat#SH30073.03). For analyses, 10^6 cells were incubated at 4℃ for 15 minutes in staining buffer (1X PBS, 5.6mM Glucose, 0.1% BSA, 0.1% NaN_3) with various monoclonal antibodies obtained from BD Biosciences Pharmingen (San Diego, CA), except where indicated, and conjugated to: fluorescein-isothiocyanate (anti-mouse CD3ε, Cat#553067; anti-IgM, Cat#553408; anti-mouse IgM^b, Cat#553520; anti-IgD, Cat#02214D; anti-mouse CD21, Cat#553818), phycoerythrin (anti-mouse IgM^a, Cat#553517;

anti-mouse CD23, Cat#553139; anti-mouse CD43, Cat#553271), allophycocyanin (anti-mouse B220, Cat#553092; anti-mouse CD5, Cat#550035), or biotin (anti-mouse IgM^b, Cat#553519; anti-mouse IgM^a, Cat#553515; anti-mouse IgD, Southern Biotech Cat#1120_08). Cells were then washed in washing buffer (1X PBS, 5.6mM Glucose, 0.1% NaN_3) and biotin-conjugated monoclonal antibodies were revealed with streptavidin-allophycocyanin (Pharmingen, Cat#554067) or streptavidin-phycoerythrin (Pharmingen, Cat#13025D). In most cases, propidium iodide was added before analyses to exclude dead cells. Side and Forward Scatter were used to gate on lymphocytes. Flow cytometry analyses were performed either on a FACScan™, FACSCalibur, or FACSVantage™ (BD Biosciences, San Jose, CA); all cell sorting was done with the FACSVantage™. For flow cytometry analyses and sorting of immature, bone marrow B cells, $B220^+$ cells were first enriched by positive magnetic selection with the MACS™ B220-microBeads kit (Miltenyi Biotech, www.miltenyibiotec.com, Germany, Cat#130-049-501). Data were acquired with CellQuest or Pro CellQuest (associated with the FACS™ instruments) and then further analyzed with FlowJo software (Tree Star, Inc., Ashland, OR).

IV. Polymerase Chain Reactions (PCR)

1. To genotype mice:

All genotyping PCR reactions were carried out for 40 cycles with an annealing temperature of 60℃. PCR kits with HotStar Taq polymerase were used

(Qiagen; www1.qiagen.com; Cat#203205), and the manufacturer's protocol followed.

To confirm inheritance of the targeted *Igh*^{a} allele, three primers were combined to generate two PCR products, one derived from the wild-type *Igh*^{b} locus (322bp) , and the other from the targeted *Igh*^{a} locus (848bp). The PCR products generated by these three primers (#4, #8, and #2) overlap the region of VDJ insertion. The primer sequences were:

#2: 5'CAGAGGGAGTTCACACAGAGCATG3' (within the 3' homology region of B1-8iΔEμ, nucl. 136031-136054, GenBank AC073553)

#4: 5'TCTTTACAGTTACTGAGCACACAGGAC3' (Immediately 5' of the leader exon of B1-8V_H, nucl. 312629-312655, GenBank BN000872)

#8 (Eμ): 5'CTTCCCTCTGATTATTGGTCTCCATTC3' (nucl. 135733-135759, GenBank AC073553)

To confirm neo^r deletion in progeny of mice mated to the EIIa-cre transgenic line, two primers (#9 and #10) were used that annealed only to the targeted *Igh*^{a} alleles. These primers generated an ~1500bp PCR product from the Neo^{r}B1-8iΔEμ^a allele (before neo^r deletion) and a 400bp product from the B1-8iΔEμ^a allele (after neo^r deletion).

#9: 5'CCCACCATCACAGACCTTTCTCCATAG3' (within the 5' homology region of the targeting vectors, nucl. 132108-132134, GenBank AC073553)

#10: 5'CT<u>G</u>AGGGCAGCAGTACAATGA<u>T</u>GAGTC3' (within the 5' flank of B1-8V_H and ~ 280 bp 3' of loxP-flanked neo^r. Primer differs by two nucleotides (underlined) from nucleotides 311488-311514, GenBank BN000872)

In order to genotype mice carrying B1-8i^{a} allele, two additional primers were used (Figure 3.3):

E3HR: 5'CTCCACCAACACCATCACACAGATTC3' (with the 3' homology region of targeting vector to generate B1-8i mice (Sonoda E1997); complementary of nucl. 134588-134613, GenBank AC073553)

Probe-J_H4: 5'CTATGGACTACTGGGGTCAAGGAAC3' (within J_H4, nucl. 134365-134389, GenBank AC073553)

In order to distinguish between "a " and " b" allotype *Igh* alleles, another two primers were used (Figure 3.7):

b_only_F:5'CTGTGACGAAAGGATGGACCATCTAG3' (~ 9kb upstream of DQ52, nucl. 122946-122971, GenBank AC073553)

b_only_R:5'CCAAGACCACTACCATGTGGATGAC3' (~ 9kb upstream of DQ52, complementary to nucl. 123538-123562, GenBank AC073553)

In order to distinguish Rag1+ and Rag1- mice, another two primers were used (Figure 3.17):

Rag1-F; 5'CAAGCGACAAAGCAGTTCACCAAG3' (nucl.4993-5016, GenBank NC_000068)

Rag1-R: 5'GCTTCTCACTCACATCCCCCATTC3' (complementary to nucl. 6508-6531, GenBank NC_000068)

2. To analyze Igh gene rearrangements in isolated B-lineage cells:

A protocol described previously (Perlot et al. 2005) was followed with slight modification. Briefly, genomic DNA was isolated by conventional procedures from

sorted cells. Alternatively, cells were resuspended in 10mM Tris-HCl, pH 8.0; 0.1mM EDTA (50μl/ per 10^5 cells), proteinase K was added to a concentration of 0.5mg/ml, and the cells were then incubated for 2.5 hours at 50℃, followed by denaturation at 95℃ for 10 minutes. Serial dilutions of the purified DNA (or cell lysates) were used as template to specifically amplify DJ and VDJ rearrangements derived only from the wild-type *Igh*^{b} allele. Allele-specificity was achieved by using a 3' primer that derived from sequences 3' of J_H4 and that are missing on the targeted *Igh*^{a} allele of both B1-8i and B1-8iΔEμ mice. The 5' primers used in these analyses were "degenerate" primers that were designed to anneal to the D_H genes and the following V_H gene families:

D_H family primer (D_HL):

5'GGAATTCGMTTTTTGTSAAGGGATCTACTACTGTG3'. This is a degenerate primer that anneals to most murine D_H sequences (Schlissel et al. 1991)

D_HQ52: 5'CCACAGGCTCGAGAACTTTAGCG3'. This primer anneals to the most J_H-proximal murine D_H sequence, DQ52 (Perlot et al. 2005).

V_HJ558 family primer:

5'GCGAAGCTTARGCCTGGGRCTTCAGTGAAG3' (Perlot et al. 2005)

V_HQ52 family primer:

GCCAAGCTTCTCACAGAGCCTGTCCATCAC (Perlot et al. 2005)

V_H7183 family primer:

GCGAAGCTTGTGGAGTCTGGGGGAGGCTTA (Perlot et al. 2005)

Promiscuous V_H primer:

GGGAATTCGAGGTGCAGCTGCAGGAGTCTGG (Kantor et al. 1997)

Each of these primers was used in conjunction with the following primer which lies 3' of J_H4 (and cannot anneal to the targeted *Igh*^{a} alleles):

5' AGGCTCTGAGATCCCTAGACAG3' (nucl. 134530-134551, GenBank AC073553)

DNA amounts were normalized to a PCR product derived from the *Igh* locus 3'RR element hs4 present as one copy/haploid genome in all cells. Primers for hs4 were:

HS4-5': 5'CCAAAAATGGCCAGGCCTAGG3'

(nucl. 25419564-25419584, GenBank NT_166318)

HS4-3': 5'AGGTCTACACAGGGGCTCTG3'

(nucl. 25418984-25419003, GenBank NT_166318)

All PCR reactions were carried out for 30 cycles (95℃ for 30 seconds; 60 ℃ for 1 minute; 72℃ for 3 minutes). PCR products were size-fractionated on 1.5% agarose gels, blotted and probed with a ^{32}P-labeled J_H4 probe (probe described in "Southern blots").

V. Real-time, Reverse Transcriptase PCR

Total RNA was isolated with the RNeasy™ mini-prep kit (Qiagen, www1.qiagen.com, Cat#74106). Real-time RT-PCR analyses of Cμ mRNA were performed with the Qiagen QuantiTect SYBR Green RT-PCR kit (Qiagen, Cat#204243). Samples were normalized using primers and probe for mRNA from the housekeeping gene *hgprt1* (hypoxanthine/guanine phosphoribosyl

transferase) or *gapdh* (glyceraldehydes 3-phosphate dehydrogenase) and the TaqMan®, one-step RT-PCR kit (TaqMan® gene expression assay ID:Mm03024075_m1 for *hgprt1* and Mm99999915_g1 for *gapdh*; one-step RT-PCR kit, Cat#4309169, Applied Biosystems, Foster City, CA). All real-time RT-PCR analyses were performed on a 7500 Real-Time PCR System from Applied Biosystems. Data analyses were accomplished with a program supplied by Applied Biosystems (User bulletin #2; http://docs.appliedbiosystems.com/pebiodocs/04303859.pdf).

For analyses of Igμ transcripts in splenic B cells, B cells were enriched by negative selection (B cell isolation kit Cat#130-090-862; Miltenyi Biotech, www.miltenyibiotec.com, Germany). For analyses of Igμ transcripts in pre-B cells, enrichment was by positive selection for B220+ cells (B220-microBeads kit; Miltenyi Biotech).

Igμ transcripts were amplified with a 5' primer that annealed to the unique V-D-J junction sequence of V_HB1-8, and a 3' primer that annealed to a sequence within the C_H1 exon of Cμ. DNA sequences were:

junction primer: 5'CGCAAGATACGATTACTACGG3'

Cμ primer: 5'GAAGACATTTGGGAAGGACTG3'

(nucl. 140198-140218, GenBank AC073553)

VI. Somatic hypermutation analysis

Somatic hypermutation analysis in V186.2-γ1 transcripts

Three 6~10 week old wild-type mice, four 6~9 week old heterozygous B1-8iΔEμ/*Igh* mice, and three 8 week old heterozygous B1-8i/*Igh* mice, were *i.p.* injected with 100μg 4-hydroxy-3-nitrophenylacetyl chicken gamma globulin (NP-CGG) (Bioseach Technologies, Novato, CA; Cat# N-5055) in alum (PIERCE,http://www.piercenet.com; Cat#77161) according to manufacturer's instruction, and boosted 1 or 2 times 3 weeks after previous injection. One week after the last injection (the first or second boost), spleens were then harvested, and total RNA were purified with Qiagen RNeasy® Mini kit (Qiagen; Cat#74104). V186.2-γ1 transcripts, the mRNA made by the dominant responding B cells to NP, were specifically amplified by RT-PCR from total splenic RNA with primer#23 and primer#24 (VH186.2F and Cγ1R primers used in Maramatsu M2000; anneals to V_H186.2 leader sequence and Cγ1 CH1 sequence, respectively) using Qiagen one-step RT-PCR kit (Qiagen, http://www1.qiagen.com/; Cat# 210212). The temperature program for the RT-PCR reactions was: 50℃, 30minutes; 95℃, 15minutes; 30 cycles of PCR amplification (95℃ for 1 minute; 55℃ for 1 minute; 72℃ for 2 minutes) followed by 72℃ for 10 minutes and holding at 4℃. RT-PCR products were gel-purified using QIAquick gel-extraction kit (Qiagen; Cat# 28704) and cloned into pCR®4Blunt-TOPO® vector using Zero Blunt® Topo® PCR Cloning Kit (Invitrogen™, Cat# K2880-20). Positive bacterial clones were picked and cultured in 2ml LB Broth media with 50μg/ml ampicillin over night at 37℃.

Plasmids were purified by FastPlasmid® Mini kit (5 prime http://www.5prime.com; Cat# 2300010) or Wizard® Plus SV Minipreps kit (Promega, http://www.promega.com; Cat# A1460). Plasmid concentration was determined on BECKMAN DU® Series 600 spectrophotometer. Sequence of the PCR product inserts was determined in both direction with T3 and T7 sequencing primers by GENEWIZ sequencing service (http://www.genewiz.com/). Sequencing results were analyzed for somatic hypermutation.

Our RT-PCR strategy allowed the amplification of V186.2-γ1 transcripts expressed from both alleles of double producers in heterozygous B1-8iΔEμ/*Igh* mice, but we can unequivocally distinguish the transcripts derived from wild-type allele from those derived from the B1-8iΔEμ allele based on a unique VDJ junction and one engineered mutation in the frame-work region 3 of V_HB1-8 that is knocked in. Only confirmed sequencing data by two-direction sequencing was used in the final mutation analyses. Similar results were obtained by analyzing sequences cloned from mice with 1 or 2 antigenic boosts, therefore, these data were pooled and discussed together.

Somatic hypermutation analysis in peyer's patch germinal center B cells

Peyer's patches were isolated from the intestines of 3 month old or older mice (B1-8i^a/*Igh*^{b} mice: E46/E47, 5.5 month; E77/E78, 3 month. B1-8iΔEμ^a/*Igh*^{b} mice: D169/D170, 4.5 month; D189/D191/D193, 4 month. B1-8i^a/ B1-8iΔEμ^a mice: D151, D154, D155, 3 month; D105 8 month). Single cell suspensions were made by crushing tissues between frosted glasses slides and filtering through a 40μm

cell strainer (BD Falcon™, Cat #352340). Cells were then stained with PNA, and antibodies against B220 and CD95 (APC Rat anti-mouse B220, BD Pharmingen Cat#553092; PE Hamster anti-mouse CD95, BD Pharmingen Cat#554258; PNA-FITC, Vector Laboratories, Cat#FL-1071). Germinal center B cells ($B220^{+}CD95^{+}PNA^{high}$) were isolated by sorting. Sorted cells were lysed in 10mM Tris-HCl, pH 8.0; 0.1mM EDTA (50μl/per 10^5 cells). Proteinase K was added to a concentration of 0.5mg/ml, and the mixture was incubated for 2.5 hours at 50□ and at 95□ for 10 minutes. Cell lysates were used as DNA template for PCR cloning the DNA fragment containing the V_HB1-8 knock-in (V_H186.2-DFL16.1-J_H2) and the 214 bp intron sequence immediately following J_H2. Two primer pairs, #4 & E3HR and #4 & #2, were used to specifically amplify this region from either the B1-8i^a or B1-8iΔEμ^a allele, respectively (Figure 3.3A, 3.3B, 3.7). High-fidelity PfuUltra® Hotstart DNA polymerase (Stratagene, Cat#600390) were used. The temperature program of these PCR reactions was: 95□ for 2 minutes, 30 cycles of reaction (95□, 30 seconds; anneal, 30 seconds; 72□, 60 seconds), 10 minutes incubation at 72□, and holding at 4□. The annealing temperature was 65□ in the first cycle, and it went down to 60□ at a pace of 1□/cycle and stayed at 60□ thereafter. The PCR products were purified, cloned and sequenced as described for V186.2-γ1 cDNA clones. Somatic hypermutation was analyzed in both VH186.2 and the 214 bp intron sequence.

Sequence analysis

For each clone, sequences obtained by sequencing with T3 and T7 primers, respectively, were aligned by bl2seq program available at

http://blast.ncbi.nlm.nih.gov/bl2seq/wblast2.cgi or downloadable from http://www.ncbi.nlm.nih.gov/Ftp/. Consensus sequences of PCR product inserts were obtained. Only sequences of good quality were used in further analyses. Mutations in the variable region were analyzed by V-Quest program available at http://imgt.cines.fr/ (Brochet et al. 2008), and mutations in the intron following the variable region were identified by aligning germline sequences with consensus sequences of PCR products.

VII. Enzyme-Linked ImmunoSorbent Assay (ELISA)

Blood samples were collected from wild-type *Igh*$^{a/a}$, *Igh*$^{a/b}$, *Igh*$^{b/b}$ and mice generated by mating B1-8iΔEμ^a/I*gh*^{b} and B1-8iΔEμ^a/I*gh*^{b} mice (or mating B1-8iΔEμ^a/I*gh*^{b} and *Igh*$^{b/b}$ mice). Blood samples were centrifuged at 12000 rpm for 5 minutes, and sera (supernatant) were collected and stored at 4□. For ELISA analyses to genotype mice bearing B1-8iΔEμ^a alleles, 100μl 1μg/ml Rat anti-mouse IgM antibody (BD Pharmingen, Cat# 553405) was coated overnight at room temperature. After blocking for two hours with 200 μl blocking solution (1XPBS, 3% BSA, 0.1% NaN_3) and washing for three times with washing solution (1XPBS, 0.5% tween-20), 100μl 1:500 diluted serum samples were applied. After one hour incubation and washing for three times, 100μl 1μg/ml biotin-labeled mouse anti-mouse IgM^a antibody (mouse γ1, κ) (BD Pharmingen, Cat# 553515) or biotin-labeled mouse anti-mouse IgM^b antibody (mouse γ1, κ) (BD Pharmingen, Cat# 553519) was added, respectively, in order to detect a or b allotype IgM. After incubating for one hour and washing for three times, 100μl 1:1000 diluted

avidin-Horseradish Peroxidase (HRP) (BD Pharmingen, Cat# 554058) was applied, and incubated for one hour. After washing for three times, HRP substrates were applied and results were obtained by reading ELISA plates at 405 nm.

Chapter 3: Results and discussion: effect of Eμ-deletion on allelic exclusion

Background and Overview

Immunoglobulin heavy chain (IgH) genes are assembled through an ordered process of joining V, D, and J gene segments into a functional V region-coding sequence (VDJ recombination). A regulatory element, Eμ, lying just downstream of the J segments, was initially discovered as a transcriptional enhancer (Banerji et al. 1983; Gilles and Tonegawa 1983; Neuberger 1983), but Eμ deletion studies subsequently demonstrated that it was essential for promoting efficient VDJ recombination, as well (Chen et al. 1993b; Serwe and Sablitzky 1993; Sakai et al. 1999b; Perlot et al. 2005; Afshar et al. 2006). A model emerged in which Eμ promoted heavy chain variable (V_H) gene assembly and then served to enhance transcription of the newly-formed IgH gene.

Although recombination can theoretically occur on either or both *Igh* alleles, only one allele is expressed in individual B cells, a phenomenon termed “allelic exclusion” (Jung et al. 2006). Allelic exclusion insures that individual B lymphocytes express antigen receptors (Ig) of a single antigen-specificity, a fundamental requirement of the clonal selection theory put forth by MacFarlane Burnet over fifty years ago (Burnet 1957).

Several models have been proposed to explain allelic exclusion. In all models, it is assumed that VDJ recombination occurs at a low frequency and that two-thirds of such rearrangements result in a reading frame that cannot be translated into a full-length heavy chain (non-functional rearrangement). While these assumptions predict that cells with functional rearrangements on both alleles will be rare, they do not explain why such cells would be almost entirely absent from the normal B lymphocyte repertoire. Models to explain the absence of such cells fall into two general groups: those that invoke selective processes acting at the level of the cell and those that invoke feedback mechanisms affecting VDJ recombination itself. An early model in the former group proposed that expression of μ chains derived from both *Igh* loci would lead to toxic levels of heavy chain, thereby resulting in cell death (Wabl and Steinberg 1982). Gene targeting experiments in which both *Igh* loci were modified to carry pre-assembled V_H genes contradicted this model; in almost all B cells of these animals, both *Igh* alleles were expressed (Sonoda et al. 1997).

Studies of transformed precursor B cells and of *Igμ* transgenic mice supported an alternate, regulated model of V-DJ recombination (Alt et al. 1984; Storb 1987). In this regulated model, it was proposed that μ chain expression from a productive *Igh* allele prevents V-DJ recombination on the other, precluding development of allelically “included” B lineage cells (Mostoslavsky et al. 2004; Jung et al. 2006). In *Igμ* transgenic mice, DJ assembly is common on the endogenous *Igh* loci of mature B cells, but full VDJ assembly is rare, suggesting that early expression of the *Igμ* transgene suppresses the second step (V-DJ

recombination) in V_H gene assembly within the endogenous loci. While allelic exclusion is rarely perfect in transgenic mice (Stall et al. 1988), it has been thought this results from the variable levels and/or timing of transgene expression as compared to IgH genes lying in their natural position within the *Igh* locus. Consistent with the "level" hypothesis, doubling a multi-copy Ig transgene (by mating) led to both higher transgene expression levels and greater allelic exclusion than when the same transgene multimer was left "hemizygous" (Watanabe et al. 1999). Allelic exclusion appeared virtually complete when a pre-assembled variable region gene was inserted into one allele of the natural *Igh* locus (by gene targeting) (Sonoda et al. 1997).

The μ heavy chain encoded by a newly-formed Igμ gene assembles with "surrogate" light chain (composed of VpreB1/2 and λ5) and with the signaling molecules Igα and Igβ to form a pre-B cell receptor (pre-BCR) (Clark et al. 2005; Martensson et al. 2007). It is through the pre-BCR that developing B cells "sense" successful assembly of an Igμ gene on one allele and signal arrest of any further assembly on the other allele (reviewed in Papavasiliou et al. 1997; Martensson et al. 2007). Even within the context of this feed-back regulation, there would be the opportunity for developing cells with two functional Igμ alleles, if gene assembly and Igμ-mediated signaling were sufficiently separated in time.

In the present study, we provide evidence that a breach of allelic exclusion, at the level of V_H gene assembly, occurs quite regularly in developing B cells but, under normal circumstances, this results in few, if any, detectable double producers. When the first allele to assemble a V_H gene lacks Eμ, however, there is

a dramatic increase in double-producers both within the bone marrow and among peripheral B cells. This striking effect is not the result of a failure to inhibit V_H assembly on the second chromosome; rather, the change takes place at the pre-B to immature B cell transition. One of Eμ's functions, subsequent to VDJ recombination, is to facilitate the survival of newly-generated B cells expressing a single *Igh* allele. In its absence, a second checkpoint for allelic exclusion is breached.

Figure 3.1 Targeting strategy used to generate B1-8iΔEμ mice.

Igh^b: partial restriction endonuclease map of the wild-type *Igh*^{b} locus. Thick vertical bars delineate exons for DQ52, J_{H1-4}, and the first two exons of the μ constant region (Cμ). Sμ = μ switch region; hatched oval = Eμ. B = BamHI, H = HindIII. *Igh*^{a}: partial restriction map of the unmodified *Igh*^{a} locus. Shaded boxes (5'H and 3'H) = regions of homology with targeting vector (below). Targeting vector: LoxP*Neo*^{R} = loxP-flanked neomycin-resistance gene (white arrowheads = loxP sites), B1-8V_H promoter region (shaded) and coding sequences (thick vertical lines). *HSV-TK* (black box) = negative selection gene for homologous recombination. neo^{R}B1-8iΔEμ^a: predicted structure of *Igh*^{a} allele after homologous recombination. B1-8iΔEμ^a: predicted structure of modified *Igh*^{a} allele, after neo^R gene deletion. Regions corresponding to the DNA probes used in genotyping genomic Southern in Figure 3.2 are shown (probes A and B).

Figure 3.1 Targeting strategy used to generate B1-8iΔEμ mice.

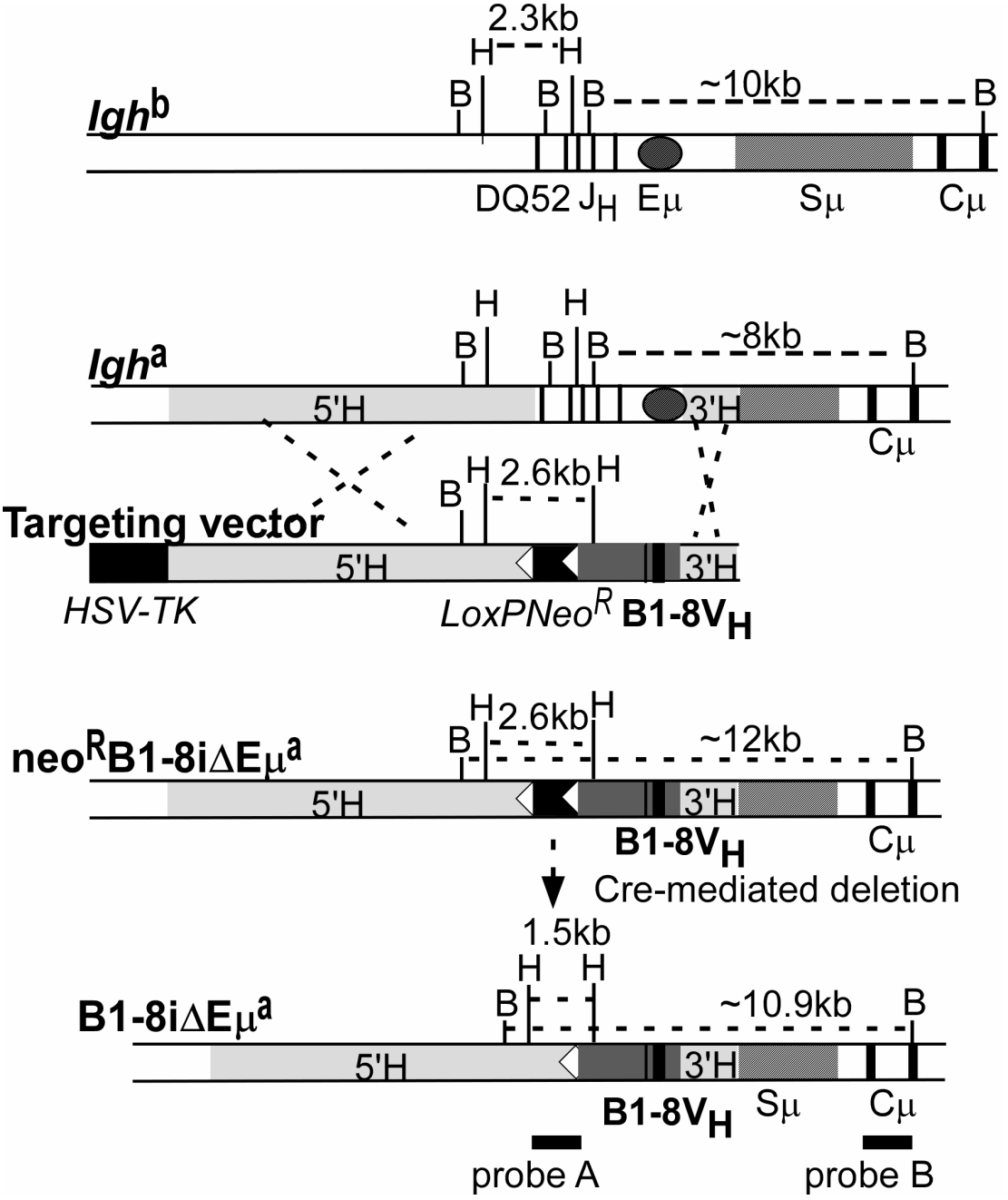

Results

1. Generating a mouse strain that carries an Eμ-deficient, V_H-assembled Igh^a allele

Because VDJ recombination is rare on an allele lacking Eμ, B cell development is dramatically impaired in mice homozygous for this deletion (Perlot et al. 2005; Afshar et al. 2006). This has made it difficult to assess Eμ's functions subsequent to V_H gene assembly, particularly since it is possible that special circumstances (e.g. compensatory mutations) are required to generate the assembled IgH genes found in such animals. In order to circumvent this problem and also to study the behavior of an Eμ-deficient allele in competition with a wild-type one, we generated mice bearing an *Igh* allele that lacked Eμ but included a fully-assembled V_H upstream of the constant region (C_H) gene cluster (Figure 1.4). Both core Eμ and flanking matrix attachment regions (MARs) were deleted, each of which has been shown necessary for the expression of Igμ transgenes in developing B cells (Cockerill et al. 1987; Forrester et al. 1994).

For these experiments, a 3.7kb region, including the most proximal D_H gene segment (DQ52), all the J_H gene segments and Eμ, was replaced, by gene-targeting, with a loxP-flanked neomycin resistance gene (neo^r) and a fully assembled variable region (V_H) gene (see targeting strategy, Fig. 3.1). The V_H gene and ~2kb of 5' flanking sequence were isolated from the B1-8 hybridoma which produces a 4-hydroxy-3-nitrophenyl acetyl (NP)-binding antibody (Reth et al. 1978; Bothwell et al. 1981). Embryonic stem cells (E14.1 line) were transfected

with the targeting vector, and clones undergoing the desired gene replacement were recovered by drug-selection.

Igh locus structure in the ES clones and the resulting mouse line from one of these ES clones was confirmed by genomic Southern blot (Figure 3.2 and data not shown). As shown in Figure 3.2A, an 8kb BamHI fragment spanning Eμ and the first two exons of Cμ in the *Igh*^{a} germline locus was replaced with a 12kb BamHI fragment in the targeted locus of neo^{r}B1-8iΔEμ^{a}/*Igh*^{b} heterozygous mice. The 12kb BamHI fragment from this mutant allele was easily distinguished from the 10kb BamHI fragment derived from the wild-type *Igh*^{b} allele of these mice (Fig 3.2A).

neo^{r}B1-8iΔEμ^{a}/*Igh*^{b} mice were mated to the EIIa-*cre* transgenic mouse line (Lakso et al. 1996) in order to remove loxP-flanked *neo*^{r} from the mutant allele. Progeny that had undergone *neo*^{r} deletion were further mated to wild-type C57BL/6 mice to ensure that deletion had occurred in the germline. As shown in Figures 3.2B, a DNA probe (probe A) derived from the region upstream of DQ52 (and, therefore, upstream of the induced deletion), detects a 2.3kb HindIII fragment in wild-type *Igh*^{a} and *Igh*^{b} loci, and a 2.6kb HindIII fragment from the modified *Igh*^{a} locus (left panel). This 2.6 kb HindIII fragment is reduced to 1.5kb upon *neo*^{r} deletion (right panel). Deletion of *neo*^{r} from the targeted locus was also confirmed by the decrease in size of the BamH I fragment detected by probe B from 12kb to ~10.9 kb (Figure 3.2A *right panel*, lane B1-8iΔEμ$^{a/a}$.) In addition, deletion of *neo*^{r} from the targeted locus was confirmed by polymerase chain reaction (PCR), using primers (#9 and #10) that flanked *neo*^{r} (Figure 3.3A). As

Figure 3.2 Genomic Southern blot to identify the neo^{R}B1-8iΔEμ^{a} allele and the B1-8iΔEμ^{a} allele.

(A) *Left*: Southern blot of liver DNA from wild-type F_1 mouse (*Igh*$^{a/b}$) and mouse heterozygous for the modified *Igh*^{a} allele before neo^{R} deletion (neo^{R}B1-8iΔEμ^{a}/*Igh*^{b}); *Right*: Southern blot of liver or tail DNA from wild-type 129 (*Igh*$^{a/a}$), C57 (*Igh*$^{b/b}$), progeny of a (B1-8iΔEμ^{a}/*Igh*^{b} X B1-8iΔEμ^{a}/*Igh*^{b}) mating, and a (neo^{R}B1-8iΔEμ^{a}/*Igh*^{b} X neo^{R}B1-8iΔEμ^{a}/*Igh*^{b}) mating. The genotype of each sample is labeled on the top, the size of DNA is labeled on the left, the corresponding allele for each band is labeled on the right, and the restriction enzyme used to digest genomic DNA and the probe used to hybridize are labeled under the blots. * the *Igh*^{b} allele and B1-8iΔEμ^{a} allele are not well distinguished under these conditions, and both alleles could be present in the marked progeny based on Mendelian genetics. (B) *Left*: Southern blot of liver DNA from wild-type 129 (*Igh*$^{a/a}$), C57 (*Igh*$^{b/b}$), and mouse heterozygous for the modified *Igh*^{a} allele before neo^{R} deletion (neo^{R}B1-8iΔEμ^{a}/*Igh*^{b}); *Right*: Southern blot of liver DNA from wild-type F1 mice (*Igh*$^{a/b}$), mice heterozygous for the modified *Igh*^{a} allele before neo^{R} deletion (neo^{R}B1-8iΔEμ^{a}/*Igh*^{b}) or after neo^{R} deletion (B1-8iΔEμ^{a}/*Igh*^{b}). Blots are labeled as in (A). Note: *Igh*$^{a/b}$ = *Igh*^{a}/*Igh*^{b}; *Igh*$^{a/a}$ = *Igh*^{a}/*Igh*^{a}; *Igh*$^{b/b}$ = *Igh*^{b}/*Igh*^{b} ;B1-8iΔE$\mu^{a/a}$ = B1-8iΔEμ^{a}/B1-8iΔEμ^{a}; neo^{R}B1-8iΔE$\mu^{a/a}$ = neo^{R}B1-8iΔEμ^{a} /neo^{R}B1-8iΔEμ^{a}

Figure 3.2 Genomic Southern blot to identify the neo^{R}B1-8iΔEμ^{a} allele and the B1-8iΔEμ^{a} allele

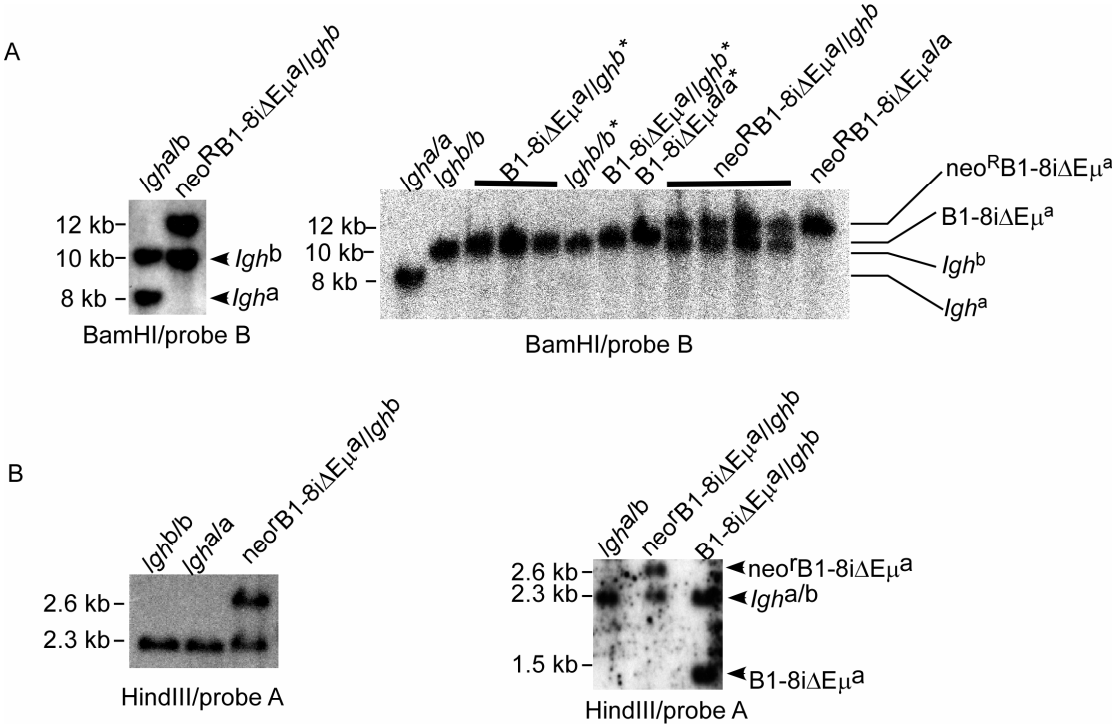

Figure 3.3 PCR reactions to identify B1-8i^{a} and B1-8iΔEμ^{a} alleles.

(A) Primers used in genotyping PCR reactions. A partial map of the I*gh*$^{a/b}$, B1-8i^{a}, B1-8iΔEμ^{a} alleles is shown. DQ52, J_H1-4 in the wild-type allele, and the B1-8 V_H coding sequences in both B1-8i^{a} and B1-8iΔEμ^{a} alleles are shown as thick black vertical lines. Hatched boxes: 5'H is the 5' homology arm used to generate both B1-8i^{a}, B1-8iΔEμ^{a} alleles, 3'H(B1-8i^{a}) is the 3' homology arm used to generate the B1-8i^{a} allele (Sonoda et al. 1997), and 3'H(B1-8iΔEμ^{a}) is the 3' homology arm used in the present study to generate the B1-8iΔEμ^{a} allele. The location of Eμ is depicted by a horizontal line labeled as "Eμ". The location and orientation of the following primers are shown on the map by bended arrows: primer #9, #10, #4, Junction, JH4_probe, E3HR, #8, #2. (B) Primer combinations used in PCR reactions to distinguish *Igh*$^{a/b}$, B1-8i^{a}, and B1-8iΔEμ^{a} alleles. (C) DNA template 1-5 were analyzed by PCR reactions for Igh$^{a/b}$, neo^{R}B1-8iΔEμ^{a}, and B1-8iΔEμ^{a} alleles using either primer combination "#4, #8, #2" (*upper*) or combination "#9, #10" (*lower*). (D) DNA template 1-3 were analyzed by PCR for I*gh*^{b} and B1-8i^{a} alleles using primer combination "Junction, Probe_JH4, E3HR", and DNA template 4-5 were analyzed by PCR for I*gh*^{b} and B1-8iΔEμ^{a} alleles using primer combination "Junction, #8, #2". In (C) and (D), the genotype of each sample is labeled under the gels. Note: *Igh*$^{a/b}$ = *Igh*^{a}/*Igh*^{b}; *Igh*$^{a/a}$ = *Igh*^{a}/*Igh*^{a}; *Igh*$^{b/b}$ = *Igh*^{b}/*Igh*^{b}; B1-8iΔE$\mu^{a/a}$ = B1-8iΔEμ^{a}/B1-8iΔEμ^{a}; neo^{R}B1-8iΔE$\mu^{a/a}$ = neo^{R}B1-8iΔEμ^{a} /neo^{R}B1-8iΔEμ^{a}.

Figure 3.3 PCR reactions to identify B1-8i^{a} and B1-8iΔEμ^{a} alleles

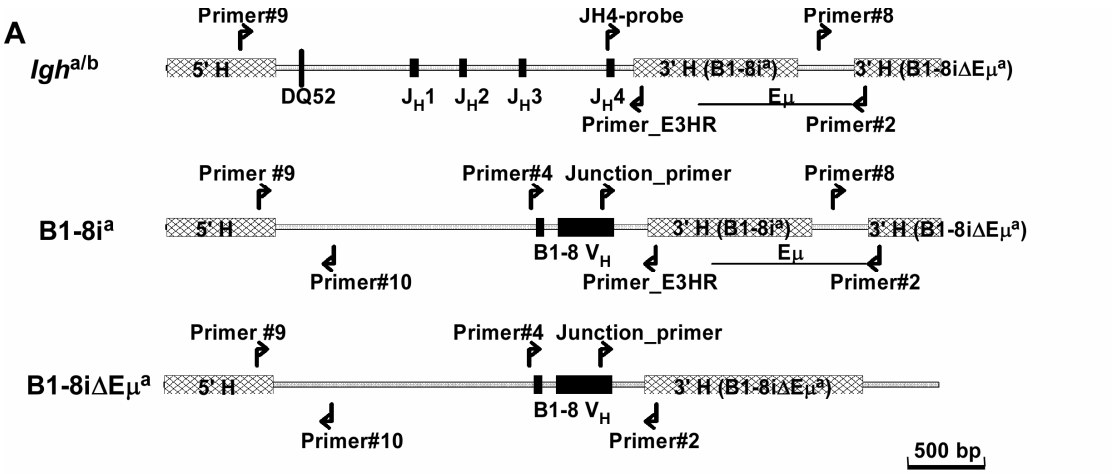

B PCR primers for genotyping B1-8i^{a} and B1-8iΔEμ^{a} mice

Primer-combinations	primer pair	product size	*Igh* $^{a/b}$	B1-8i^{a}	B1-8iΔEμ^{a}
#9, #10	#9 & #10	~400 bp	-	+	+
#4, #8, #2	#4 & #2	848 bp	-	-	+
	#8 & #2	322 bp	+	+	-
Junction, #8, #2	Junction & #2	387 bp	-	-	+
	#8 & #2	322 bp	+	+	-
#4, Probe-JH4, E3HR	#4 & E3HR	834 bp	-	+	-
	Probe-JH4 & E3HR	249 bp	+	-	-
Junction, Probe-JH4, E3HR	Junction & E3HR	373 bp	-	+	-
	Probe-JH4 & E3HR	249 bp	+	-	-

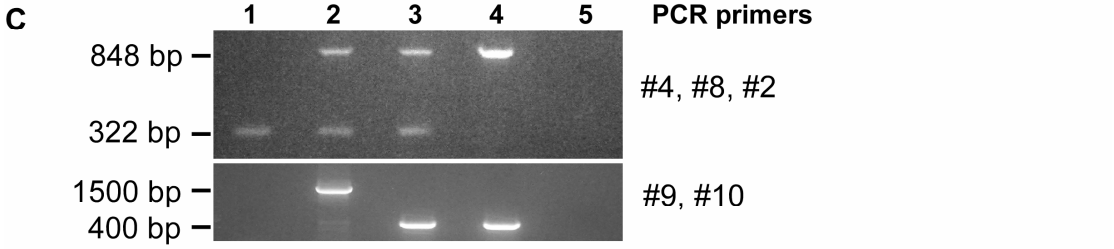

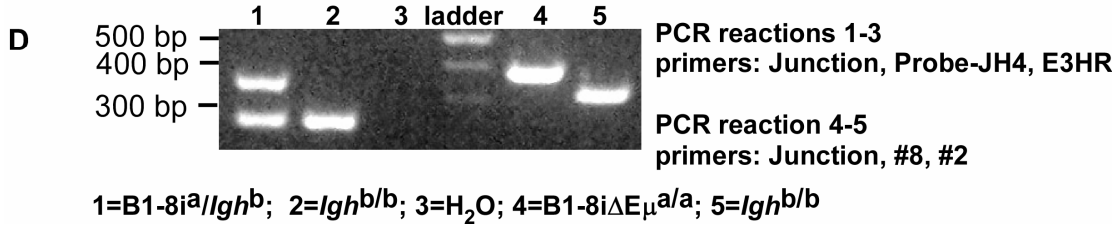

Figure 3.4 ELISA used to genotype mice bearing B1-8i$\Delta E\mu^a$ alleles.

B1-8i$\Delta E\mu^a$/*Igh*^{b} mice were found to contain both a and b allotype IgM in serum. Therefore ELISA to detect a and b allotype IgM was used to distinguish I*gh*$^{b/b}$, B1-8i$\Delta E\mu^a$/I*gh*^{b} and B1-8i$\Delta E\mu^{a/a}$ mice. For each serum sample, two reactions (duplicates) to detect either IgM^a or IgM^b were done avoid false positive, and results of both reactions are shown in the graph. Note: *Igh*$^{a/a}$ = *Igh*^{a}/*Igh*^{a}; *Igh*$^{a/b}$ = *Igh*^{a}/*Igh*^{b}*; Igh*$^{b/b}$ = *Igh*^{b}/*Igh*^{b}; B1-8i$\Delta E\mu^{a/a}$ = B1-8i$\Delta E\mu^a$/B1-8i$\Delta E\mu^a$; –Coating Ab = non-coating antibody control, PBS = non-serum control. * Sera of mice generated by mating B1-8i$\Delta E\mu^a$/I*gh*^{b} and B1-8i$\Delta E\mu^a$/I*gh*^{b} mice.

Figure 3.4 ELISA used to genotype mice bearing B1-8i$\Delta E\mu^a$ alleles.

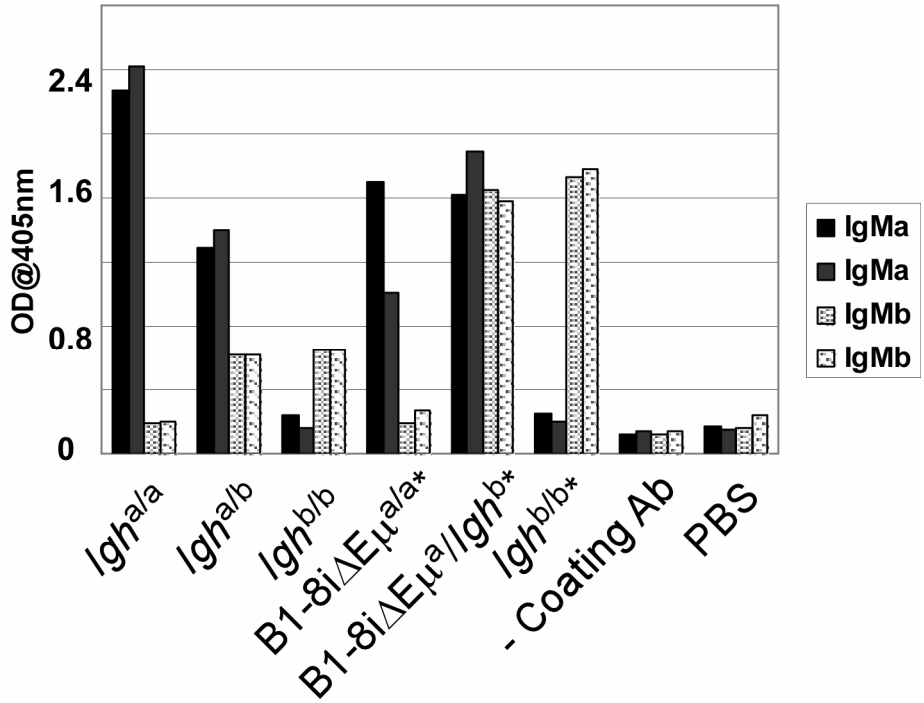

shown in Figure 3.3C (bottom panel), the PCR product was reduced from 1.5kb (sample #2) to ~0.4kb (samples #3, #4). Heterozygotes carrying the Eμ-deficient allele with assembled B1-8V_H gene (and no *neo*^{r}) were designated B1-8iΔEμ^a/*Igh*^{b}. Homozygous mutant animals were generated in brother-sister matings, and referred to as B1-8iΔEμ$^{a/a}$ mice (or homozygous B1-8iΔEμ mice).

A matched mouse strain for B1-8iΔEμ^a mice was generated previously (Sonoda et al. 1997), and it carries a modified "a" *Igh* allele with exactly the same V_H knockin but with Eμ untouched (B1-8i^a allele, Figure 1.4 and 3.3A). Since identification of the mice used for this study requires a distinction among wild-type alleles (*Igh*$^{a/b}$), the B1-8i allele, and the B1-8iΔEμ^a allele. PCR reactions were used in most genotyping experiments. The primers used in these reactions are shown in Figure 3.3A and 3.3B. A typical PCR reaction to genotype mice which could be wild-type, B1-8iΔEμ^a/*Igh*^{b}, or B1-8iΔEμ$^{a/a}$ (homozygous) mice involved the primer combination "#4, #8, #2" as shown in Figure 3.3C, or the primer combination "Junction, #8, #2" as shown in Figure 3.3D (Samples 4-5). Primer combination "Junction, probe-J_H4, E3HR" was used to distinguish wild-type alleles from the B1-8i^a allele as shown in Figure 3.3D (Samples 1-3). After the discovery that the serum of B1-8iΔEμ^a/*Igh*^{b} mice contained both a and b allotype IgM antibody, ELISAs to detect IgM^a and IgM^b were also used as a way to genotype mice that could be wild-type, B1-8iΔEμ^a/*Igh*^{b}, or B1-8iΔEμ$^{a/a}$ (Figure 3.4).

2. IgM from an Eμ-deficient allele can drive B cell development

One of the first questions that arise with respect to Eμ function following the formation of a functional IgH gene is whether transcription of the newly-formed gene is Eμ dependent. Other enhancers that can drive IgH gene transcription lie at the far 3' end of the locus, but it has not been established whether or not this regulatory region, the 3'RR, is functional immediately following IgH gene formation in pro-B cells.

If transcription of newly-formed IgH genes were Eμ-dependent, expression of the B1-8iΔEμ^a allele would be delayed until other transcription control elements (e.g. the 3'RR) became functional. Despite this delay, B cell development could proceed normally in animals heterozygous for this allele since V-D-J recombination could proceed with normal efficiency on the other, wild-type *Igh*^{b} allele. There would likely be a defect in B cell development in mice homozygous for the B1-8iΔEμ^a allele, however, since, in these mice, both *Igh* alleles would lack expression at the stage required for signaling the pro-B to pre-B transition. If, on the other hand, transcription of newly-formed IgH genes were Eμ-independent, B1-8iΔEμ^a/B1-8iΔEμ^a homozygotes would undergo normal B cell development, and, as predicted by the regulated model of V-DJ recombination, B1-8iΔEμ^a/*Igh*^{b} animals would be restricted to expression of the B1-8iΔEμ^a allele. Complete "allelic exclusion" has been reported previously, in fact, for a mouse carrying the

Figure 3.5. Spleen and bone marrow B cell profiles in homozygous B1-8i^a and B1-8iΔEμ^a mice.

(A) Flow cytometry profiles of splenic lymphocytes from adult homozygous B1-8i^a and B1-8iΔEμ^a mice, stained for B220 (B cell marker) and CD3ε (T cell marker). (B) Surface IgM^a and relative Igμ transcript levels in splenic B cells of homozygous B1-8i^a and B1-8iΔEμ^a mice. Left: histogram of splenic cells stained with antibody to IgM^a. Right: qRT-PCR results, using primers for B1-8i μ-mRNA and normalized to *hgprt1* mRNA (see Materials and Methods). μ-mRNA from B1-8i^a B cells set as 1.0; wild-type *Igh*^{b} homozygotes = negative control. (C) Bone marrow B cell subsets in homozygous B1-8i^a and B1-8iΔEμ^a mice. *Upper panels*: Bone marrow cells gated for B220+ (B-lineage) cells and analyzed for CD43 and IgM expression. *Lower panels*: Bone marrow B220+ cells analyzed for IgD and IgM. Data shown are representative of three animals of each genotype.

Figure 3.5. Spleen and bone marrow B cell profiles in homozygous B1-8i^a and B1-8iΔEμ^a mice.

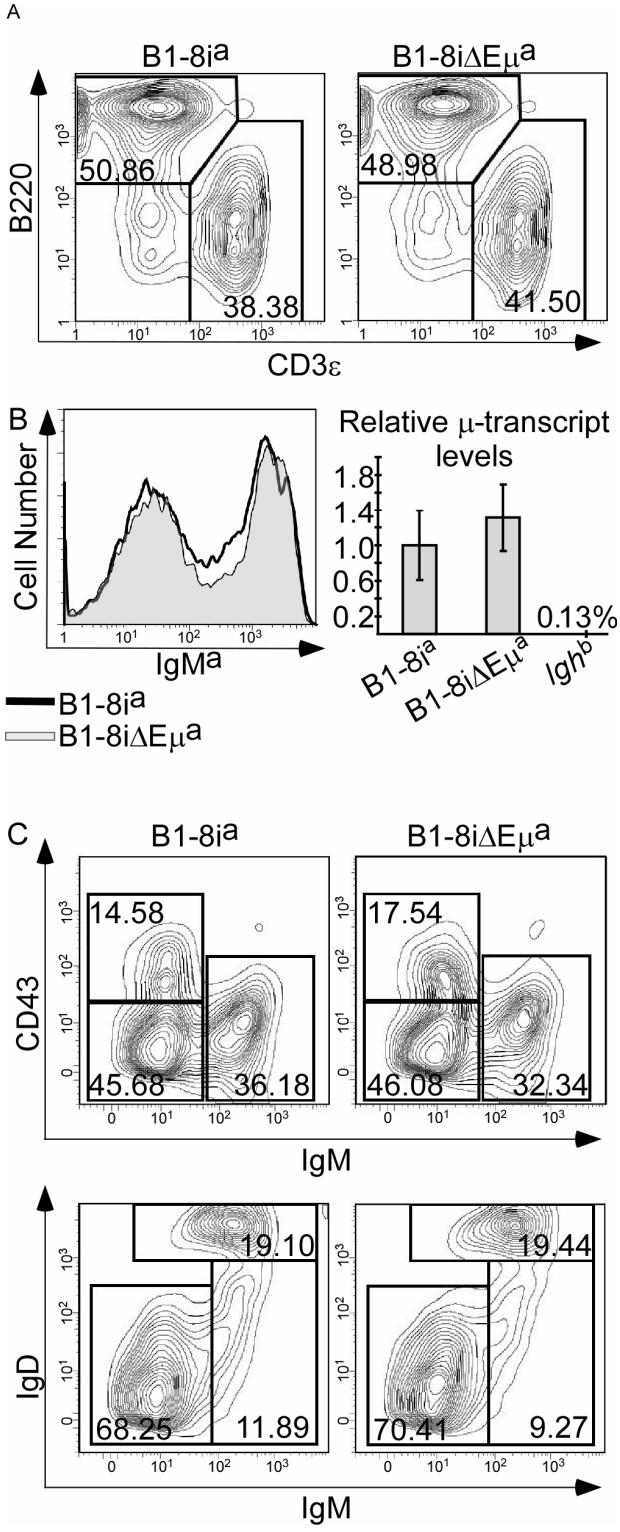

Table 3.1: Absolute cell numbers in wild-type and homozygous mutant mice. Cells recovered from bone marrow and spleen of individual mice were counted (total cells). Aliquots were stained for B-lineage markers (B220, CD43, IgD, IgM in bone marrow) and for CD3ε (T cells) and B220 (B cells) in spleen. Cell number for lymphocyte subpopulations were calculated based on total cell count and the percentage total cells comprising each subpopulation (determined by flow cytometry).

*$p < 0.001$ (vs Igh^b/Igh^b)

Table 3.1. Absolute cell numbers in wild-type and homozygous mutant mice

Genotype (homozygotes)	*Igh*^{b} (n = 3)	B1-8i^{a} (n = 3)	B1-8iΔEμ^{a} (n = 3)
Bone marrow (x 10^6)			
total cells	25.83 ± 2.84	21.83 ± 6.45	21.50 ± 1.00
lymphocytes	7.22 ± 0.24	4.94 ± 1.17	5.10 ± 0.56
B220+	4.20 ± 0.12	1.84 ± 0.44*	2.22 ± 0.37*
pro-B	0.49 ± 0.07	0.27 ± 0.06	0.35 ± 0.10
pre-B	2.09 ± 0.26	0.78 ± 0.17	0.88 ± 0.31
immature B	0.44 ± 0.05	0.21 ± 0.07	0.19 ± 0.07
mature B	0.88 ± 0.13	0.40 ± 0.14	0.53 ± 0.20
Spleen (x 10^6)			
total cells	33.00 ± 2.18	31.67 ± 4.80	36.50 ± 5.07
lymphocytes	26.85 ± 2.88	25.46 ± 4.09	29.59 ± 3.59
B cells	14.36 ± 2.68	12.97 ± 2.32	14.60 ± 0.40
T cells	9.28 ± 0.67	9.61 ± 1.35	11.16 ± 1.95

same B1-8iV_H gene (by gene replacement) as that used in the present study (Sonoda et al. 1997).

As shown in Figure 3.5A, the proportion of B cells in the splenic lymphocytes of B1-8i$\Delta E\mu^a$ homozygous animals was normal, showing no difference from that in B1-8i homozygous mice. Comparisons of multiple mice with these genotypes are summarized in Table 3.1. The level of IgM^a on the surface of resting, splenic B lymphocytes was also the same, whether the B cells' *Igh* loci contained or lacked Eμ (Figure 3.5B panel). Quantitative measurements of Igμ mRNA produced by splenic B cells were done, using real-time reverse-transcriptase polymerase chain reaction using primers that specifically detect the VDJ-μ transcripts expressed from the knock-in alleles (real-time RT-PCR; Experimental Procedures). B cells expressing Eμ-deficient genes produced as much (or more) Igμ mRNA as B cells with Eμ-containing genes. After normalizing to GAPDH mRNA, transcripts from the Eμ deficient allele were about 30% more abundant than those from the allele that retained Eμ on average (Figure 3.5B right panel).

The splenic B cell profile in B1-8i$\Delta E\mu^a$ homozygous mice suggested that B cell development was proceeding normally in these animals. Since it was possible, however, that peripheral expansion of a small precursor population was masking a central defect, we also analyzed bone marrow in these animals. As shown in Figure 3.5C, the pro-B ($B220^+/IgM^-/CD43^+$), pre-B ($B220^+/IgM^-/CD43^-$), and immature/mature B cell ($B220^+/IgM^+/CD43^-$) subsets were found in similar proportions in homozygous B1-8i^a and B1-8i$\Delta E\mu^a$ animals (Figure 3.5C, upper

panels; also see Table 3.1). When antibodies to IgD and IgM were used to distinguish immature (IgM^+/IgD^-) from mature B cells (IgM^+/IgD^+) in the bone marrow, these were also found at comparable levels (Figure 3.5C, lower panel). The total number of B-lineage cells in the bone marrow of these homozygous mutant mouse lines was reduced with respect to wild-type (≥ 50% wild-type, Table 3.1) but was the same for the two mutant lines, indicating that the difference from wild-type was a function of the V_H gene knock-in *per se* and was not affected by the presence/absence of Eμ. The well populated B lineage cells in both bone marrow and spleens demonstrated that the B1-8iΔ$E\mu^a$ allele can be expressed early enough to drive B cell development.

As noted earlier, in the absence of assembled V_H gene insertion, Eμ-deficient mice (c$E\mu^{\Delta/\Delta}$ mice) have small spleens (~50% wild-type) with a reduced percentage of splenic B cells (~40% wild-type) (Perlot et al. 2005), and more importantly, the number of pre-B and immature B cells is about only 5-10% of wild-type levels). The very different phenotype of the B1-8iΔ$E\mu^a$ homozygous mice demonstrates that these defects in the c$E\mu^{\Delta/\Delta}$ mice are due to the impairment in V-D-J assembly. Subsequent to V_H gene assembly (as in B1-8iΔ$E\mu^a$ mice), Eμ is required neither to promote B cell development nor to support normal levels of IgM on the surface of resting B cells.

3. Allelic exclusion is compromised in the absence of Eμ

In the regulated model of V-DJ joining, successful V_H gene assembly on one allele inhibits further rearrangement on the other allele, ensuring that

Figure 3.6. IgM allotype expression in B1-8i^{a}/*Igh*^{b} and B1-8iΔEμ^{a}/ *Igh*^{b} mice.

(A) Flow cytometry profiles of lymphocytes in bone marrow, spleen, and the peritoneal cavity, stained with antibodies to IgM^{a} and IgM^{b}. (B) IgM allotype expression on immature and mature B cells of the bone marrow. B220^{+} cells were enriched and then stained with antibodies to IgM^{a}, IgM^{b}, and IgD. Plots are of cells gated for IgM^{a} alone (left-most panels), or for cells that were IgM^{a}, IgD- (middle panels; immature B cells), or IgM^{a}+, IgD+ cells (right-most panels; mature B cells) and then analyzed for IgM^{a} and IgM^{b}. In both (A) and (B), the number in upper right quadrant = % double-positive cells relative to total IgM+ cells. (C) Percentage IgM^{a+b+} of total IgM^{+} cells at different stages of development and in different tissues. N= numbers of animals analyzed.

Figure 3.6 IgM allotype expression in B1-8iμ^a /*Igh*^{b} and B1-8iΔEμ^a/ *Igh*^{b} mice

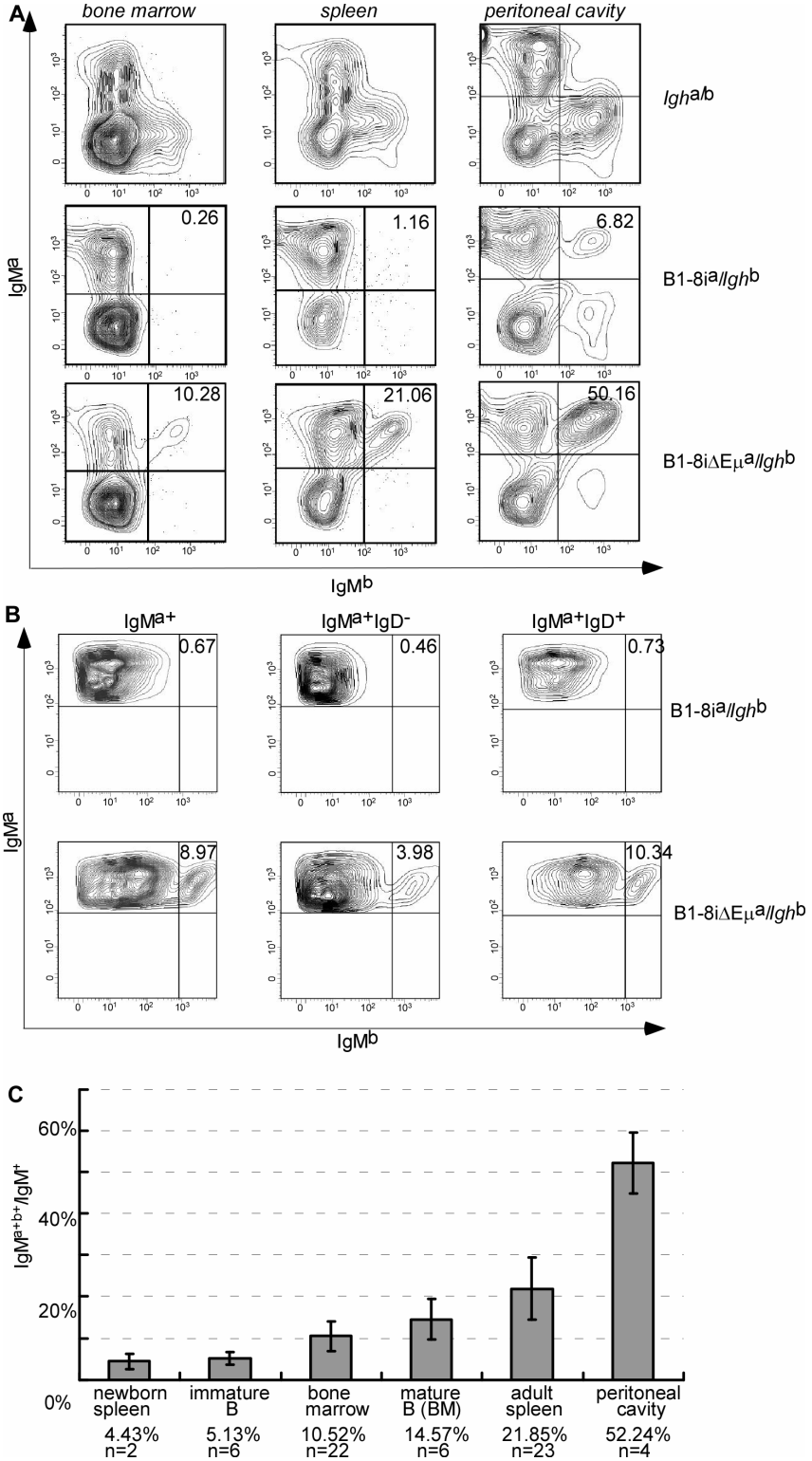

individual B cells express antibody with only one antigen-specificity (reviewed in Mostoslavsky et al. 2004; Jung et al. 2006). Having discovered that Igμ from the Eμ-deficient B1-8iΔEμ^a allele could drive normal B cell development, we expected that B cells from mice heterozygous for this locus, like those from mice heterozygous for the B1-8i locus, would express only the modified *Igh*^{a} allele. Since the mutant *Igh* allele was created in ES cells derived from the 129/Ola (129) strain (*Igh*^{a}), and this allele was bred to the C57BL/6 (C57) strain (*Igh*^{b}), anti-allotype reagents were used to distinguish expression of the two alleles in B cells.

As shown in the middle of Figure 3.6A, splenic B cells from wild-type mice heterozygous for the *Igh*^{a} and *Igh*^{b} alleles express either IgM^a or IgM^b but not both. Splenic B cells from B1-8i^a/*Igh*^{b} mice expressed only the B1-8i^a allele, but, surprisingly, allelic exclusion was clearly compromised in B1-8iΔEμ^a/*Igh*^{b} animals. While all B cells in these animals expressed IgM of the *Igh*^{a} allotype, ~20% of these cells also expressed IgM^b. Double-expressing B cells were also seen in the bone marrow of B1-8iΔEμ^a/*Igh*^{b} animals but not in the bone marrow of wild-type *Igh*$^{a/b}$ heterozygotes or B1-8i^a/*Igh*^{b} heterozygotes (Figure 3.6A, left). Double producers comprised ~10% of all IgM+ cells in B1-8iΔEμ^a/*Igh*^{b} bone marrow, a smaller percentage than was seen in spleen (compare *left* and *middle* panels, Figure 3.6A).

The smaller proportion of double producers suggested there might be an expansion of double producers after they left bone marrow. In fact, analysis of B cells in peritoneal cavity showed an even higher proportion of double producers,

~50% (Figure 3.6A, right). Therefore, immature B cells, the earliest stage of B lineage cells that express IgM, were analyzed. IgM^a-positive, B220+ bone marrow cells were further fractionated to allow separate analyses of immature B cells ($IgM^{a+}IgD^-$) and mature B cells ($IgM^{a+}IgD^+$), while no double producers were detected in either immature or mature B cells in B1-8i^a/*Igh*^{b} mice, B1-8i$\Delta E\mu^{a/a}$ mice double-producers were less frequent in the immature B cell population of B1-8i$\Delta E\mu^a$/*Igh*^{b} animals than in the mature B cell population (Figure 3.6B). Analyses of multiple animals are summarized in Figure 3.6C. Overall, therefore, these analyses suggested that a small subset of allelically-included immature B cells arise in B1-8i$\Delta E\mu^a$/*Igh*^{b} animals (but not in B1-8i^a/*Igh*^{b} animals), and this subset is expanded as cells exit the bone marrow and move to peripheral tissues (e.g. spleen, and peritoneal cavity).

The dominance of single producers at immature B cells, and the well-populated precursor B cell subsets (Table 3.2) in B1-8i$\Delta E\mu^a$/*Igh*^{b} mice are consistent with the results obtained from analyses of homozygous B1-8i$\Delta E\mu^a$ mice: the B1-8i$\Delta E\mu^a$ allele can be expressed early enough to drive B cell development.

4. The presence of double producers in B1-8i$\Delta E\mu^a$/*Igh*^{b} mice is not due to genetic background.

Since the B1-8i$\Delta E\mu^a$ allele was derived from E14.1 cells with the 129 genetic background, and progeny carrying the B1-8i$\Delta E\mu^a$ allele were mated with wild-type C57 mice to generate B1-8i$\Delta E\mu^a$/*Igh*^{b} mice, most B1-8i$\Delta E\mu^a$/*Igh*^{b} mice

Table 3.2: Absolute cell numbers in wild-type and heterozygous mutant mice.

Cells recovered from bone marrow of individual mice were counted (total cells). Aliquots were stained for B-lineage markers (B220, CD43, IgD, IgM in bone marrow) Cell number for lymphocyte subpopulations were calculated based on total cell count and the percentage total cells comprising each subpopulation (determined by flow cytometry).

*$p < 0.05$ (vs Igh^b/Igh^b)

Table 3.2: Absolute cell numbers in wild-type and heterozygous mutant mice.

Genotype	***Igh*$^{b/b}$**	**B1-8iΔEμ^{a}/*Igh*^{b}**	**B1-8i^{a}/*Igh*^{b}**
	n=4	**n=4**	**n=4**
Bone marrow (x 10^6)			
total cels	**47.50±9.57**	**40.00±0.00**	**45.50±16.46**
lymphocytes	**28.68±6.57**	**22.63±0.73**	**23.93±8.24**
B220+	**8.25±2.73**	**4.33±0.41***	**3.67±0.45***
pro-B	**0.36±0.06**	**0.35±0.02**	**0.33±0.07**
pre-B	**6.22±2.09**	**3.05±0.39**	**2.13±0.30**
immature B	**0.97±0.33**	**0.40±0.07**	**0.41±0.10**
mature B	**1.27±0.36**	**0.79±0.15**	**0.88±0.14**

Figure 3.7.Generate and identify B1-8i^{a}/*Igh*^{b} mice with the 129 genetic background or B1-8iΔEμ^{a}/*Igh*^{b} littermates.

Upper: Mating used to generate B1-8i^{a}/*Igh*^{b} mice with the 129 genetic background or B1-8iΔEμ^{a}/*Igh*^{b} littermates. Progeny's genotypes are predicted and useful ones are in black.

Lower left; PCR reactions used to distinguish *Igh*^{b} from *Igh*^{a} allele. The primer pair "b_only_F and b_only_R" allows the reliable generation of a relatively small PCR product (617 bp) from only the *Igh*^{b} allele.

Lower right, PCR reactions used to genotype progeny produced by "B1-8i^{a}/*Igh*^{b} X B1-8iΔEμ^{a}/*Igh*^{b}" mating. Genotypes were determined based on three PCR analysis as listed in the following table:

primers	PCR product	*Igh*^{a} allele	*Igh*^{b} allele	B1-8i^{a} allele	B1-8iΔEμ^{a} allele
Primer#4 and E3HR	834 bp	**-**	**-**	**+**	**-**
Primer$4, #8, and #2	848 bp	**-**	**-**	**-**	**+**
	322 bp	**+**	**+**	**+**	**-**
b_only_F and b_only_R	small (617 bp)	**-**	**+**	**-**	**-**
	big (unknown size)	**+/?**	**+/-**	**+/-**	**+/-**

Figure 3.7. Generate and identify B1-8i^{a}/*Igh*^{b} mice with 129 genetic background or B1-8iΔEμ^{a}/*Igh*^{b} littermate.

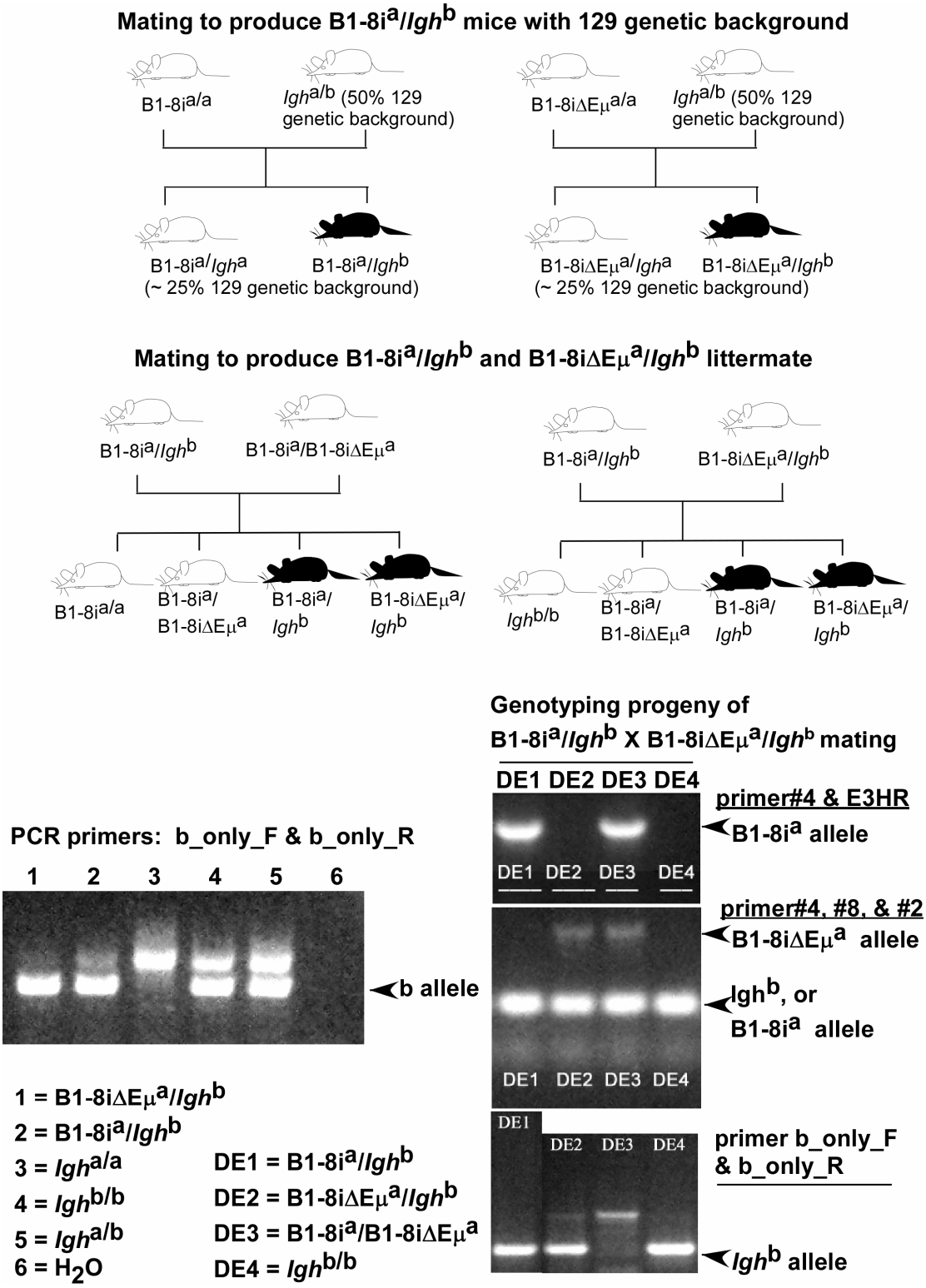

Figure 3.8 Double producers map to the B1-8i$\Delta E\mu^a$ allele, not to genetic background.

Frequencies of double producers in spleen were analyzed as in Figure 3.6 and summarized. Note: a/a = mice with two “a” allotype immunoglobulin heavy chain loci; E/b = B1-8i^a/*Igh*^{b} mice; D/b = B1-8i$\Delta E\mu^a$/*Igh*^{b} mice; n = the number of mice analyzed;

Figure 3.8 Double producers map to the B1-8i$\Delta E\mu^a$ allele, not to genetic background .

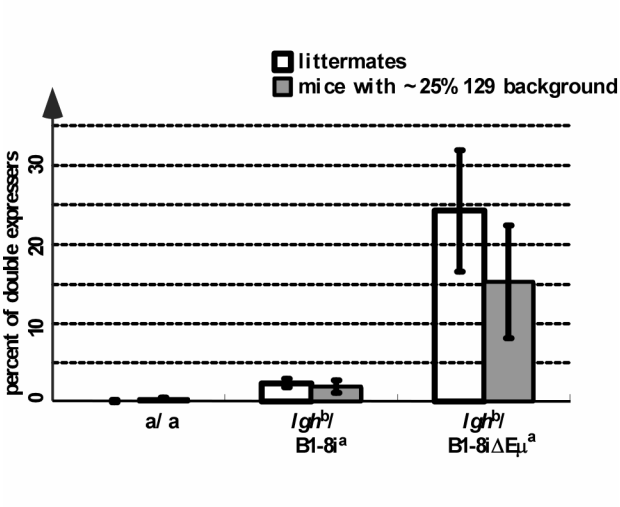

	littermates	mice of ~25% 129 backgrounc
a/a	0.08 (n=2)	0.36 (n=2)
E/b	2.33 (n=6)	1.91 (n=6)
D/b	24.2 (n=7)	15.25 (n=3)

used in this study have mixed 129 and C57 genetic background (Most B1-8i$\Delta E\mu^a$/*Igh*^{b} mice are the progeny of 3-6 backcrosses to C57). On the other hand, B1-8i^a/*Igh*^{b} was also generated with E14.1 cells, but these mice were mated with CB.20 mice that have the BALB/c genetic background (After we received the B1-8i$\Delta E\mu^a$.homozygous mice, B1-8i^a/*Igh*^{b} mice were generated by mating with C57 mice). It is not clear, however, how much of the 129 genetic background is retained in the B1-8i^a/*Igh*^{b} mice used in this study. Since different in genetic background might influence the phenotype of allelic exclusion, two experiments were conducted to test whether the large number of double producers in B1-8i$\Delta E\mu^a$/*Igh*^{b} mice was due to its genetic background.

In the first experiment, both homozygous B1-8i$^{a/a}$ and B1-8i$\Delta E\mu^{a/a}$ mice were mated to wild-type F1 animals (C57 X 129) (Figure 3.7). This mating introduced the C57 genetic background into B1-8i^a/*Igh*^{b} progeny, and it also brought the amount of 129 genetic background to a similar level in B1-8i^a/*Igh*^{b} and B1-8i$\Delta E\mu^a$/*Igh*^{b} progeny. In the second experiment, B1-8i^a/*Igh*^{b} and B1-8i$\Delta E\mu^a$/*Igh*^{b} littermates were generated by mating either B1-8i^a/*Igh*^{b} and B1-8i$\Delta E\mu^a$/*Igh*^{b} mice or B1-8i^a/*Igh*^{b} and B1-8i^a/B1-8i$\Delta E\mu^a$ mice (Figure 3.7). The generated B1-8i^a/*Igh*^{b} and B1-8i$\Delta E\mu^a$/*Igh*^{b} littermates would have similarly mixed genetic background of 129, C57, and BALB/c. Pairs of PCR primers that generated a “b” allele-specific product were used to distinguish B1-8i^a/*Igh*^{b} and B1-8i$\Delta E\mu^a$/*Igh*^{b} from B1-8i^a/*Igh*^{a} and B1-8i$\Delta E\mu^a$/*Igh*^{a} mice, respectively, all of which were generated in the first experiment (Figure 3.7, lower left). In order to identify B1-8i^a/*Igh*^{b} and B1-8i$\Delta E\mu^a$/*Igh*^{b} mice in the second experiment, primer

combinations to identify B1-8i, B1-8iΔEμ^a and *Igh*^{b} alleles were used (Figure 3.7, lower right, also see Figure 3.3).

Analysis of B1-8i^a/*Igh*^{b} and B1-8iΔEμ^a/*Igh*^{b} mice generated for both experiments showed that large numbers of double producers were always observed in B1-8iΔEμ^a/*Igh*^{b} mice, but not in B1-8i^a/*Igh*^{b} mice (Figure 3.8). Therefore, the "double-producer" phenotype observed in B1-8iΔEμ^a/*Igh*^{b} mice not due to genetic background, but due to the absence of Eμ from the knockin allele.

5. DNA rearrangement on the wild-type allele of B1-8iΔEμ^a/*Igh*^{b} mice is inhibited but not eliminated

It has been estimated that less than one-third of V-DJ rearrangements result in a functional gene. The ~10% (bone marrow) or ~20% (spleen) double-producers in B1-8iΔEμ^a/*Igh*^{b} animals should represent, therefore, only ~33% of the total attempts at V_H gene assembly taking place on the wild-type *Igh*^{b} allele in B cells of these mice. Since Igμ from the B1-8iΔEμ^a allele is sufficient to drive B cell development forward, as determined in mice homozygous for this allele, most aberrant rearrangements on the *Igh*^{b} allele would be expected to persist in the mature, IgM^{a+b-} B cells of these mice.

To estimate the frequency of such rearrangements, we took advantage of a BamHI restriction fragment length polymorphism (RFLP) within the V_H-D_H interval that distinguishes *Igh* loci from the C57BL/6 and 129/Ola mouse strains. A probe lying within this V_H-D_H interval (probe C, Figure 3.9A) was used to hybridize to BamHI-digested liver DNA from 129/Ola (*Igh*^{a}) and C57BL/6 (*Igh*^{b}) mice and revealed a 9.6kb fragment from the *Igh*^{a} allele and a 7.5kb from the *Igh*^{b} allele

Figure 3.9. V-DJ rearrangements on the wild-type *Igh*^{b} allele of B1-8iΔEμ^{a}/*Igh*^{b} mice.

Overview of the *Igh*^{a} *and Igh*^{b} *loci*, showing positions of hybridization probes (Probe C, Probe D). Probe C detects a sequence that will be deleted upon V-DJ joining. Probe D detects a sequence 3' of the *Igh* loci and retained on both alleles in all cells. The size of BamH I fragment detected by Probe C and Probe D on both a and b alleles are shown. (B) Strategy of the analysis: *Left*, sorted IgM$^{a\text{-}b+}$ B cells are predicted to lose the "b" BamH I fragment and retain less "a" BamH I fragment relative to liver cells; *Right*, the level of V-DJ recombination on the wild-type *Igh*^{b} allele is estimated by the loss of the "b" BamH I fragment. * Since the knock-in allele (B1-8iΔEμ^{a}) is fixed and does not undergo recombination, the "a" BamH I fragment will be fully retained. (C) *Left*, detection of the BamH I fragment from a and b alleles by Probe C. Liver DNAs from wild-type C57(*Igh*$^{b/b}$) and F1 (*Igh*$^{a/b}$) mice was digested by BamH I and hybridized with probe C. *Right*, assay for V-DJ rearrangement on the *Igh*^{a} and *Igh*^{b} alleles in wild-type F_1 (*Igh*$^{a/b}$) and B1-8iΔEμ^{a}/*Igh*^{b} mice. Genomic DNA extracted from liver and from splenic IgM$^{a\text{-}b+}$ cells isolated by flow cytometry from wild-type *Igh*$^{a/b}$ (*left*) and IgM^{a+b-} cells sorted from B1-8iΔEμ^{a}/*Igh*^{b} (*right*) mice. DNAs were digested with BamHI and hybridized with probes C (*upper*) and D (*lower*). (D) Quantitative analysis (ImageQuant™) of the two blots shown in (C) and a repeat experiment. Band intensities in liver set to 100%. White bars = *Igh*^{a} allele; black bars = *Igh*^{b} allele. (Normalization was to probe D for WT Igh$^{a/b}$ mice; normalization was to the Igh^{a} fragment in *B1-8iΔEμ^{a}/Igh*^{b} *mice*)

Figure 3.9. V-DJ rearrangements on the wild-type *Igh*^{b} allele of B1-8i$\Delta E\mu^{a}$/*Igh*^{b} mice

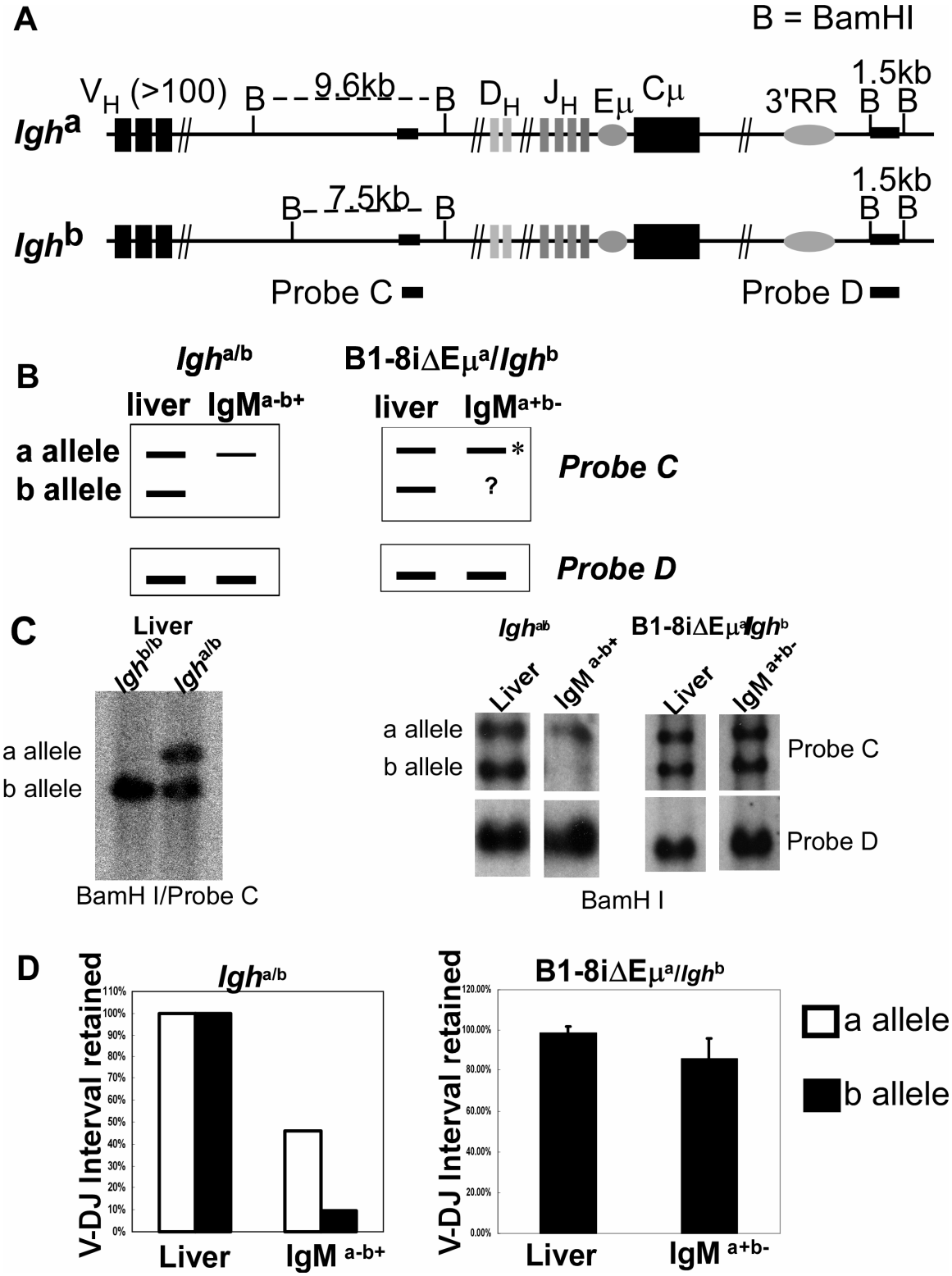

(Figure 3.9C). Because of their location, these BamHI fragments will be deleted upon fusion of any V_H with any D_H gene segment on the *Igh*^{a} and *Igh*^{b} alleles, respectively. For example, IgM^{a-b+} cells sorted from wild-type mice would lack the *Igh*^{b}-derived 7.5kb BamHI fragment. The number of V-DJ rearrangements on the *Igh*^{b} allele in IgM^{a+b-} B cells from B1-8iΔEμ^a/*Igh*^{b} mice can be estimated by the level of the *Igh*^{b}-derived 7.5kb BamHI fragment relative to liver since V_H-D_H rearrangement would eliminate this fragment (Figure 3.9B).

Splenic B cells were sorted from wild-type *Igh*$^{a/b}$ F_1 animals and from B1-8iΔEμ^a/*Igh*^{b} mice. IgM^{a-b+} cells from wild-type *Igh*$^{a/b}$ mice almost entirely lacked the smaller BamHI fragment that was derived from the *Igh*^{b} allele (residual fragment results from contaminating cells in sorted populations) and retained only ~45% germline (liver) levels of the larger BamHI fragment from the *Igh*^{a} allele (Figure 3.9C right, and 3.9D left). A BamHI fragment mapping 3' of the *Igh* loci (probe D, Figure 3.9A) was used to normalize DNA loading in these experiments. These results are consistent with earlier studies and demonstrate the inefficiency of the V_H assembly process such that many B cells (in this case, ~55%) have undergone (unsuccessful) V-D-J gene assembly on the unexpressed *Igh*^{a} allele, before they attempt (and succeed at) assembly on the *Igh*^{b} allele (Alt et al. 1984; ten Boekel et al. 1998).

In IgM^a+ B cells from B1-8iΔEμ^a/*Igh*^{b} mice, the B1-8 V_H gene has been inserted upstream of Cμ on the *Igh*^{a} allele and all germline J_H genes have simultaneously been removed. As noted earlier, the B1-8 V_H gene was modified to inhibit V_H gene replacement events, so the 9.6kb BamHI fragment lying

between the V_H and D_H genes on this chromosome should not be lost in any B cells from these mice (early studies reported no evidence for V-D rearrangements (Alt et al. 1984)). As shown in Figure 3.9C, this fragment did, in fact, remain in DNA isolated from IgM^{a+b-} B cells. The smaller BamHI fragment from the *Igh*^{b} allele was also present in these cells and was present at 85-95% germline levels (Figure 3.9D, right). Quantification of the genomic Southern data, in fact, showed no statistically-significant difference in the levels of this *Igh*^{b}-derived BamHI fragment in liver as compared to IgM^{a+b-} B cells of B1-8i$\Delta E\mu^a$/*Igh*^{b} mice (Figure 3.9D, right). We conclude that in most cells expressing only the B1-8i$\Delta E\mu^a$ allele, no attempts at V_H-D_HJ_H rearrangement have taken place on the wild-type *Igh*^{b} allele. The frequency of IgM^{a+b+} B cells (~10% in bone marrow and ~20% in spleen) in these animals, therefore, is not matched rare aberrant V-DJ rearrangements on the *Igh*^{b} allele in splenic IgM^{a+b-} B cells.

To address this issue further, we turned to a more sensitive measure of V-DJ rearrangement. A PCR strategy, as show in Figure 3.10, was used to specifically detect V-DJ rearrangements on the wild-type *Igh* allele. A J_H4 primer combined with V_H family primers was used since the JH4 primer does not anneal to either the B1-8i$\Delta E\mu^a$ allele or B1-8i^a allele. A wild-type *Igh* allele-specific J_H4 probe was hybridized to blotted PCR products to further increase the sensitivity and specificity of this analysis. In a control experiment (Figure 3.10, lower right), PCR products for VDJ rearrangements were only detected in DNA isolated from tissues that contained B cells with V-DJ rearrangements in wild-type *Igh* alleles

Figure 3.10. PCR strategy of V-DJ rearrangement analysis on the wild-type *Igh* allele.

Upper, locus maps showing positions of PCR primers and probes for dectecting V-DJ rearrangements on the Igh^{b} allele. 5' primers specific for individual V_H gene families (V_H family primer) were used in combination with a 3' primer (J_H4 primer), present on the wild-type $Igh^{a/b}$ allele but missing on both the B1-8i^{a} and B1-8i$\Delta E\mu^{a}$ alleles. The J_H4 probe, used to detect V-DJ rearrangement PCR products, is also present only on the wild-type $Igh^{a/b}$ allele but not the B1-8i^{a} or B1-8i$\Delta E\mu^{a}$ allele.

Lower left, the rearrangements to different J_H results in different sizes of V-DJ rearrangement PCR products.

Lower right: representative blot demonstrating allele-specific amplification. WT = wild-type $Igh^{a/b}$ B1-8i$\Delta E\mu^{a}$ and B1-8i^{a} = mice homozygous for these respective alleles. H_2O = no DNA template control.

Figure 3.10. PCR strategy of V-DJ rearrangement analysis on the wild-type *Igh* allele.

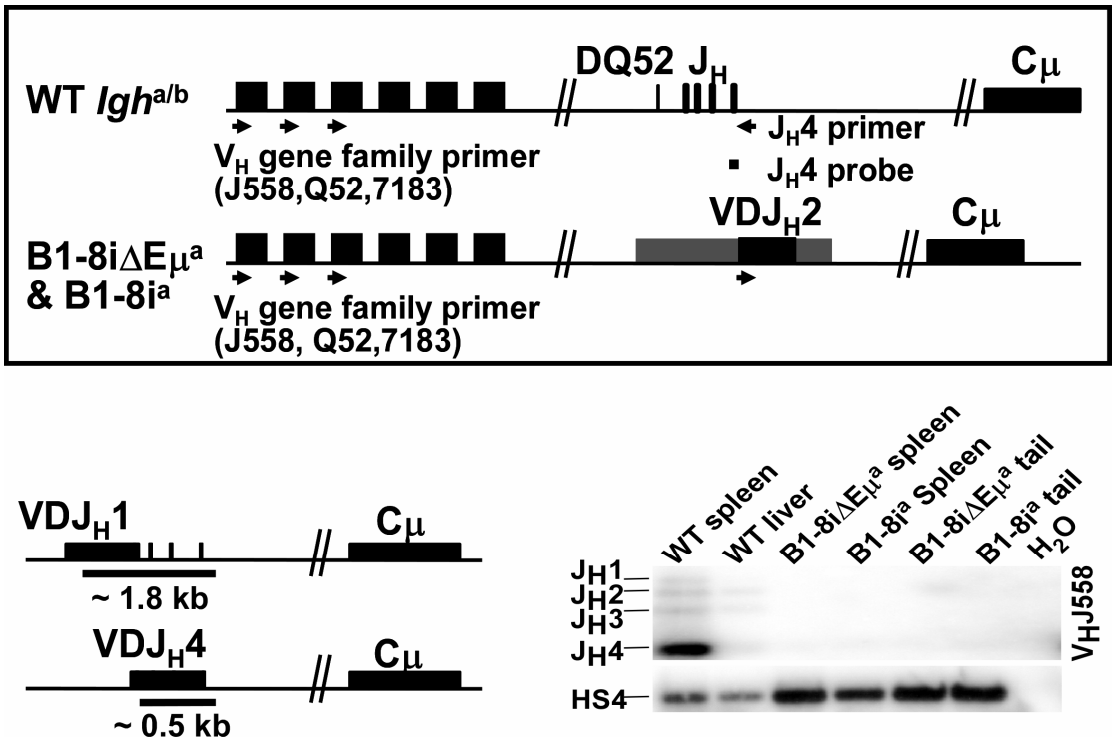

Figure 3.11. V-DJ rearrangements on the wild-type *Igh*^{b} allele of splenic B cells in B1-8i^{a}/*Igh*^{b} and B1-8iΔEμ^{a}/*Igh*^{b} mice.

A) Splenic B cells from mice of the indicated genotypes (*Igh*$^{a/b}$ and B1-8iΔEμ^{a}/*Igh*^{b}) were sorted on the basis of phenotype (IgM^{a+b-}, IgM^{a+b+}). PCRs were carried out on 5-fold serial dilutions of DNA templates (four lanes/cell type). PCR strategy detects V-DJ rearrangements on only the *Igh*^{b} allele in B1-8iΔEμ^{a}/*Igh*^{b} mice (both alleles in wild-type *Igh*$^{a/b}$ mice). VDJ rearrangements involving each J_H gene segment are indicated (J_H1, J_H2, etc.). V_H family primers are indicated to right of panels (V_HJ558, etc.) PCR of HS4 (a 3'RR element) normalized DNA input.

B) As in (A), but a primer designed to anneal to all V_H families (Kantor et al. 1997, promiscuous V_H primer) was included.

C) Summary of cloning and sequencing analysis of VDJ rearrangements in splenic B cells. PCR product for V_H-D_H-J_H4 rearrangements was gel-purified, cloned, and sequenced.

Figure 3.11. V-DJ rearrangements on the wild-type *Igh*^{b} allele of splenic B cells in B1-8i^a/*Igh*^{b} and B1-8iΔEμ^a/*Igh*^{b} mice.

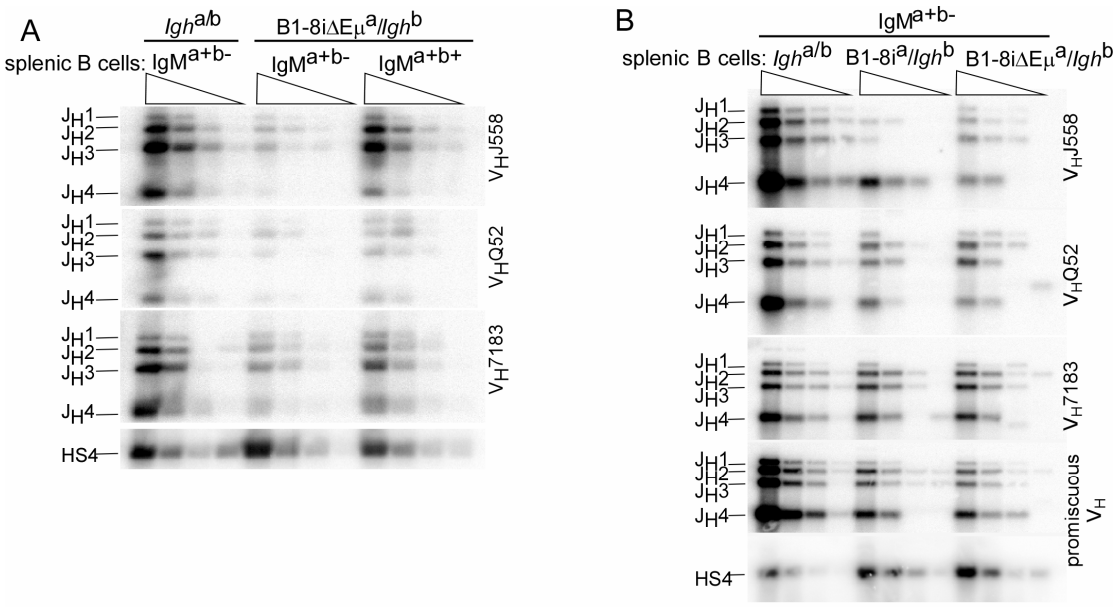

C

genotype	Cells	rearrangements	productive/all clones
B1-8iΔEμ^a/*Igh*^{b}	IgM^{a+b+}	V_H7183-D_H-J_H4	7 / 7
		V_HJ558-D_H-J_H4	7 / 7
B1-8iΔEμ^a/ *Igh*^{b}	IgM^{a+b-}	V_H7183-D_H-J_H4	1 / 19
B1-8i^a/ *Igh*^{b}	IgM^{a+b-}	V_H7183-D_H-J_H4	0 / 18

(wild-type spleen), demonstrating this primer's allele-specificity. An hs4 fragment was also amplified to normalize the amount of DNA template.

This PCR strategy was first used to confirm, at the molecular level, that IgM^{a+b+} cells identified by flow-cytometry in B1-8iΔEμ^a/*Igh*^{b} animals had, in fact, successfully assembled Igμ genes on their wild-type *Igh* alleles. Splenic IgM^{a+b+} cells were isolated by flow-cytometry and analyzed for V-DJ rearrangement on the wild-type allele. PCR products for V_HJ558-D_H-J_H4 and V_H7183-D_H-J_H4 rearrangements were cloned and sequenced. Of the 14 independent clones sequenced, all of them revealed a successfully assembled ("productive") V_H gene on the *Igh*^{b} allele (Figure 3.11C).

This PCR strategy was also used to analyze genomic DNA from IgM^{a+b-} splenic B cells, looking for aberrant VDJ rearrangements on the wild-type (and unexpressed) *Igh*^{b} allele. Semi-quantitative PCR was used to quantify VDJ rearrangements on the wild-type *Igh*^{b} allele of splenic B cells from B1-8iΔEμ^a/*Igh*^{b} mice, and comparisons were made with IgM^{a+b-} splenic B cells from wild-type *Igh*$^{a/b}$ mice (Fig. 3.11A). In the wild-type mice, this PCR strategy does not distinguish between rearrangements on the *Igh*^{a} *and Igh*^{b} alleles (J_H4 primer will anneal to both alleles) so that the PCR products generated are bi-allelic (from both alleles). As shown in Figure. 3.11A, PCR products were detected with each of the V_H family primers in DNA isolated from IgM^{a+b-} splenic B cells from B1-8iΔEμ^a/*Igh*^{b} mice. V-DJ rearrangements (presumably aberrant) had taken place, therefore, on the silent *Igh*^{b} allele of some of these splenic B cells. PCR products representing these events, however, were 1/5 to 1/25 as abundant as

those seen in wild-type mice, indicating that V-DJ assembly on the *Igh*^{b} allele was relatively rare in IgM^{a+b-} splenic B cells. In contrast, V-DJ rearrangements on the *Igh*^{b} allele were readily detectable in IgM^{a+b+} double-producers from the B1-8iΔEμ^a/*Igh*^{b} mice, where these V_H gene assemblies resulted in a productive *Ig*μ^b gene (Figure 3.11A). In this population of double-producers, the PCR products derive from *Igh*^{b} rearrangements that have taken place in every B cell in the sorted population. Compared with the IgM^{a+b-} cells from the same animal, these PCR products were (like those from wild-type cells) 5- to 25-fold more abundant. These PCR results are consistent with the genomic Southern data, suggesting that most IgM^{a+b-} cells have not undergone V_H-D_HJ_H rearrangement on the *Igh*^{b} allele. The PCR studies confirm, however, that some such rearrangements have taken place.

As shown in Figure 3.6B, only ~ 5% immature B cells from B1-8iΔEμ^a/*Igh*^{b} mice express both IgM^a and IgM^b, This should be matched by ~10% IgM^{a+b-} cells of aberrant V_H-D_HJ_H rearrangements on the *Igh*^{b} allele. The splenic B cells profile is consistent with this estimate: semiquantitative PCR showed that about 4-20% IgM^{a+b-} cells have undergone V_H-D_HJ_H rearrangement on the *Igh*^{b} allele.

One simple explanation for the “double producer” phenotype in B1-8iΔEμ^a/*Igh*^{b} mice is a failure of feed-back inhibition process normally mediated by a successfully assembled IgH gene. This failure could be due to the absence of Eμ on the B1-8iΔEμ^a allele. Given the rare aberrant rearrangements detected on the wild-type *Igh*^{b} allele in splenic IgM^{a+b-} cells of B1-8iΔEμ^a/*Igh*^{b} mice, an even lower number of rearrangements or a complete prohibition of rearrangement was

Figure 3.12. V-DJ rearrangements on the wild-type *Igh*^{b} allele of pre-B cells in B1-8i^{a}/*Igh*^{b} and B1-8iΔEμ^{a}/*Igh*^{b} mice.

A) D-J rearrangements on the *Igh*^{b} allele of pre-B cells. Semi-quantitative PCR analysis was carried out as described in Figure 3.11 (A) and material and methods. Cells were isolated by flow-cytometry (B220+CD43-IgM-) from six mice of each of the indicated genotypes. The D_HL primer anneals to most D_H genes; DQ52 anneals only to D_HQ52. Same allele-specific 3'primer (J_H4) as in (Figure 3.11). Liver DNA from *Igh*$^{a/b}$ mice (lane 13) and spleen cell DNA from homozygous B1-8i^{a} and homozygous B1-8iΔEμ^{a} mice (lanes 14 &15), respectively, were included as controls. H_2O = no template control.

B) Pre-B cells were isolated as in (A) and PCR reactions using the V_H gene family primers were carried out as described in Figure 3.11(A).

Figure 3.12. V-DJ rearrangements on the wild-type *Igh*^{b} allele of pre-B cells in B1-8i^{a}/*Igh*^{b} and B1-8iΔEμ^{a}/*Igh*^{b} mice.

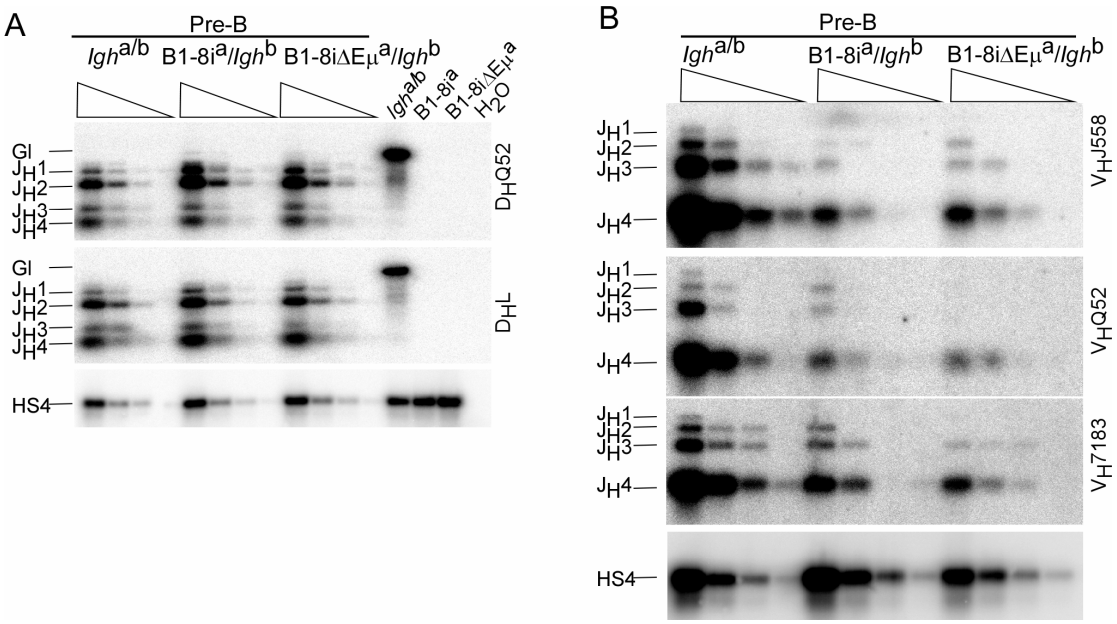

expected on the wild-type *Igh*^{b} allele in splenic IgM^{a+b-} cells of B1-8i^a/*Igh*^{b} mice. However, comparative analyses of IgM^{a+b-} spleen cells from B1-8i^a/*Igh*^{b} and B1-8iΔEμ^a/*Igh*^{b} mice showed a similar amount of V_H-D_HJ_H rearrangement (Figure 3.11B). In addition to the V_H family-specific primers described above, these experiments included a primer designed to anneal to all known V_H gene families (Kantor et al. 1997). Either with family primers for individual V_H families, or with the primer for all V_H genes, similar amounts of V-DJ rearrangement were detected. Splenic B cells in B1-8i^a/*Igh*^{b} included those that had undergone V_H-D_HJ_H assembly on the unexpressed *Igh*^{b} allele as in B1-8iΔEμ^a/*Igh*^{b} mice, demonstrating that the knock-in B1-8μ^a allele, like the B1-8iΔEμ^a allele, was not entirely prohibiting V-DJ recombination on the allelic (*Igh*^{b}) chromosome. The quantitative analysis further suggested that B1-8iΔEμ^a/*Igh*^{b} mice did not have a great deal more V-DJ rearrangement on the wild-type allele, in precursor B cells, than did B1-8i^a/*Igh*^{b} mice

6. V-DJ rearrangements on the wild-type allele are evident in pre-B cells from both B1-8iΔEμ^a/*Igh*^{b} and B1-8i^a/*Igh*^{b} mice

The same PCR approach was used to estimate the frequency of *Igh*^{b} allele rearrangements in pre-B cells of both B1-8iΔEμ^a/*Igh*^{b} and B1-8i^a/*Igh*^{b} mice. Pre-B cells comprise the pool that has just ceased Ig heavy chain rearrangement and is beginning the process of Ig light chain gene assembly. Semi-quantitative PCR assays of DNA from these cells showed that this pool had undergone D-J joining on the wild-type *Igh*^{b} allele at the same frequency as pre-B cells from normal *Igh*$^{a/b}$ mice (Figure 3.12A). V-DJ joins were also evident on the *Igh*^{b} alleles of pre-B cells

from both B1-8i$\Delta E\mu^a$/*Igh*^{b} and B1-8i^a/*Igh*^{b} mice. These, however, were both present at ~1/5-1/25 the frequency seen in normal pre-B cells (Figure 3.12B).

To estimate the frequency of precursors that had undergone V-DJ on the *Igh*^{b} allele, we made the following assumptions. In normal pre-B cells, this PCR strategy detects V-DJ joins on both alleles. In these cells, at least one allele has undergone functional V-DJ rearrangement (in order to progress to the pre-B cell stage), and an estimated 40% of the cells also carry a non-functional V-DJ rearrangement on the second allele (Alt et al. 1984; ten Boekel et al. 1998). If each pre-B cell in B1-8i$\Delta E\mu^a$/*Igh*^{b} and B1-8iμ^a/*Igh*^{b} mice had undergone V-DJ rearrangement on the single *Igh*^{b} allele (no feedback inhibition), then PCR products representing these rearrangements would be ~1.0/1.4 (71%) the level seen in a population of normal pre-B cells. Instead, semi-quantitative analyses showed them to be no greater than 20% (4%-20%) the level seen in normal pre-B cells. This suggested that between 6% and 28% (4/71 to 20/71) of the pre-B cells in B1-8i$\Delta E\mu^a$/*Igh*^{b} and B1-8iμ^a/*Igh*^{b} mice carried assembled V_H genes (productive or non-productive) on the *Igh*^{b} allele. The B1-8i$\Delta E\mu^a$ and B1-8iμ^a alleles were clearly inhibiting, but not entirely prohibiting, V-DJ recombination on the allelic chromosome. This feedback inhibition was Eμ-independent. The effect on immature and peripheral B cell phenotype was not.

7. An Eμ-dependent checkpoint for allelic exclusion at the pre-B to immature B cell transition

V_H gene assembly on the *Igh*^{b} allele resulted in a significant population of splenic B cells expressing both *Igh* alleles in mice of one genotype

Table 3.3 Frequency of "productive" V_H assembly as determined by DNA cloning and sequence analysis.

VDJ-rearrangements were amplified by PCR and cloned from DNA of sorted pre-B or mature B cells from B1-8i^a/*Igh*^{b} or B1-8iΔEμ^a/*Igh*^{b} mice. Only unique sequences were analyzed. V-D-J rearrangements were analyzed by V-Quest, which was also used to determine whether the V_H assembly was "productive" or "non-productive".

Table 3.3 Frequency of "productive" V_H assembly as determined by DNA cloning and sequence analysis.

V_H7183-D_H-J_H4 rearrangements

genotype	B cell subset	productive	non-productive	total	% of productive
***Igh*$^{b/b}$**	pre-B	11	9	20	55.0%
***Igh*$^{b/b}$**	immature B	13	5	18	72.2%
B1-8i^{a}/***Igh*^{b}**	pre-B	15	22	37	40.5%
B1-8i^{a}/***Igh*^{b}**	immature B	10	22	32	31.3%
B1-8iΔEμ^{a}/***Igh*^{b}**	pre-B	12	24	36	33.3%
B1-8iΔEμ^{a}/***Igh*^{b}**	immature B	3	14	17	17.6%

V_HJ558-D_H-J_H4 rearrangements

genotype	B cell subset	productive	non-productive	total	% of productive
***Igh*$^{b/b}$**	pre-B	24	3	27	88.9%
***Igh*$^{b/b}$**	immature B	17	3	20	85.0%
B1-8i^{a}/***Igh*^{b}**	pre-B	16	1	17	94.1%
B1-8i^{a}/***Igh*^{b}**	immature B	19	1	20	95.0%
B1-8iΔEμ^{a}/***Igh*^{b}**	pre-B	36	1	37	97.3%
B1-8iΔEμ^{a}/***Igh*^{b}**	immature B	3	0	3	100.0%

Table 3.4 Analysis of VH7183-DH-JH4 rearrangements in pre-B cells of B1-8i^{a}/*Igh*^{b} and B1-8iΔEμ^{a}/*Igh*^{b} mice

V_H-D_H-J_{H4} junction sequences on the wild-type *Igh*^{b} allele of B1-8i^{a}/*Igh*^{b} and B1-8iΔEμ^{a}/*Igh*^{b} pre-B cells. V_H7183D_HJ_{H4} rearrangements were cloned by PCR from genomic DNA of isolated pre-B cells, using a V_H7183 family primer and J_H4 primer. DNA sequences were analyzed by the IMGT/V-QUEST program (http://imgt.cines.fr). Because of ambiguity, assigned D_H genes were manually revised, where necessary, using IMGT/V-QUEST results as guidance, and junctions without a perfect alignment of 7 or more nucleotides to a C57BL/6 D_H gene were not assigned a D_H gene. Under "Productivity," P=productive, NP=non-productive. CDR3 lengths were given for productive clones (IMGT/V-QUEST program assigns the CDR3 to sequences between Cys 104 in the V_H and Trp/Phe in the conserved Trp/Phe-Gly-X-Gly motif in J_H). Clones were isolated in two separate experiments: in one experiment, clones were obtained from pre-B cells of an individual B1-8i^{a}/*Igh*^{b} and an individual B1-8iΔEμ^{a}/*Igh*^{b} mouse; in the second experiment, pre-B cells were isolated from a pool of two mice for each genotype.

* in this rearrangement, the V_H and J_H genes can be identified, but the Cys 104 was missing so the junction was not analyzed

** the V_H used in this rearrangement is from another (non-7183) V_H family.

Table 3.4 Analysis of V_H7183-D_H-J_H4 rearrangements in pre-B cells of B1-8i^a/*Igh*^{b} and B1-8iΔEμ^a/*Igh*^{b} mice.

B1-8i^a/*Igh*^{b} preB cells V_H7183-D_H-J_H4 rearrangements

V name	3'V-REGION	N1	P	D-REGION	N2	D name	Productivity	CDR3 length
IGHV5-2	tgtgcaaga	ctt		ctacg	tgc		P	12
IGHV5-2	tgtgcaaga	c		atagtaaccac	ttgacg	IGHD3-1	P	12
IGHV5-2	tgtgcaaga	cat		gtctatgc	cacgggggg		P	14
IGHV5-2	tgtgcaaga	caag		taactggg		IGHD4-1	P	10
IGHV5-2	tgt	ccc		tggtt		IGHD2-3	P	8
IGHV5-2	tgtgcaaga	ca		taactggg		IGHD4-1	P	11
IGHV5-2	tgtgcaaga	ctt		ctacg	tgc		P	12
IGHV5-2	tgtgcaaga	c		actacggtagtagc		IGHD1-1	NP	
IGHV5-2	tgtgcaaga	cgactg		ggtggt			NP	
IGHV5-2	tgtgcaaga			tggttactac	a	IGHD2-3	NP	
IGHV5-2	tgtgcaaggac			ctcccgcta	t		NP	
IGHV5-2	tgtgcaaga	c		atagtaactac	aacgagct	IGHD3-1	NP	
IGHV5-2	tgtgcaaga	c		atagtaactac	gacgagct	IGHD3-1	NP	
IGHV5-2	tgtgc			tactata	t	IGHD3-1	NP	
IGHV5-2	tgtgcaaga			tggttacga	gagagggggggggt	IGHD2-7	NP	
IGHV5-2	tgtgcaaga	c		tagtaactac	gtat	IGHD3-1	NP	
IGHV5-2	tgtgcaaga	catgggc		ccaaataggg	g		NP	
IGHV5-2	tgtgcaaga	c		atgg	gg		NP	
IGHV5-2	tgtgcaaga	c		actatagtaact	ggggg	IGHD3-1	NP	
IGHV5-2	tgtgcaaga	c		atagtaactac	gacgagct	IGHD3-1	NP	
IGHV5-2	tgtgcaaga			ctactatagtaac	cctgt	IGHD3-1	NP	
IGHV5-4	tgtgcaaga	ga		tctccgggggtg	gtct		P	13
IGHV5-4	tgtgcaaga	g		atggtaactac	gt	IGHD2-8	P	13
IGHV5-4	tgtgcaaga			gtac			NP	
IGHV5-4	tgtgcaag			ctactatagtaac	ga	IGHD3-1	NP	
IGHV5-4	tgtgcaaga	gat		ctatgattacgac	gacggcccc	IGHD2-4	NP	
IGHV5-4	tgtgcaaga	gagagttct	t	agacagctcagg	gacggg	IGHD3-2	NP	
IGHV5-4	tgtgcaaga	gatgg		ggtagtagc	aatctc	IGHD1-1	NP	
IGHV5-6	tgtgcaagaca			taagacg	a		P	12
IGHV5-6	tgtgcaagaca			ttattactacg	agggctac	IGHD1-1	P	11
IGHV5-6	tgtgcaagac	cg		gggaggttcta	g		NP	
IGHV5-12	tgtgcaaga	catg		actatgactacgac	ggttgg	IGHD2-4	P	15
IGHV5-12	tgtgcaaga	c		atgtctatgac	cccct	IGHD2-3	P	14
IGHV5-12	tgtgcaaga	catcctc		atggttactac	gtcc	IGHD2-3	NP	
IGHV5-9-1*	(Cys 114 is missing)						NP	
IGHV5-17	tgtgcaagg	Cgaatcagccag		attactacggtagtag	ggaag	IGHD1-1	P	17
IGHV5-17	tgtgcaagg	aggaacggg		actacggtagtag	aag	IGHD1-1	P	15

B1-8iΔEμ^a/*Igh*^{b} preB cells V_H7183-D_H-J_H4 rearrangements

V name	3'V-REGION	N1	P	D-REGION	N2	D name	Productivity	CDR3 length
IGHV5-1	tgtttgaga	cat		cctact	tt		NP	
IGHV5-1	tgtttgaga	c		tggtaac		IGHD2-8	NP	
IGHV5-2	tgtgcaag	cat		cttcgg			P	7
IGHV5-2	tgtgcaaga			catcgggg	cccc		P	12
IGHV5-2	tgtgcaaga	gaccg					P	9
IGHV5-2	tgtgcaag	cat		cttcgg			P	7
IGHV5-2	tgtgcaaga	cat		tactatgattacgac	ggg	IGHD2-4	P	14
IGHV5-2	tgtgcaaga	cat		gacagctcaggctac	ac	IGHD3-2	NP	
IGHV5-2	tgtgcaaga	ca		ggggcagctcaggc	cct	IGHD3-2	NP	
IGHV5-2	tgtgcaaga			tgattacga		IGHD2-4	NP	
IGHV5-2	tgtgcaag	g		ctgaagt	agga		NP	
IGHV5-2	tgcgcaaga			tctactatgattacgac	gggg	IGHD2-4	NP	
IGHV5-2	tgtgcaaga			cctactatag		IGHD3-1	NP	
IGHV5-2	tgtgcaaga	c		tagc			NP	
IGHV5-2	tgtgcaaga	catgg		atagtaactac	ggaagg	IGHD3-1	NP	
IGHV5-2	tgtgcaaga	ct		gtaactac	g	IGHD3-1	NP	
IGHV5-2	tgtgcaaga	caagtaa		aaagggg	cttg		NP	
IGHV5-2	tgtgcaaga			ctatgattacgac	ggga	IGHD2-4	NP	
IGHV5-2	tgtgcaaga	tttccccttg		ggtaactac	g	IGHD2-8	NP	
IGHV5-2	tgtgcaaga	c		atggtaactac	g	IGHD2-8	NP	
IGHV5-2	tttgcaaga			tgattacga		IGHD2-4	NP	
IGHV5-2	tgtgcaaga	cgga		ggtagtagctac	gggg	IGHD1-1	NP	
IGHV5-4	tgtgcaaga	gatc		acgatagtaactac	g	IGHD3-1	P	14
IGHV5-4	tgtgcaaga	gataact	a	tctactatggttacga	gcgacccct	IGHD2-7	NP	
IGHV5-4	cgtgcaaga	gaa		ggaatggtaagg		IGHD2-8	NP	
IGHV5-4	tgtgcaaga			gatagcccagg	gacgggg	IGHD3-2	NP	
IGHV5-6	tgtgcaag	ccctcg	a	tttattactacgg	tagtagct	IGHD2-3	NP	
IGHV5-9	tgtgcaaga			tctatgatggttactac	g	IGHD2-3	P	14
IGHV5-9	tgtgcaag	gc		ataa	g		P	8
IGHV5-9	tgtgcaaga	t		ggtaacacgg		IGHD2-8	NP	
IGHV5-9-1	tgtacaaga			gagggttact		IGHD2-3	P	12
IGHV5-9-1	tgtacaaga	gacgggggcct		gggacag	g	IGHD4-1	P	14
IGHV5-9-1	tgtacaaga	gaggagatgg		taccctcaata			NP	
IGHV5-16	tgtgcaaga	gatcaga		atgattacgac	ggg	IGHD2-4	P	14
IGHV5-17	tgtgcaagg	ccc		acgggg			NP	
IGHV7-3**	tgtgcaagatat	ctg		aactggg	ctagg	IGHD4-1	P	12

Table 3.5 Analysis of V_HJ558-D_H-J_H4 rearrangements in pre-B cells of B1-8i^a/*Igh*^{b} and B1-8iΔEμ^a/*Igh*^{b} mice

Analysis was done in a similar way as for Table 3.4 except that D_H assignment is fully based on V-QUEST analysis. V_HJ558-D_H-J_{H4} rearrangements were cloned by PCR from genomic DNA of isolated pre-B cells, using a V_HJ558 family primer and J_H4 primer. DNA sequences were analyzed by the IMGT/V-QUEST program (http://imgt.cines.fr).

Table 3.5 Analysis of V_HJ558-D_H-J_H4 rearrangements in pre-B cells of B1-8i^a/*Igh*^{b} and B1-8i$\Delta E\mu^a$/*Igh*^{b} mice.

B1-8i^a/*Igh*^{b} preB cells V_HJ558-D_H-J_H4 rearrangements

V name	REGION	P	N1	P	D-REGION	D name	Productivity	CDR3 length
IGHV1-7	tgtgcaaga				.....tggg..	IGHD4-1	P	10
IGHV1-7	tgtgcaaga		tcagggaagagat		....ttactacggtagtagctac	IGHD1-1	P	19
IGHV1-18	tgtgcaaga		tgaggg		........tacggtagtagc...	IGHD1-1	P	14
IGHV1-19	tgtgcaag.		g		..tattactacggtagtagctac	IGHD1-1	P	18
IGHV1-19	tgtgcaa..		a		.ctactatggtaac...	IGHD2-1	NP	
IGHV1-26	tgtgcaag.			gtct	agacagctcaggctac	IGHD3-2	P	17
IGHV1-36	tgtgcaaga		g		...atcactacggtagta.....	IGHD1-1	P	13
IGHV1-50	tgtgcaaga				gagggcctac	IGHD5-1	P	12
IGHV1-55	tgtgcaaga		ggggag		..tattactacggtag.......	IGHD1-1	P	15
IGHV1-61	tgtgcaaga		agg		......atgattacgac	IGHD2-4	P	14
IGHV1-63	tgtgcaaga		tc		.......ctacggtag.......	IGHD1-1	P	10
IGHV1-74	tgtgc....		cct		agacagctcaggctac	IGHD3-2	P	13
IGHV1-76	tgtgcaaga	t	tc				P	7
IGHV1-81	tgtgcaaga		g		.........atggtg........	IGHD1-1	P	9
IGHV1-81	tgtgcaaga		g		......actacggtagtagctac	IGHD1-1	P	17
IGHV1-81	tgtgcaaga		aagaggga		cctactata........	IGHD3-1	P	15

B1-8i$\Delta E\mu^a$/*Igh*^{b} preB cells V_HJ558-D_H-J_H4 rearrangements

V name	REGION	P	N1	P	D-REGION	D name		CDR3 length
IGHV1-9	tgtgcaag.		cccc		............cgaggg.	IGHD2-14	P	9
IGHV1-18	tgtgcaaga		aggggg		.ctactactatt.....	IGHD2-4	P	12
IGHV1-19	tgtgcaaga		ggggg		.......tgattacgac	IGHD2-4	P	16
IGHV1-22	tgtgcaaga		ggg		...attactacggtag.......	IGHD1-1	P	12
IGHV1-22	tgtgcaaga				cacccggg..	IGHD4-1	P	10
IGHV1-22	tgtgcaaga				tttattactacggtagtagctac	IGHD1-1	P	14
IGHV1-26	tgtgcaaga		tcgggg		........gattacgac	IGHD2-4	P	16
IGHV1-26	tgtgcaaga				.......aggtactacgg.	IGHD2-14	P	11
IGHV1-26	tgtgcaaga				.....tgggac	IGHD4-1	P	12
IGHV1-36	tgtgtaaga		g		........cggg....	IGHD3-2	P	8
IGHV1-50	tgtgcaaga		c		.tttttactacggtagtag....	IGHD1-1	P	14
IGHV1-53	tgtgcaaga				......atggttact..	IGHD2-3	P	13
IGHV1-53	tgtgcgaga		gggggggttg		.....gatggttact..	IGHD2-3	P	15
IGHV1-53	tgtgcaaga		ggggggg		.ttattactacggtagtagc...	IGHD1-1	P	19
IGHV1-55	tgtgcaaga		agggg		.......tagcctgagctgt.........	IGHD6-1	P	15
IGHV1-55	tgtgcaaga		cctcttc		.ttagtactacggtagtagctac	IGHD1-1	P	17
IGHV1-55	tgtgcaa..		c		ccaag............	IGHD2-11	P	10
IGHV1-56	tgtgcaaga		a				P	8
IGHV1-58	tgtgcaaga		t		........ggttctatgg.	IGHD2-14	P	8
IGHV1-58	tgtgcaaga		g		...attactacggtagtagc...	IGHD1-1	P	16
IGHV1-58	tgtgcaaga		g		...attactacggtagtagc...	IGHD1-1	P	16
IGHV1-58	tgtgcaaga	t	gggggg		tctatga..........	IGHD2-3	P	11
IGHV1-61	tgtgcaaga				.ctcct............	IGHD3-1	P	9
IGHV1-69	tgtgcaaga		gaaat		.......tggttactac	IGHD2-3	P	15
IGHV1-69	tgtgcaaga		tcggggg		...attactacggtagtagc...	IGHD1-1	P	22
IGHV1-72	tgtgcaaga				.....tggaac	IGHD4-1	P	7
IGHV1-75	tgtgcaag.		gga		..........cctgagctgt.........	IGHD6-1	P	13
IGHV1-76	tgtgca...		c		....ctatgattacg..	IGHD2-4	NP	
IGHV1-77	tgtgcaaga		tcgaaagc		..tattactacggtagtagctac	IGHD1-1	P	17
IGHV1-77	tgtgcaaga		ggggag	a	tttattactacggtagtagc...	IGHD1-1	P	19
IGHV1-78	tgtgcaaga		aggggatttg		......atgattacgac	IGHD2-4	P	14
IGHV1-81	tgtgcaaga		ggaaa		.......tagcctgagctgt.........	IGHD6-1	P	15
IGHV1-81	tgtgcaaga		gaaagggtttat		..atacc...	IGHD5-2	P	8
IGHV1-81	tgtgcaaga		aagcc		..tattactacggtag.......	IGHD1-1	P	13
IGHV1-81	tgtgcaaga		acctcggt		tttatt..................	IGHD1-1	P	13
IGHV1-84	tgtgcaaga		agcc		cctact...........	IGHD3-1	P	12
IGHV1-85	tgtgcaaga		gtgc		...acagggagg......	IGHD3-3	P	12

Figure 3.13 Usage of V_H in V_H7183-D_H-J_H4 rearrangements in pre-B cells of B1-8i^a/*Igh*^{b} and B1-8iΔEμ^a/*Igh*^{b} mice

V_H usage in the V_H7183-D_H-J_H4 rearrangements presented in Table 3.4 was analyzed. The proportion of each V_H7183 family member used in these rearrangements is shown. Other = V_H from other family.

Figure 3.13 Usage of V_H in V_H7183-D_H-J_H4 rearrangements in pre-B cells of B1-8i^a/*Igh*^{b} and B1-8iΔEμ^a/*Igh*^{b} mice

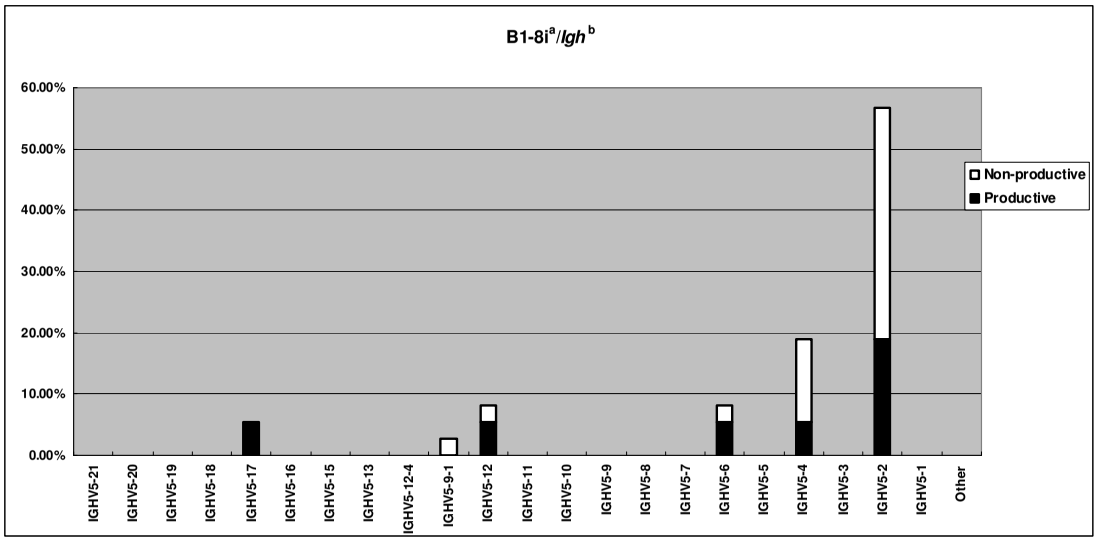

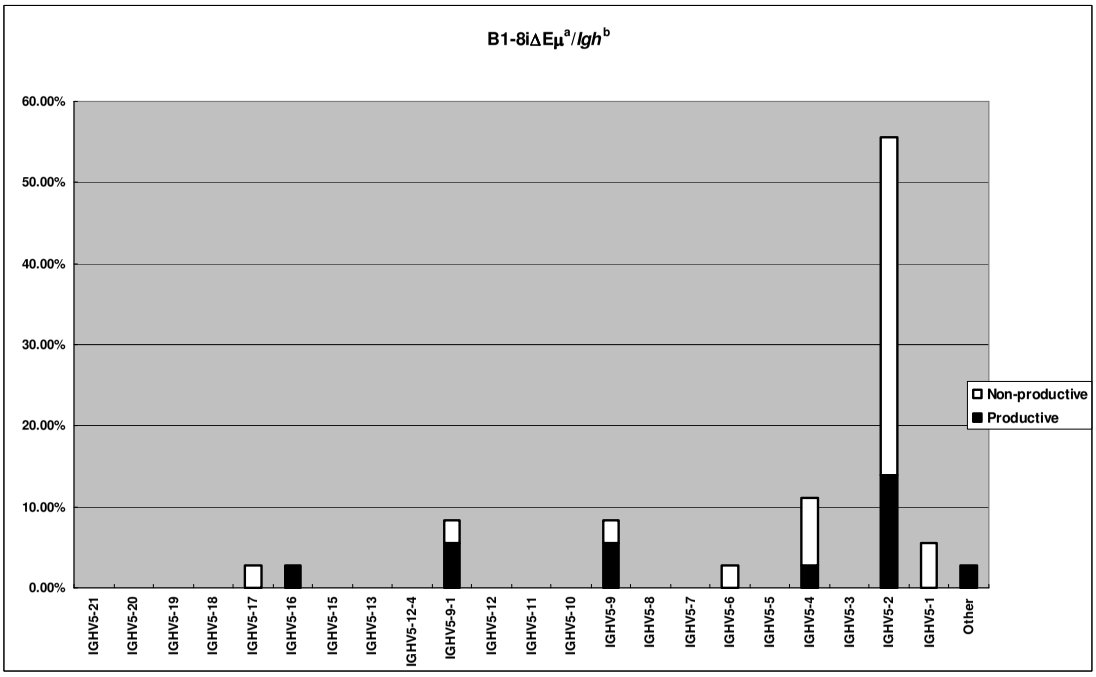

Figure 3.14 Usage of D_H in V_H7183-D_H-J_H4 rearrangements in pre-B cells of B1-8i^a/*Igh*^{b} and B1-8iΔEμ^a/*Igh*^{b} mice

D_H usage in the V_H7183-D_H-J_H4 rearrangements presented in Table 3.4 was analyzed. The proportion of each D_H used in these rearrangements is shown. ND = cases in which D_H can not be determined.

Figure 3.14 Usage of D_H in V_H7183-D_H-J_H4 rearrangements in pre-B cells of B1-8i^a/*Igh*^{b} and B1-8i$\Delta E\mu^a$/*Igh*^{b} mice

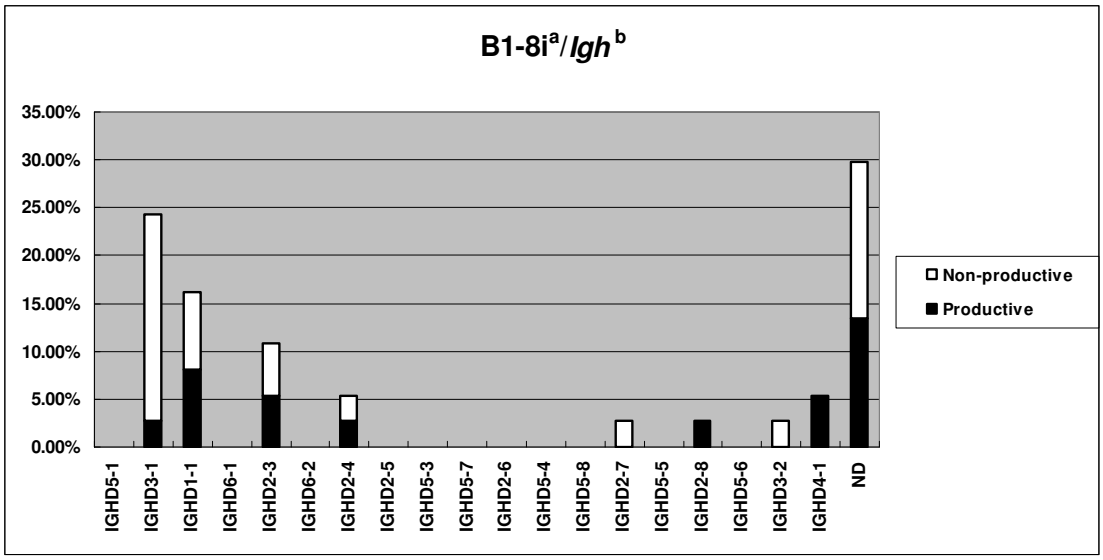

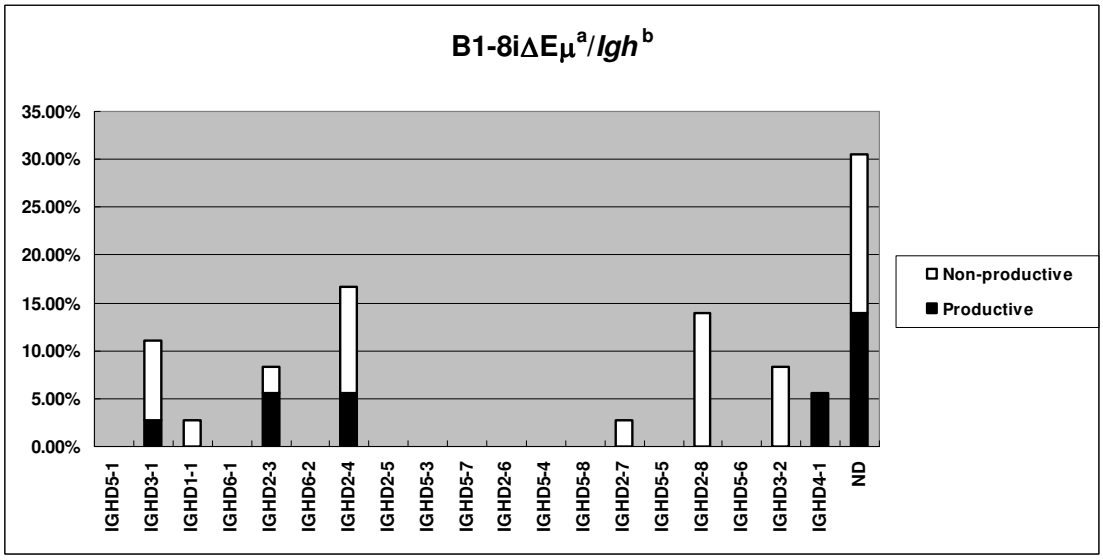

Figure 3.15 Length of CDR3 in V_H7183-D_H-J_H4 rearrangements in pre-B cells of B1-8i^a/*Igh*^{b} and B1-8iΔEμ^a/*Igh*^{b} mice

The length of CDR3 of the productive V_H7183-D_H-J_H4 rearrangements presented in Table 3.4 and from some wild-type pre-B cells (data not shown), was analyzed. The proportion of rearrangements with various CDR3 length (as shown on X axis) is shown.

Figure 3.15 Length of CDR3 in V_H7183-D_H-J_H4 rearrangements in pre-B cells of B1-8i^a/*Igh*^{b} and B1-8iΔEμ^a/*Igh*^{b} mice

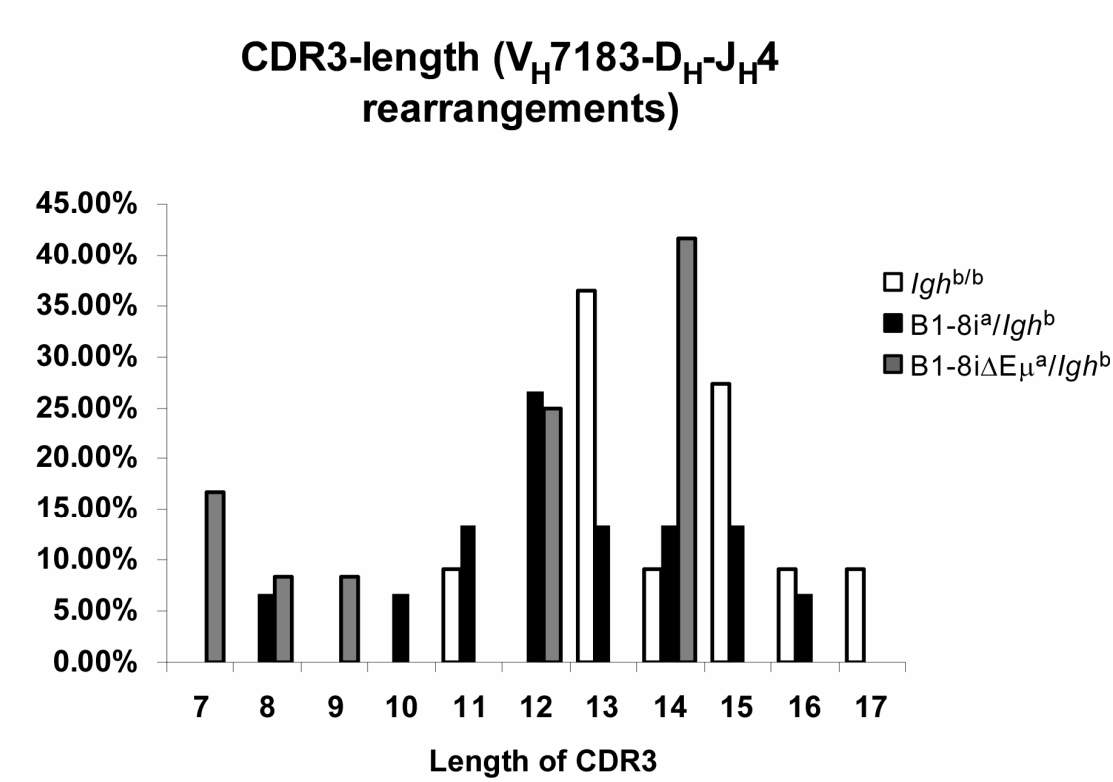

Figure 3.16 Number of N nucleotides at V-DJ junction of V_H7183-D_H-J_H4 rearrangements in pre-B cells of B1-8i^a/*Igh*^{b} and B1-8iΔEμ^a/*Igh*^{b} mice.

The number of N nucleotides at V-DJ junction of the V_H7183-D_H-J_H4 rearrangements presented in Table 3.4 was analyzed. The proportion of V-DJ junctions with various numbers of N nucleotides (as shown on X axis) is shown.

Figure 3.16 Number of N nucleotides at V-DJ junction of V_H7183-D_H-J_H4 rearrangements in pre-B cells of B1-8i^a/*Igh*^{b} and B1-8iΔEμ^a/*Igh*^{b} mice.

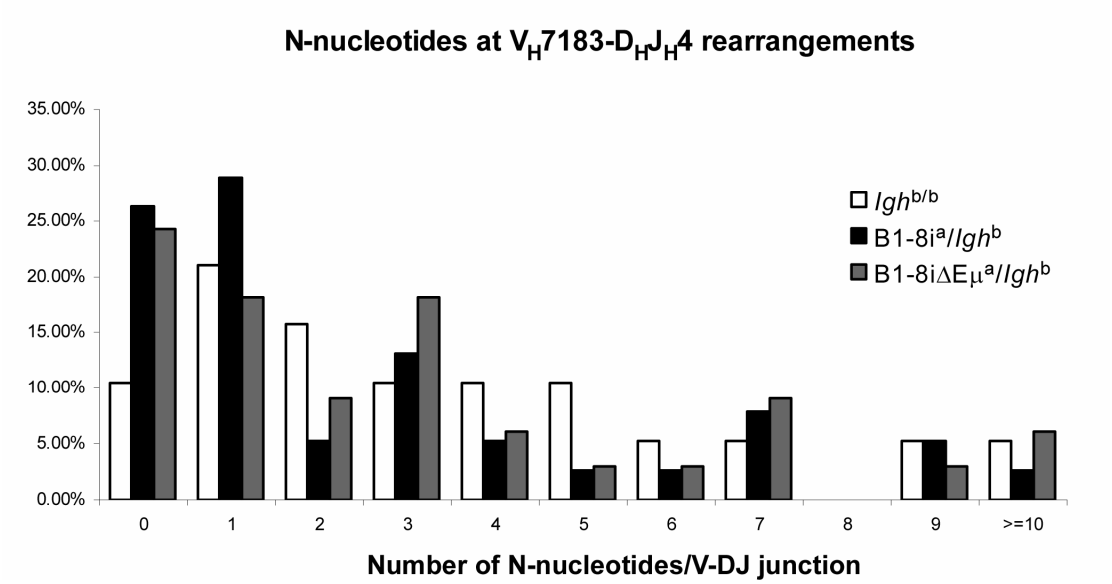

(B1-8i$\Delta E\mu^a$/*Igh*^{b}) but not the other (B1-8i^a/*Igh*^{b}). One question we asked was whether the V_H gene rearrangements we were detecting in the pre-B cells of these two mouse lines differed in some fundamental way (e.g. frequency of productive rearrangements). Pre-B cells were harvested from mice of both genotypes, DNA isolated, and assembled V_H genes from the *Igh*^{b} allele cloned and sequenced. Fifteen out of 36 unique V_H7183-D_H-J_H4 rearrangements cloned from pre-B cells of the B1-8i^a/*Igh*^{b} genotype, were both in-frame and lacked a stop codon (productive rearrangements) (Table 3.3 and Table 3.4). Similarly, 12 out of 36 unique V_H7183-D_H-J_H rearrangements isolated from B1-8i$\Delta E\mu^a$/*Igh*^{b} pre-B cells were productive (Table 3.3 and Table 3.4). Interestingly, V_HJ558-D_H-J_H4 rearrangements cloned from pre-B cells of both B1-8i^a/*Igh*^{b} and B1-8i$\Delta E\mu^a$/*Igh*^{b} mice were mostly productive (16/17 from B1-8i^a/*Igh*^{b} pre-B cells, and 36/37 from B1-8i$\Delta E\mu^a$/*Igh*^{b} pre-B cells), and this was also true for wild-type pre-B cells (24/27 productive) (Table 3.3, 3.5).

Closer examination of productive V_H7183-D_H-J_H4 rearrangements showed no fundamental difference between those isolated from B1-8i^a/*Igh*^{b} and B1-8i$\Delta E\mu^a$/*Igh*^{b} animals, either in the 7183 V_H family members used (Table 3.4, Figure 3.13), the D_H segments used (Table 3.4, Figure 3.14), the length of CDR3 (Table 3.4, Figure 3.15), or the number of N-nucleotides in the V-D junctions (Table 3.4, Figure 3.16). N-nucleotides were found in the V-D junctions in greater than 70% of the sequences analyzed, and 40% of these had 3 or more N-nucleotides at this junction. In junctions with N-nucleotides, the average length was 3.5 (B1-8i^a/*Igh*^{b} mice) and 4.3 (B1-8i$\Delta E\mu^a$/*Igh*^{b} mice) nucleotides. Notably,

this contrasts with light chain genes where N-nucleotides are much more rare (~10% of junctions) and are found in much lower numbers/junction (generally 1 or 2) (Victor et al. 1994). We conclude that the precursors to double-producers can be found in bone marrow from both B1-8i$\Delta E\mu^a$/*Igh*^{b} and B1-8i^a/*Igh*^{b} mice and that, as discussed below, V_H assembly on the *Igh*^{b} allele has likely occurred prior to the pre-B cell stage.

To test the possibility that presence of Eμ on the B1-8i^a allele was in some way prohibiting surface expression of a μ-chain from the other, productively-rearranged *Igh*^{b} allele, we sorted IgM^{a+b-} cells (single-producers) from both B1-8i$\Delta E\mu^a$/*Igh*^{b} and B1-8i^a/*Igh*^{b} mice and cloned V_H7183-D_H-J_H rearrangements from them. In an initial experiment focusing only on B1-8i$\Delta E\mu^a$/*Igh*^{b} mice, 4 out of 5 V_H7183-D_H-J_H rearrangements cloned from IgM^{a+b-} cells were unproductive, while 7 of 7 V_H7183-D_H-J_H rearrangements cloned from IgM^{a+b+} cells (double-producers) were productive. In a second experiment involving both B1-8i$\Delta E\mu^a$/*Igh*^{b} and B1-8i^a/*Igh*^{b} mice, all V_H7183-D_H-J_H rearrangements cloned from IgM^{a+b-} cells (single-producers) were unproductive (14 unique clones from B1-8i$\Delta E\mu^a$/*Igh*^{b} cells and 18 unique clones from B1-8i^a/*Igh*^{b} cells). Surface expression, therefore, faithfully reflects VDJ assembly status (i.e, productive or non-productive rearrangements) on the wild-type *Igh*^{b} allele, providing no support for a model of Eμ-dependent and allele-specific silencing.

In summary, analyses of the wild-type *Igh*^{b} allele in both B1-8i^a/*Igh*^{b} and B1-8i$\Delta E\mu^a$/*Igh*^{b} mice clearly demonstrate that assembly of a functional *Igh* gene

Figure 3.17 Genotyping B1-8iΔEμ mice with wild-type or mutant *Rag1* gene by PCR.

Upper: primer Rag1-F and Rag-R were used to distinguish *Rag1*+ and *Rag1*- mice – a ~1.5kb PCR product can be obtained only from wild-type *Rag1*+ DNA. *Lower*, primer Junction, #8 and #2 were used to genotype immunoglobulin heavy chain alleles as shown in Figure 3.3. Genotype of each sample is shown at bottom.

Figure 3.17 Genotyping B1-8iΔEμ mice with wild-type or mutant *Rag1* gene by PCR

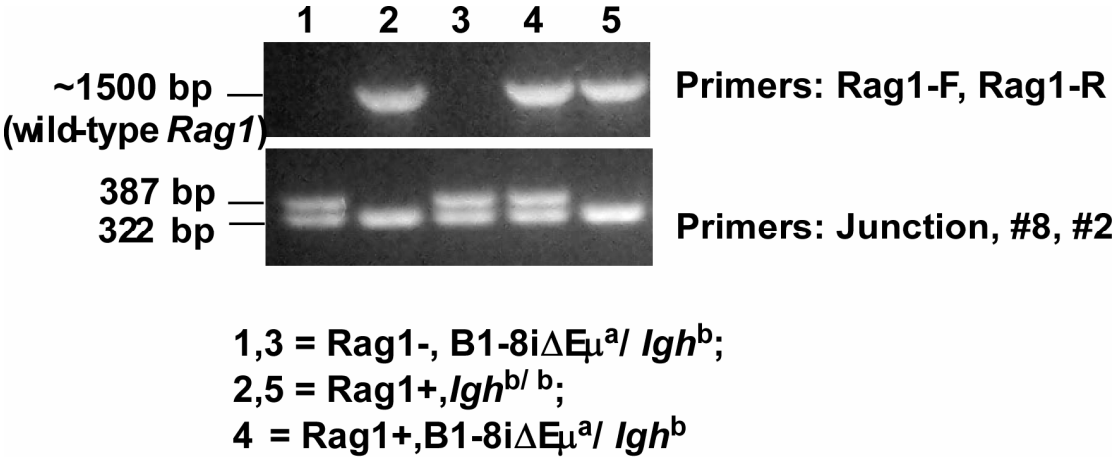

Figure 3.18. Igμ transcription and cytoplasmic Igμ protein levels in pre-B cells of mutant mice.

(A) B220+ lymphocytes from bone marrow of Rag1-deficient *Igh*$^{b/b}$, B1-8i^{a}/*Igh*^{b}, and B1-8iΔEμ^{a}/*Igh*^{b} mice were analyzed for size (forward scatter) and for CD43 expression by FACS™ . Data shown are representative of three individual mice of each genotype analyzed. (B) Igμ mRNA levels in pre-B cells isolated from the bone marrows of mice of the indicated genotypes. Data shown were generated by quantitative RT-PCR, using *hgprt1* mRNA for normalization (see Experimental Procedures), and include two experiments analyzing a total of 5 individual animals of each genotype. Negative controls were mRNA isolated from pro-B cells of an *Igh*$^{b/b}$, *Rag1*$^{-/-}$ littermate and mRNA from C57BL/6 heart tissue (*Igh*$^{b/b}$, *Rag1*$^{+/+}$). Statistical significance ($p = 0.027$) obtained by two-tailed t-test. (C) Cytoplasmic Igμ levels in B220+ bone marrow cells of Rag1$^{-/-}$ mice. Bone marrow cells of indicated genotypes stained with antibody to B220 and then fixed and stained for cytoplasmic Igμ. *Left:* Histograms of cytoplasmic Igμ *Right:* mean Igμ fluorescence in pre-B cells from multiple mice (n=number mice analyzed).

Figure 3.18. Igμ transcription and cytoplasmic Igμ protein levels in pre-B cells of mutant mice.

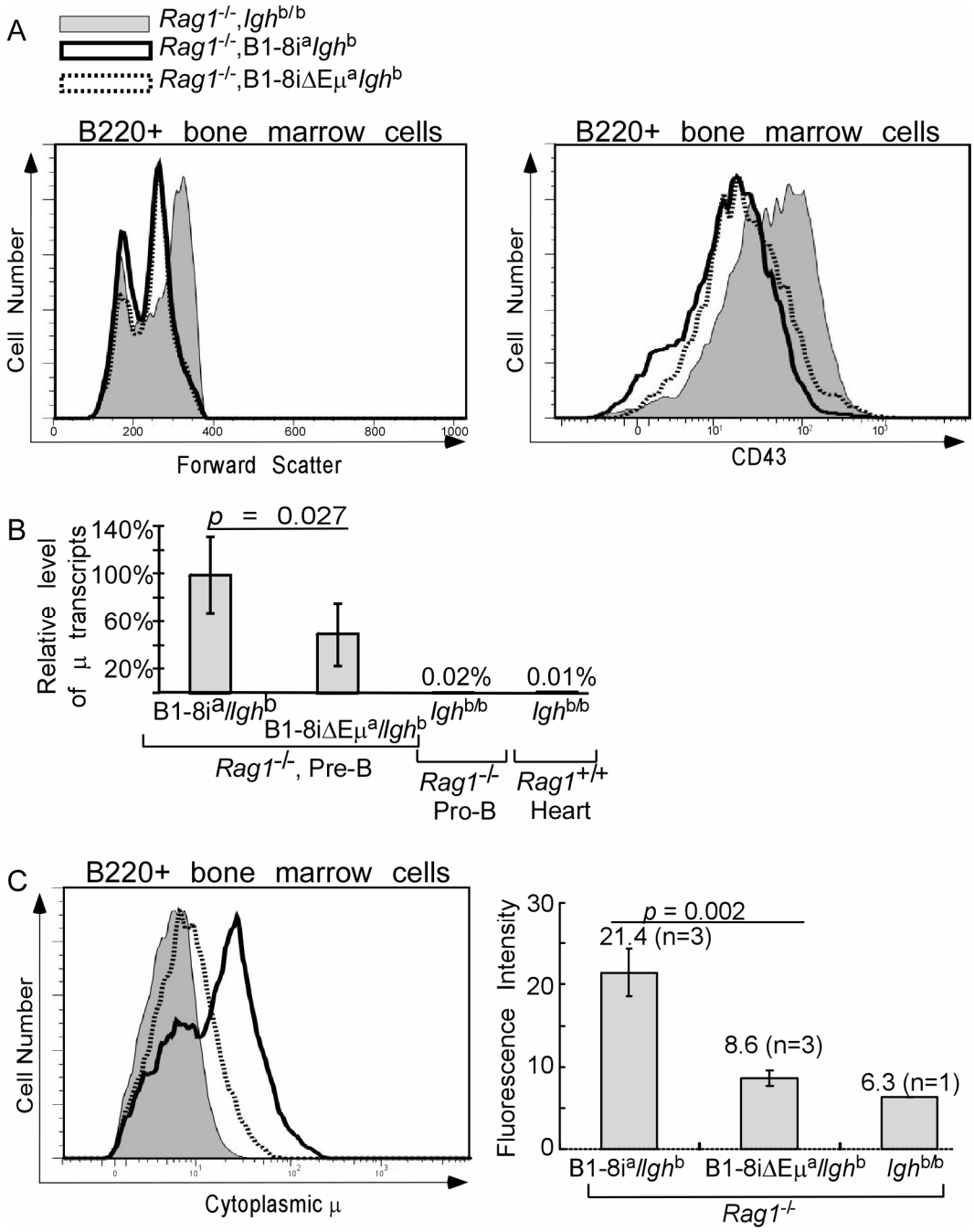

on one allele does not fully block V-DJ assembly on the other. Rather, V-DJ joining on the second allele occurs at a frequency sufficient to generate a subset of pre-B cells that express μ-heavy chain from both alleles. The fact that such double-producing cells do not progress to the immature B cell stage in B1-8i^{a}/*Igh*^{b} animals but do so in B1-8iΔEμ^{a}/*Igh*^{b} mice supports the existence of a previously unappreciated and Eμ-dependent "checkpoint" for allelic exclusion.

8. In pre-B cells, absence of Eμ results in lower μ mRNA levels

In an attempt to understand the mechanism through which Eμ might influence the development and selection of precursor B cells, we compared levels of μ mRNA generated from the B1-8i^{a} and B1-8iΔEμ^{a} alleles, respectively, in pre-B cells. To enrich for pre-B cells, B1-8i^{a} and B1-8iΔEμ^{a} mice were backcrossed to Rag1$^{-/-}$ mice to generate B1-8i^{a}/*Igh*^{b} and B1-8iΔEμ^{a}/*Igh*^{b} heterozygous mice that lacked Rag1 activity. PCR that amplifies a ~1.5kb PCR product only from the wild-type Rag-1 locus was used to distinguish Rag1+ and Rag1-deficient mice (Figure 3.17, upper reactions with primer Rag1-F and Rag1-R).

In both Rag1-deficient B1-8i^{a}/*Igh*^{b} and B1-8iΔEμ^{a}/*Igh*^{b} mice, B cell development was arrested at the pre-B cell stage because cells in these mice are incapable of assembling Ig light chain genes. Age-matched mice of each genotype were sacrificed and B220+ bone marrow cells isolated (see Experimental Procedures). As expected, no IgM+ cells were present in these bone marrow cells, and the bulk of cells were smaller and expressed lower levels of CD43 than comparable cells from *Igh*$^{b/b}$, Rag1$^{-/-}$ littermates, consistent with

their having progressed to the pre-B cell stage (Figure 3.18A). Total RNA was isolated from the B220+ bone marrow cells of B1-8i^{a}/*Igh*^{b}; Rag1$^{-/-}$ and B1-8iΔEμ^{a}/*Igh*^{b}; Rag1$^{-/-}$ mice (and from *Igh*$^{b/b}$, Rag1$^{-/-}$ littermates, as controls) and was quantified by real-time RT-PCR (5' primer for unique VDJ junction of V_HB1-8; 3' primer for C_H1 exon of Cμ, see Materials and Methods (Chapter 2).

As shown in Figure 3.18B, steady-state μ mRNA levels were roughly twice as high in cells expressing an *Igh*^{a} allele that retained Eμ than in cells expressing an Eμ-deficient allele. This is in contrast to the finding in splenic B cells where the Eμ-deficient allele produced as much or more Igμ mRNA than its Eμ-containing counterpart (Figure 3.5B, left). Bone marrow cells from both genotypes were then analyzed for cytoplasmic Igμ protein. As shown in Figure 3.18C, protein levels mirrored the mRNA levels, documenting an ~2-fold decline in Igμ protein in the pre-B cells of mice that lacked Eμ on the functional IgH allele. At this developmental stage, when pre-BCR and BCR-mediated signals are dictating B cell fate, μ heavy chain levels are measurably influenced by the presence/absence of Eμ.

9. Evidence of increased light chain editing in the developing B cells of B1-8iΔEμ^{a}/*Igh*^{b} mice

The reduced Igμ levels in the pre-B cells of B1-8iΔEμ^{a}/*Igh*^{b} mice suggested that these levels might be suboptimal for pre-BCR-mediated clonal expansion and/or BCR-mediated selection into the immature B cell pool. Increased survival of precursors expressing both alleles (double-producers) might reflect a need for

Figure 3.19 Increased frequency of λ-positive splenic B cells in B1-8iΔEμ^{a}/*Igh*^{b} mice.

Spleen cells were stained for both Igκ and Igλ and percentage λ+ cells calculated as λ/(κ+λ). Data pooled from three experiments. Nb = number mice analyzed. P-values calculated by two-tailed test.

Figure 3.19 Increased frequency of λ-positive splenic B cells in B1-8iΔEμ^a/*Igh*^{b} mice.

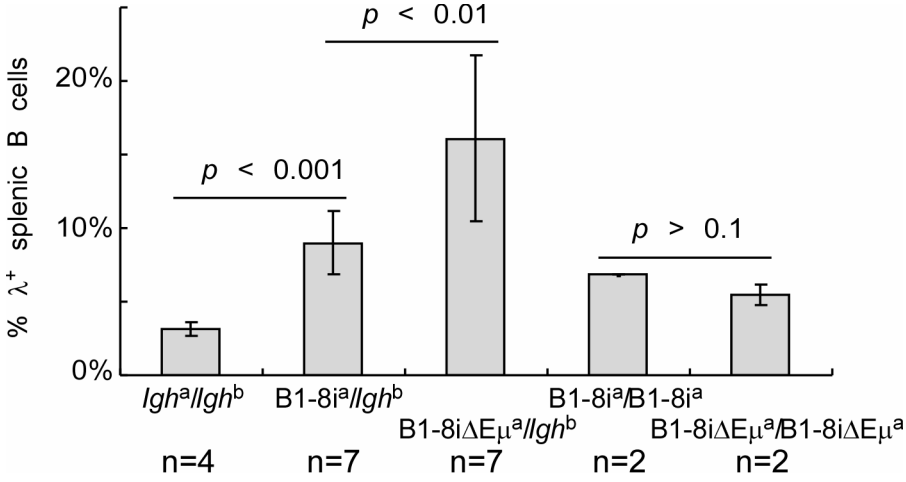

increased Igμ levels achieved by bi-allelic expression. If so, it might be expected that IgM^{a+b-} cells circumvented this problem through alternate means, perhaps by selection for light chains that yielded BCRs with superior signaling properties. This would necessitate receptor editing, and one measure of receptor editing within a population of B cells is the frequency of Igλ-positive cells.

In normal mice, Igλ+ cells make up only ~5% of splenic B cells, and analyses of the Igκ locus in Igλ-producing cells suggest that Igλ genes are usually assembled only after the opportunity to express one of the two available Igκ alleles has been exhausted (Nemazee 2006; Casellas et al. 2007; Monroe and Dorshkind 2007). We looked for Igλ-expressing splenic B cells in wild-type, B1-8iΔEμ^{a}/*Igh*^{b}, and B1-8i^{a}/*Igh*^{b} mice (Figure 3.19). Both knock-in mice had higher levels of Igλ –expressing B cells than did wild-type mice as might be expected because of the limitation to a single heavy chain. However, the frequency of Igλ-producers among B1-8iΔEμ^{a}/*Igh*^{b} splenic B cells was significantly higher than that in B1-8i^{a}/*Igh*^{b} mice (average of 16% vs 9%; p=0.01). Importantly, and consistent with the above-stated hypothesis, no such difference was observed when mice homozygous for each of these mutant alleles were compared (Figure 3.19).

10. Double-producers in B1-8iΔEμ^a/*Igh*^{b} mice are largely of the marginal zone phenotype in spleen and the B1 B cell phenotype in the peritoneal cavity

As previously shown in Figure 3.6, double-producers were found in large numbers in the peritoneal cavity of B1-8iΔEμ^a/*Igh*^{b} mice. Three kinds of phenotypically and functionally distinct B cell populations have been described in both mice and people: follicular B cells (also known as conventional B cells or B-2 B cells), marginal zone (MZ) B cells, and B-1 B cells. Follicular and MZ B cells, as their names imply, occupy distinct regions in the spleen. Follicular B cells make up the majority of B cells in blood, lymph nodes, and spleen. The peritoneal cavity, on the other hand, is largely populated by B-1 B cells, although B-1 B cells are also found in small numbers elsewhere. B-1 B cells are subdivided into those that do (B1a) and those that do not (B1b) express CD5.

In spleen, monoclonal antibodies specific for CD23, CD21, Igδ and Igμ were used to distinguish MZ (CD23^{lo}, CD21^{hi}, IgD^{lo}, IgM^{hi}) and follicular B cells (CD23^{hi}, CD21^{lo}, IgD^{hi}, IgM^{+}) (Martin and Kearney 2002). These phenotypes were determined for both single- and double-producers from the B1-8iΔEμ^a/*Igh*^{b} heterozygous mice (Figure 3.20). While single-producers were predominantly CD23^{hi}, CD21^{lo}, and IgD^{hi} (follicular cell phenotype), double producers were almost equally divided into cells with the follicular and MZ phenotypes, respectively. Consistent with the fact that these cells expressed two Igμ alleles, IgM expression was approximately twice the level of IgM^a+ single producers (Figure 3.20A).

Figure 3.20. Surface phenotype of double-producers in spleen and peritoneal cavity of B1-8iΔEμ^a/*Igh*^{b} mice.

(A) CD23, CD21, IgD, and IgM expression on splenic IgM^{a+b-} cells (single-producers; shaded curve) and IgM^{a+b+} cells (double-producers; dark line). Non-B cells were included as controls (IgM^{a-b-}; dotted line). Cells were gated on the basis of IgM^a and IgM^b expression and histograms generated for expression of the third surface marker. (B) IgD expression on peritoneal cells (plotted versus forward scatter = FSC). % total cells in three IgD gates (negative, dull, high) provided. (C) IgD levels on peritoneal cells gated as IgM^{a-b-}, IgM^{a+b-}, and IgM^{a+b+}. *Left*: Contour plot of anti-IgM^a and anti-IgM^b staining, with gates (and % total cells) indicated. *Right*: Histogram of IgD levels on gated populations, legend as in (A). (D) IgM allotype expression on peritoneal cells. Cells were stained with antibodies to CD5, IgM^a, and IgM^b. Cells gated on the basis of CD5 and IgM^a expression (left) were analyzed for IgM^a and IgM^b expression (two right plots).

Figure 3.20. Surface phenotype of double-producers in spleen and peritoneal cavity of B1-8i$\Delta E\mu^a$/*Igh*^{b} mice.

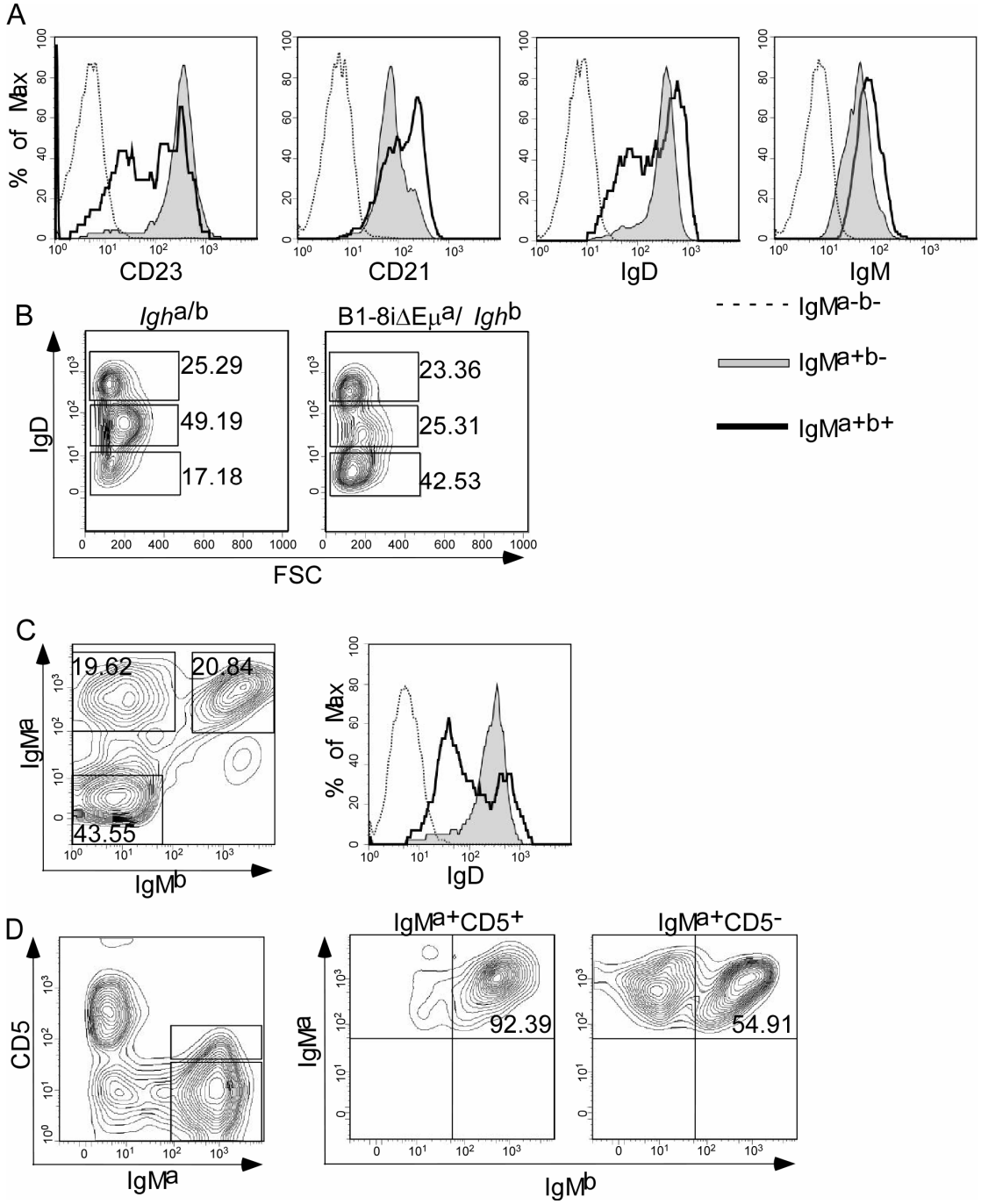

Peritoneal cells were stained with antibodies specific for Igδ, CD5, and Igμ to distinguish B-1 cells (IgD^{dull} $CD5^{+/-}IgM^{hi}B220^{lo}$) from conventional, B-2 B cells ($IgD^{hi}CD5^{-}IgM^{+}B220^{+}$). The proportion of IgM+ cells in the peritoneal cavity was decreased in both B1-8i$\Delta E\mu^{a}$/*Igh*^{b} and B1-8i^{a}/*Igh*^{b} animals relative to wild-type (~60% vs ~80%; data not shown). Among these cells, the proportion that were IgD^{dull} (B1 cells) was also reduced relative to wild-type (Figure 3.20B, compare center gates for *Igh*$^{a/b}$ and B1-8i$\Delta E\mu^{a}$/*Igh*^{b} animals). This last observation is consistent with the earlier finding that B-2 cells predominate in mice carrying a knock-in of the B1-8i V_H gene (Lam and Rajewsky 1999). When we analyzed the peritoneal cells for IgM^{a} and IgM^{b}, however, IgM^{a+} single-producers were almost uniformly IgD^{hi} (B2 phenotype), while a large proportion of the double-producers (IgM^{a+b+}) were IgD^{dull} (B1 phenotype) (Figure 3.20C). Strikingly, $CD5^{+}$ B cells were almost exclusively (~90%) double producers (Figure 3.20D). In summary, B cells expressing both *Igh* alleles were over-represented in the MZ compartment of the spleen and in the B1 B cells of the peritoneal cavity.

Based on the paucity of double producers in bone marrow at the immature B cell stage, and the extreme enrichment of double producers in B-1 cells, it was hypothesized that precursors to B-1 cells might have different regulation of allelic exclusion in B1-8i$\Delta E\mu^{a}$/*Igh*^{b} mice. There has been considerable controversy about whether B1 B cells constitute a separate lineage of cells, but transplantation experiments show that progenitors to B1 B cells predominate in fetal liver (as compared to adult bone marrow) (Hardy 1991; Hardy and Hayakawa 1991). If the double-producers were uniquely arising in this subset of cells because of a defect

in allelic exclusion only in this lineage, double-producers might be expected at higher numbers at these early stages in mouse development. To test this hypothesis, fetal liver from six B1-8i$\Delta E\mu^a$/*Igh*^{b} embryos (d16~d18) were examined for IgM+ cells. B220+ cells were gated for analysis of the two *Igh* allotypes. While there were IgM+ cells in the fetal liver at this stage in development, none of these cells expressed both IgM^a and IgM^b; rather, all expressed only IgM^a (Figure 3.21A, adult bone marrow shown as comparison)**.** To determine whether double-producers dominate the early migrants to spleen, spleen cells were isolated from newborn mice. As illustrated in Figure 3.21B and quantified in Figure 3.6C, double-producers in newborn spleen made up ~5% of IgM+ cells, much as in the immature B cells of bone marrow. Therefore, there is no enrichment of double producers in B cells generated at these early stages of mouse development. Rather, it appears that the large number of double-producers found in both spleen and peritoneal cavity results from peripheral expansion of a small pool of cells arising in the bone marrow and likely also in fetal liver.

Figure 3.21 Ontogeny of double-producers in heterozygous B1-8i$\Delta E\mu^a$/*Igh*^{b} mice.

(A) IgM allotype expression in adult bone marrow and fetal liver of B1-8i$\Delta E\mu^a$/*Igh*^{b} mice. Cells isolated from one adult bone marrow or pooled from 6 fetal livers (16~18 day embryos) were stained with FITC-conjugated anti-mouse IgM^b, PE-conjugated anti-mouse IgM^a, and APC-conjugated anti-mouse B220. Plots shown are gated for B220$^+$ cells. Numbers shown are IgM^{a+b+}/IgM+ cells x 100. (B) IgM allotype expression in splenic lymphocytes of a newborn C57BL/6 (*Igh*$^{b/b}$) mouse, a B1-8i$\Delta E\mu^a$ homozygous mouse, and a B1-8i$\Delta E\mu^a$ /*Igh*^{b} heterozygous mouse (representative of two mice analyzed). Spleen cells from 2~3 day-old newborn mice were stained with FITC-conjugated anti-mouse IgM^b and PE-conjugated anti-mouse IgM^a. Numbers shown are IgM^{a+b+}/IgM+ cells x 100. *In these cases, the number shown is IgM^{a+b+}/(IgM^{a+b-}+IgM^{a+b+}) X 100 since the signals in the lower right quadrant are due to background staining (present in mice that lack *Igh*^{b} allele, middle panel).

Figure 3.21 Ontogeny of double-producers in heterozygous B1-8i$\Delta E\mu^a$/*Igh*^{b} mice.

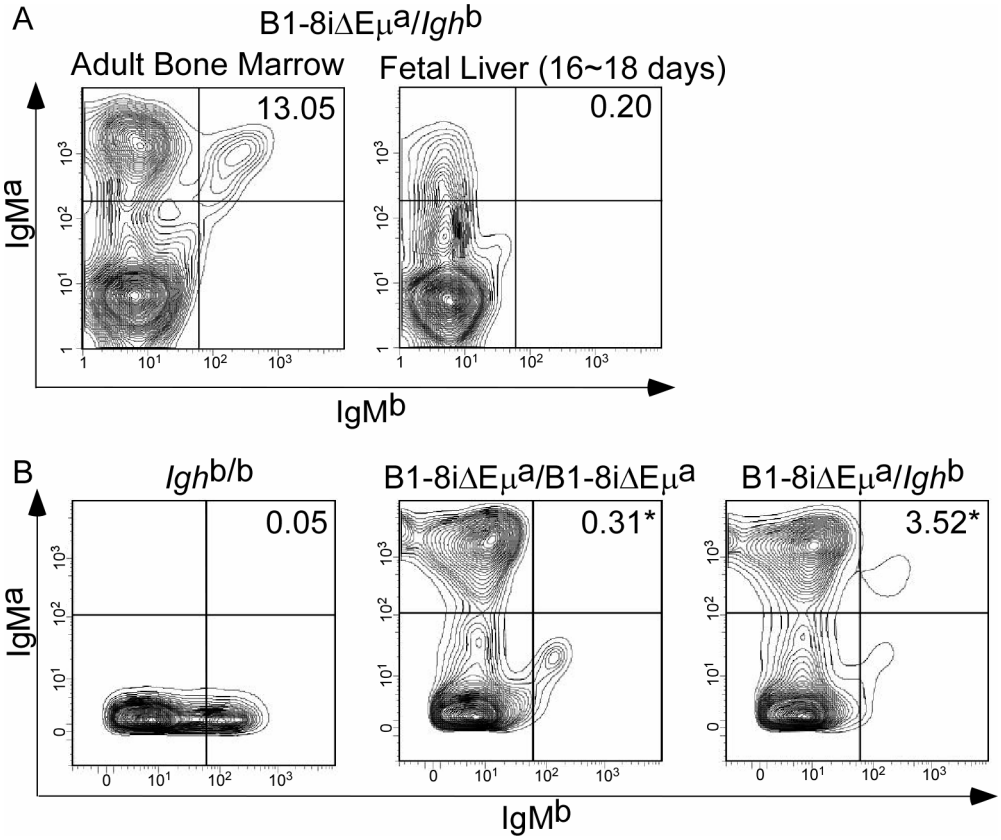

Discussion

The present study has shown that the intronic enhancer Eμ serves a critical function even after V_H gene (VDJ) assembly is complete. In mice heterozygous for an Eμ-deficient, but productively rearranged IgH gene (B1-8iΔEμ^a/*Igh*^{b}), large numbers of IgH double-producing cells arose in peripheral tissues, breaking the rules of allelic exclusion. In contrast, a matched mouse line with the same V_H knock-in but with Eμ present (B1-8i^a/*Igh*^{b}) lacked these double-producing cells. In both animals, there was evidence that the Igμ product of the assembled IgH gene was signaling a shut-down of V_H assembly on the *Igh*^{b} allele, the primary mechanism postulated to insure IgH allelic exclusion (Figure 3.9, 3.11, and 3.12). The efficiency of this feedback inhibition was unaffected (or mildly affected at most) by the presence or absence of Eμ.

This latter finding was unexpected. Eμ was initially discovered as a transcriptional enhancer and believed to serve as such in newly-formed IgH genes (Banerji et al. 1983; Gilles and Tonegawa 1983; Neuberger 1983). In that capacity, Eμ could dictate pre-BCR levels and, thereby, signaling strength in a developing B lymphocyte. In Eμ's absence, Igμ might not reach the levels required to signal an end to V-DJ recombination. But it was not at the pro- or pre-B cell stages that the B1-8iΔEμ^a/*Igh*^{b} and B1-8i^a/*Igh*^{b} mice differed. Pre-B cells of both mouse strains were dominated by those that had undergone D-J, but not V-DJ, rearrangement on their *Igh*^{b} alleles, demonstrating that feedback signals inhibiting this last step in recombination were no less efficient in the absence of Eμ.

Both B1-8iΔEμ^a/*Igh*^{b} and B1-8i^a/*Igh*^{b} mice contained rare pre-B cells with V-DJ rearrangement on their *Igh*^{b} alleles. Sequence analyses of these rearrangements revealed abundant N-nucleotides in the V-D junction (Table 3.4, 3.5, and Figure 3.16), suggesting that they occurred in pro-B cells (the only developmental stage at which terminal transferase (TdT) is expressed) (Li et al. 1993; Victor et al. 1994). Chromatin remodeling studies have documented that pro-B cells are the only developing B cells with "contracted" *Igh* alleles, facilitating V-DJ rearrangements, especially those involving distal V_H gene segments (e.g. V_HJ558) (Roldan et al. 2005). V_H J558-DJ rearrangements on the *Igh*^{b} allele were easily detected in these pre-B cells. These results suggest that subsequent to V_H gene assembly, there is sufficient delay in the assembly of, or signaling through, the pre-BCR to allow RAG-mediated rearrangements to take place in a minority of cells before they transition to the pre-B cell stage.

The potential to generate double-producers was the same in B1-8iΔEμ^a/*Igh*^{b} and B1-8i^a/*Igh*^{b} animals, so why did immature B cells with this phenotype arise only in mice lacking Eμ on the knock-in allele? Signaling through the pre-BCR is required not only to down-regulate the RAG genes (terminating V-DJ recombination), but also to promote cell proliferation and differentiation to the pre-B cell stage (reviewed in Monroe and Dorshkind 2007). If the reduced Igμ chain level in B1-8iΔEμ^a/*Igh*^{b} pro-B cells resulted in pre-BCR signals that were suboptimal for promoting this transition, we might expect that precursors to double-producers (expressing Igμ from two alleles, one with Eμ present) would be

Figure 3.22. Model of Eμ-dependent positive selection

In B1-8i^{a}/*Igh*^{b} mice, newly emerging immature B cells that express either only the knockin allele (V_HB1-8(Eμ)) or both knockin and wild-type alleles (V_HB1-8(Eμ)/ VDJ(Eμ)) can pass positive selection since they express one or two doses of a normal level of Igμ chain, respectively. But immature B cells that express both alleles are more likely to be autoreactive (94% vs 75%, respectively) assuming that 75% of newly generated B cell receptors are auto-reactive (Wardemann et al. 2003). Therefore, immature B cells that express both alleles are much less likely to pass negative selection (6% *vs* 25%).

In B1-8iΔEμ^{a}/*Igh*^{b} mice, while immature B cells that have express both alleles (V_HB1-8(ΔEμ)/VDJ(Eμ)) can pass positive selection, most newly emerging immature B cells can not. These cells express only the Eμ-deficient knockin allele (V_HB1-8(ΔEμ)) and make only about half the normal dose of Igμ chain. Consequently, most of them fails positive selection.* It is not clear whether the under-expression of the Eμ-deficient knockin allele (V_HB1-8(ΔEμ)) will enable B cell receptors made by this heavy chain to pass negative selection even if they are self-reactive, but it is certainly possible. If so, the expression of both alleles will not increase the chance for immature B cells to become autoreactive (75%). Otherwise, the chance of being autoreactive will be the same as in immature B cells expressing two alleles in B1-8i^{a}/*Igh*^{b} mice (94%).

Figure 3.22 Model of Eμ-dependent positive selection

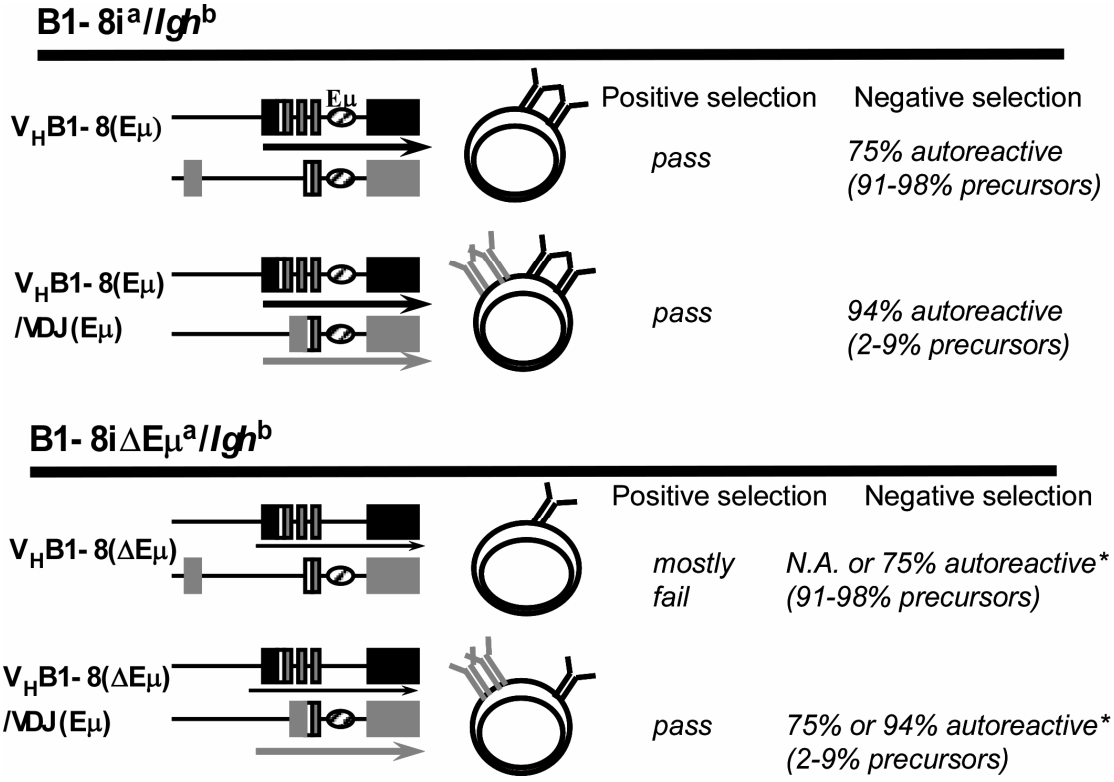

enriched in the pre-B cell population of B1-8i$\Delta E\mu^a$/*Igh*^{b} mice. This was not the case, however; these precursors were present in equal numbers in B1-8i$\Delta E\mu^a$/*Igh*^{b} and B1-8iμ^a/*Igh*^{b} mice (Figure 3.12, Table 3.4, and 3.5). In RAG-1-/- mice, the bulk of B-lineage cells in both mice assumed a pre-B cell phenotype, further supporting the idea that signaling through the Igμ chain (pre-BCR) to promote the pro- to pre-B cell transition was largely unaffected by loss of Eμ (and lower Igμ levels).

The transition from pre-B to immature B cell requires successful assembly of a functional Ig light chain gene, resulting in replacement of the pre-BCR with a BCR. The BCR on immature B cells serves two opposing purposes: it is required for survival (BCR ablation at any B cell stage tested leads to cell death), but it can also induce its own modification (receptor editing) if its signal is too strong (autoreactive BCR) (reviewed in Nemazee 2006; Monroe and Dorshkind 2007). The nature and strength of the BCR signal in immature B cells, therefore, profoundly affects cell fate. Since it is at this stage that the phenotypes of the B1-8i$\Delta E\mu^a$/*Igh*^{b} and B1-8iμ^a/*Igh*^{b} mice diverge, we propose that reduced Igμ levels in emerging immature bone marrow B cells of B1-8i$\Delta E\mu^a$/*Igh*^{b} mice result in BCR signaling that is generally below the threshold for positive selection (Figure 3.22). In normal animals, it has been suggested that this signal is antigen-independent (tonic signaling) (Bannish et al. 2001). In B1-8i$\Delta E\mu$a/Igh^b animals, the rare cells that express both *Igh* alleles (double-producers) would have a selective advantage because the increased, tonic signaling through the BCR could reach the required threshold for survival. Consistent with this model, the pre-B to immature B transition appeared normal in mice homozygous for the $\Delta E\mu$ allele. In these

animals, bi-allelic IgH gene expression would raise the Igμ level to that of normal cells expressing one intact (Eμ-containing) allele. In B1-8i^{a}/*Igh*^{b} mice, however, emerging immature B cells that express both B1-8i^{a} and the wild-type Igh^{b} allele have a disadvantage in negative selection because they are more likely to be autoreactive.

If, in the absence of Eμ, BCR density is generally not optimal for effective tonic signaling, then how do the single-producers in B1-8iΔEμ^{a}/*Igh*^{b} animals reach the immature B cell stage? Both density and signaling strength can be affected by light chain through its effects on BCR stability (the strength of heavy/light chain association) and Ag-specificity. B cells starting with a disability (low μ-chain levels) could be expected to have more stringent light chain requirements than normal, needing either light chains that form a strong and stable association with the V_HB1-8-μ chain or those that form an innocuous antigen-specificity with stronger basal signaling properties. As might be expected from cells with these more stringent requirements, light chain "editing," as reflected in the number of Igλ-producing spleen cells, was increased in B1-8iΔEμ^{a}/*Igh*^{b} B cells, as compared to B1-8i^{a}/*Igh*^{b} B cells (Figure 3.19).

Double-producers in B1-8iΔEμ^{a}/*Igh*^{b} mice expanded in peripheral tissues and were most prevalent in the CD5+ B1 B cells of the peritoneal cavity (Figure 3.20). B1 B cells (both CD5+ and CD5-) arise in fetal life, are self-renewing, give rise to most of the natural autoantibodies found circulating in the sera of healthy mice, and provide the first line of defense against invading pathogens such as influenza virus (Baumgarth et al. 2005; Baumgarth et al. 2008). The dominance of

double-producers in CD5+ B1 B cells suggests that survival signals in the B1 B cell pool are even more dependent than B2 B cells on Eμ. It has been clearly demonstrated in at least one mouse model that CD5+ B1 B cells require strong, often autoreactive BCR signals for survival. By comparison, the elevated basal signaling required by these cells can induce anergy in bone marrow-derived B2 B cells (Hardy and Hayakawa 2005). Even if the V_HB1-8/light chain combination generated an appropriately autoreactive BCR in a developing B1 B cell, it might be difficult for this BCR to provide a survival signal if the Igμ (and BCR) level were low, coming from a single ΔEμ allele. B cells that expressed a recombined, endogenous IgH allele, however, would circumvent this problem, both by generating higher Igμ levels (from the Eμ-intact allele) and by producing alternate H-chains that would increase the likelihood of forming an H+L combination with sufficiently high signaling properties.

In summary, we suggest that loss of Eμ compromises positive selection of the immature B cells in bone marrow, and perhaps even more so, of the newly arising B cells in fetal liver. In the absence of this regulatory element, rare cells that express both *Igh* alleles are not only permitted but selectively expanded, leading to the development of a substantial population of mature B cells that express two, disparate receptors. Unlike cells expressing two different light chains (ten Boekel et al. 1998; Liu et al. 2005), these heavy chain double-producers can be expected to express both types of receptor on the cell surface at comparable levels since we found that Igμ expression level was Eμ-independent in splenic B cells. It is unclear how these two-receptor cells will affect normal and/or autoimmune responses, but

it is likely significant that positive and negative selection at the pre-B to immature B cell transition is apparently “blind” to the receptor from the Eμ-deficient locus, while this receptor can be expected to have equal status at a later developmental stage (e.g. splenic B cells). Allelic exclusion with respect to the *Igh* locus, therefore, can be viewed as, at minimum, a two-step process involving both an Eμ-independent (feedback inhibition of V-DJ recombination) and an Eμ-dependent (positive selection) phase.

Chapter 4: Results and Discussion: effect of Eμ-deletion on somatic hypermutation and class switch recombination

Background and overview

During an immune response, somatic hypermutation (SHM) introduces point mutations into the immunoglobulin genes of germinal center B cells at a rate one million fold higher than that of random mutations (reviewed in: Odegard and Schatz 2006; Di Noia and Neuberger 2007; Peled et al. 2008). Somatic hypermutation was originally proposed as the mechanism generating all antibody diversity (Brenner and Milstein 1966), but it is now known that much of this diversity (e.g. in rodents and humans) is generated prior to antigen-stimulation and results from the random recombination of multiple gene segments, a process known as V(D)J recombination (reviewed in Jung et al. 2006). Somatic hypermutation's role in antibody diversity takes place after antigen stimulation of individual B cells, contributing to these cells' developing antibodies with increasing affinity for the antigen. Mutation, coupled with selection for higher-affinity antibodies, also provides a means by which the antibody response can effectively follow quickly-evolving pathogens (Longo and Lipsky 2006).

While the efficiency of an antibody response is greatly augmented by SHM and CSR, mis-targeting of these processes poses a significant threat to the integrity of the host cell's genome. In fact, the key enzyme, AID, has been implicated in tumorigenesis in a wide variety of tissue types (Kotani et al. 2007; Okazaki et al. 2007). Despite AID's presence, it has been suggested that the B cell genome is shielded from wide-spread mutation, both because of selective targeting of AID and gene-specific, high-fidelity repair of AID-generated uracils. Nevertheless, a significant number of genes has been found not to be fully protected in normal mice nor in healthy human B cells (Pasqualucci et al. 1998; Shen et al. 1998; Muschen et al. 2000; Gordon et al. 2003; Liu et al. 2008). Understanding the targeting mechanism of AID-initiated somatic hypermutation would help us to understand why this process mis-targets some non-Ig genes, and hopefully provide knowledge that can be used to protect mis-targeted genes and maintain the integrity of the host genome one day.

Although it has been extensively studied, the mechanism directing the somatic hypermutation machinery to the immunoglobulin loci remains unknown (reviewed in: Odegard and Schatz 2006; Li et al. 2007; Peled et al. 2008). The variable region coding segment (VDJ; VJ) of an assembled immunoglobulin gene is the primary, although not the exclusive, target of somatic hypermutation. Most reported non-Ig gene targets of somatic hypermutation were found to mutate at much lower frequencies than the Ig loci. *Bcl6*, for example, the most extensively mutated non-Ig gene reported thusfar, is mutated at 1/20 to 1/50 the level of immunoglobulin genes (Shen 1998, Liu 2008).Somatic hypermutation

preferentially targets RGYW/WRCY hot spots, but these hotspots can be found in almost any gene. Since V_H sequences can be replaced, in situ, with other DNA sequences without affecting the rate or extent of somatic hypermutation, the element(s) responsible for targeting must fall outside the region mutated but *in cis* with those sequences.

A positive correlation between transcription level and rate of somatic hypermutation has been established. The sequence and structure of the Ig promoter appear to be unimportant, however, since substitution of a natural Ig promoter with the rDNA promoter supports somatic hypermutation and the mutation rate is proportion to transcription levels (Fukita et al. 1998). In the immunoglobulin heavy chain locus, other known cis-control elements include Eμ and 3'RR. In one study involving an IgH transgene, it was shown that hs3b and hs4 together contributed significantly to SHM of the transgene, but targeted deletion of hs3b and hs4 within the natural *Igh* locus had no effect on SHM levels (Terauchi et al. 2001; Morvan et al. 2003).

In parallel with the *Igh* locus, the murine Igκ locus also contains an intronic enhancer (Eκ) and 3' enhancer (3' Eκ), and like Eμ, Eκ is required for efficient assembly of κ variable region genes. Both 3'Eκ and Eκ were shown to be required for somatic hypermutation in transgenic studies (Betz et al. 1994), but Eκ knockout mice were reported to have normal somatic hypermutation, and deletion of 3'Eκ from the endogenous Igκ locus showed that 3'Eκ was not required, but quantitatively important for somatic hypermutation. The decrease in somatic hypermutation frequency was likely due to the decrease in transcription in the

absence of 3'Eκ (van der Stoep et al. 1998; Inlay et al. 2006). Eκ consists of a core enhancer and one matrix attachment region (MARκ). Interestingly, deletion of MAR alone leads to an increase in the proportion of Igκ alleles free of mutations in Peyer's patch germinal center B cells (Yi et al. 1999).

In the present study, we took advantage of our experimental system, and analyzed both somatic hypermutation and class-switch recombination in B1-8iΔEμ mice. These processes were directly compared in B1-8ΔEμ mice and B1-8i mice. We found that SHM was reduced to approximately one-third wild-type levels upon Eμ deletion, although there was no concomitant reduction in transcription. The rate of CSR was moderately affected, although this was only obvious in direct comparisons of Eμ-containing and Eμ-deficient alleles simultaneously expressed in individual B cells (double-producers). We conclude that Eμ makes both significant and unique contributions to SHM such that remaining elements in the *Igh* locus are unable to fully supplant Eμ's functions. Given that loss of Eμ does not result in decreased IgH gene transcription, we suggest that Eμ plays a more direct role in recruiting the SHM/CSR machinery to the *Igh* locus.

Table 4.1 Somatic hypermutation frequency in germinal center B cells of Peyer's patches in B1-8i/*Igh* and B1-8iΔEμ/*Igh* mice

Somatic hypermutation was analyzed in sorted Peyer's patch germinal center B cells from B1-8i/*Igh* and B1-8iΔEμ/*Igh* mice. Detailed protocol is described in "Materials and Methods" (Chapter 2). Both V_H and the following intronic sequences were cloned and sequenced, but mutations in these two regions were separately analyzed for both B1-8i and B1-8iΔEμ alleles. The total number of independent clones, number of clones without mutations, the total number of point mutations identified, and the mutation frequency is shown. Data were pooled from the analyses of multiple animals of the same genotype.

Table 4.1 Somatic hypermutation frequency in germinal center B cells of Peyer's patches in B1-8i/*Igh* and B1-8iΔEμ/*Igh* mice

Region	**V_H**		**Intron**	
Genotype	**B1-8i/*Igh***	**B1-8iΔEμ/*Igh***	**B1-8i/*Igh***	**B1-8iΔEμ/*Igh***
Allele	**B1-8i**	**B1-8iΔEμ**	**B1-8i**	**B1-8iΔEμ**
No. of sequences	**46**	**53**	**46**	**53**
No. of germline sequences	**16**	**18**	**18**	**21**
Total point mutations	**551**	**517**	**205**	**238**
Mutation frequency 1[a]	**4.07%**	**3.32%**	**1.52%**	**1.53%**
Mutation frequency 2[b]	**6.25%**	**5.02%**	**2.49%**	**2.53%**
[a] Mutation frequency 1 was calculated as follows: total number of mutations/total number of base pairs analyzed for all sequences.				
[b] Mutation frequency 2 was calculated with only those sequences that contained at least 1 mutation.				

RESULTS

1. The Eμ-deficient allele is well-mutated in germinal center B cells of Peyer's patch

In order to study the effect of Eμ deletion in somatic hypermutation, we first analyzed the IgH genes of germinal center B cells in Peyer's patches. Germinal center B cells were sorted as $B220^{+}CD95^{+}PNA^{high}$ cells, and PCR was used to amplify the knock-in $V_HB1\text{-}8$ gene ($V_H186.2\text{-}DFL16.1\text{-}J_H2$) and the immediately following 214 bp intron sequence shared by the B1-8i and B1-8iΔEμ alleles. On both the B1-8i and B1-8iΔEμ alleles, we observed an overall lower somatic hypermutation frequency in the intronic region relative to the V_H region. This could reflect the intron's greater distance from the V_H promoter (Rada and Milstein 2001) and/or positive selection for mutations within V_H coding sequences. As shown in table 4.1, both the V_H region and the intron region of the B1-8iΔEμ were well mutated, with a mutation frequency of 5.02% and 2.53% for mutation sequences, respectively. There was no significant difference in mutation frequency for the B1-8i and B1-8iΔEμ alleles. (6.25% *vs* 5.02% for V_H region, and 2.49% *vs* 2.53% for intron region; Table 4.1).

In Peyer's patch germinal center B cells, therefore, there is no evidence to suggest that Eμ deletion has an effect on somatic hypermutation. Since germinal center reactions are chronically active within Peyer's patches (Gonzalez-Fernandez and Milstein 1993; Gonzalez-Fernandez et al. 1994; Griebel 1996), we reasoned that accumulation of multiple rounds of mutations

might be masking the effect of Eμ-deletion on the frequency of somatic hypermutation. We further hypothesized that an effect resulting from Eμ deletion might be revealed when competition was introduced, or when antigen-driven somatic hypermutation was analyzed after a short-term germinal center reaction.

2. The Eμ-deficient allele is less efficiently mutated when put in competition with an allele carrying Eμ.

In order to test the first hypothesis, mice heterozygous for the B1-8i and B1-8iΔEμ alleles (B1-8i/B1-8iΔEμ mice) were generated to introduce competition between these two alleles for the somatic hypermutation machinery. Since the same sets of cells were used to analyze somatic hypermutation on both alleles, there were no differences in terms of purity of sorted germinal center B cells, nor was there the possibility of variation caused by separate treatment of samples. In addition, both alleles are experiencing an exactly the same conditions for somatic hypermutation in each cell.

Although substantial levels of mutation in both V_H coding and intronic sequences were observed on both the B1-8i and B1-8iΔEμ alleles (summarized in Table 4.2), and the mutation frequency was not significantly different if only the mutated clones were considered, the B1-8iΔEμ-derived clones showed a significantly lower mutation frequency in both the V_H coding sequences (3.39% *vs* 4.83%, $p<0.05$) and intronic sequences (1.55% *vs* 2.27%, $p<0.05$). This difference was based mainly on the larger number of B1-8iΔEμ clones that were free of mutations (Figure 4.1). While there were only 3/49 V_H clones and 7/49 intron clones that were free of mutations for the B1-8i allele, 11/42 V_H clones ($p <$

Table 4.2 Somatic hypermutation frequency in germinal center B cells of Peyer's patches in B1-8i/B1-8iΔEμ mice

Somatic hypermutation was analyzed in sorted Peyer's patch germinal center B cells from B1-8i/B1-8iΔEμ mice as in Table 4.1. Both V_H and the following intronic sequences were separately analyzed for mutations on both B1-8i and B1-8iΔEμ alleles. The number of independent clones, number of clones without mutations, the total number of point mutations identified, and the mutation frequency are shown. Data were pooled from the analyses of multiple animals of the same genotype.

Table 4.2 Somatic hypermutation frequency in germinal center B cells of Peyer's patches in B1-8i/B1-8iΔEμ mice

Region	V_H		Intron	
Genotype	B1-8i/B1-8iΔEμ			
Allele	B1-8i	B1-8iΔEμ	B1-8i	B1-8iΔEμ
No. of sequences	49	42	49	42
No. of germline sequences	3	11***	7	12*
Total point mutations	696	418	327	192
Mutation frequency 1[a]	4.83%	3.39%**	2.27%	1.55%**
Mutation frequency 2[b]	5.15%	4.59%	2.65%	2.18%
[a] Mutation frequency 1 was ca;culated as follows: total number of mutations/total number of base pairs analyzed for all sequences.				
[b] Mutation frequency 2 was calculated with only those sequences that contained at least 1 mutation.				
* $p<0.1$ (χ^2 test)				
** $p<0.05$ (unpaired two-tail *t*-test)				
*** $p<0.001$ (χ^2 test)				

Figure 4.1 Distribution of clones with varying numbers of mutations in sequences cloned from Peyer's patch germinal center B cells of B1-8i/B1-8iΔEμ mice.

For the mutations shown in Table 4.2, the number of mutations in each V_H region and intronic region was counted. The proportion of clones with various numbers of mutations is presented in pie charts. In each pie chart, the number at the center is the total number of clones analyzed for the indicated region and allele; the color of each portion represents the number of mutations as indicated in the legend; the percentage of the total represented by each portion is labeled outside the portion. For example, for the B1-8 V region, 50 clones were examined and 27% of these 50 clones had >20 mutations in the 294 bp of this V region.

Figure 4.1 Distribution of clones with varying numbers of mutations in sequences cloned from Peyer's patch germinal center B cells of B1-8i/B1-8iΔEμ mice

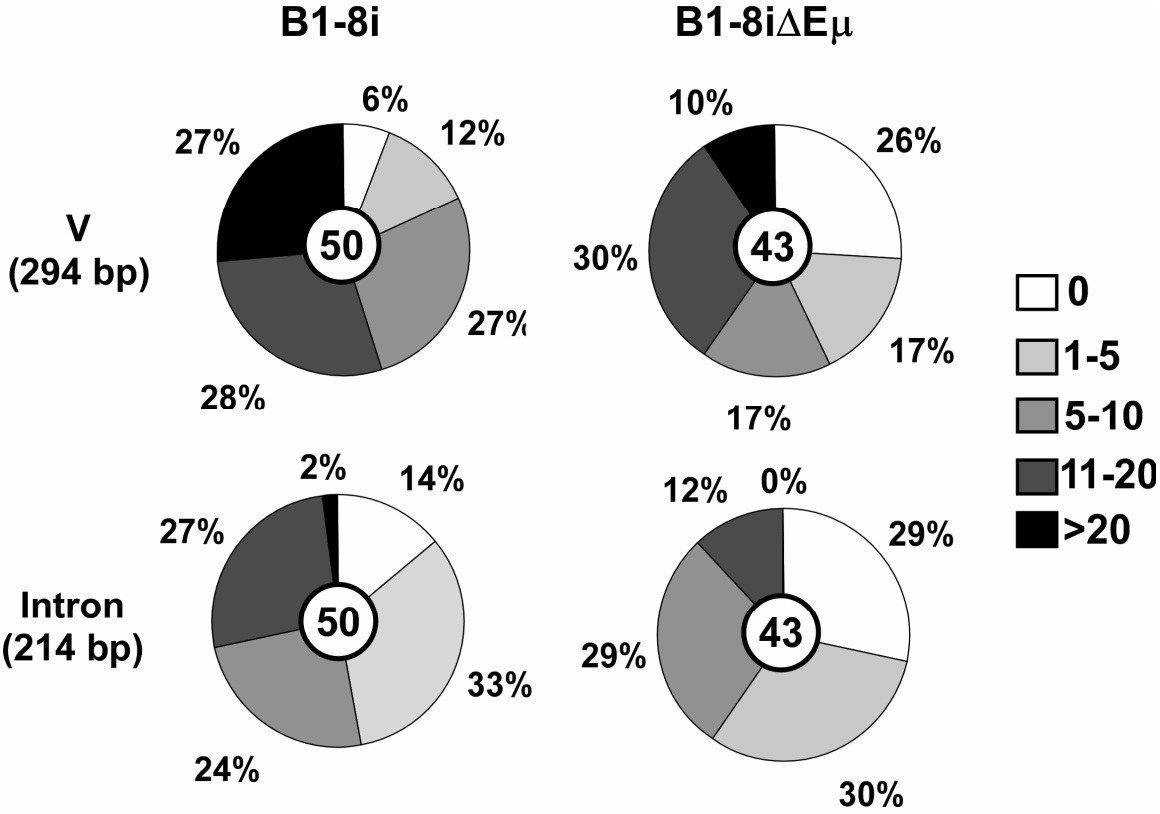

Figure 4.2 Correlation between mutation number in the V region and that in the following intronic sequences.

For each sequence cloned from the B1-8i or B1-8iΔEμ allele in B1-8i/*Igh*, B1-8iΔEμ/*Igh*, or B1-8i/B1-8iΔEμ mice, mutations were counted separately for V_H and the following intron. The number of mutations in the intron was plotted against the number of mutations in the V_H region. The correlation efficiency (R) was calculated by the "CORREL" function in the Microsoft Excel program, and the *p* value was calculated by the "TDIST" function in the Microsoft Excel program, based on a *t* value that is calculated as $R^*((\text{degree of freedom})/(1-R^2))^{1/2}$.

Figure 4.2 Correlation between the mutation number in the V region and that in the following intronic sequences

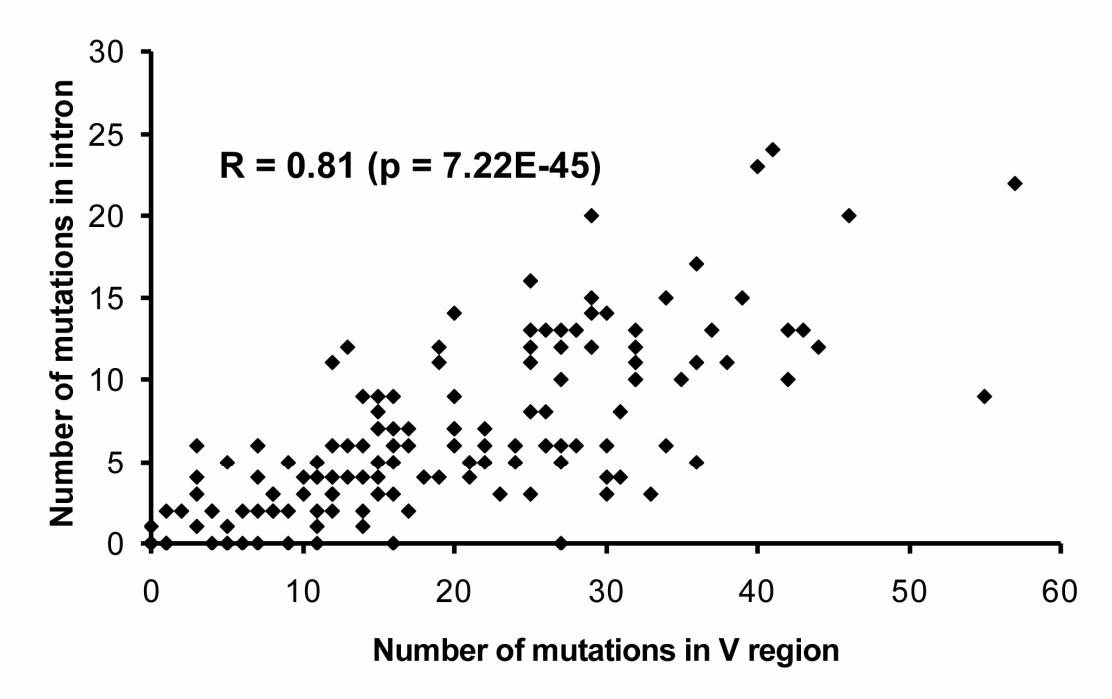

0.01) and 12/42 intron clones (p<0.1) were free of mutations for the B1-8iΔEμ allele. These analyses suggested that the B1-8iΔEμ allele was less efficiently mutated when put in competition with the B1-8i allele.

3. Strong correlation between the number of mutations in VH coding sequences and that in the following intronic sequences

Since mutations occurring in intronic sequences are not subject to selection, but mutations occurring in V_H coding sequences can change the encoded amino acids and therefore become subject to antigenic selection, analyzing mutations in intronic sequences is considered a better strategy to study natural or “real” mutation rate than is analyzing mutations in productive V_H sequences. Our experimental system allowed the analysis of both V_H sequences and the following intron, and this provides us an opportunity to assess the effect of selection on somatic hypermutation analyses.

The relationship between the number of mutations in V_H coding sequences (with selection) and that in the following intronic sequences (without selection) was analyzed for correlation. As shown in Figure 4.2, there was a very strong positive correlation between the number of mutations in the V_H region and the number of mutations in the intronic region (R = 0.81, p=7.22E-45). This strong correlation indicates that although selection pressure for mutations in V_H and intron are different, the mutation frequency in the two regions faithfully reflect each other. This might be explained by the physical association of the two regions on the same allele, such that exposure of the intron to mutations is dictated by

mutation and selection of the associated V_H. For example, early mutation of the V_H to a high affinity antigen-binding state could result in clonal expansion of cells with low overall mutations.

Based on the data shown in Figure 4.2, we predict that analyses of V_H and intron sequences provide the same information about mutation frequency, particularly, when comparing two alleles with the same target sequences. However, the nature of the mutations might differ between V_H and intron sequences when the V_H region is under strong selection pressure.

4. Dramatic decrease in somatic hypermutation on the Eμ-deficient allele of splenic B cells expressing Igγ1

In order to analyze antigen-driven somatic hypermutation after a short-term germinal center reaction, we immunized mice with 4-hydroxy-3-nitrophenylacetyl chicken gamma globulin (NP-CGG) and boosted with this antigen one or two times in 3-week intervals. The immunization protocol was designed to maximally recruit B cells expressing the B1-8i IgH chain into germinal centers since this IgH, combined with λ1 and many κ light chains, forms an antibody with NP-specificity. mRNA was isolated from the spleens of immunized mice, and γ1 transcripts with V_H186.2 (V_HB1-8 is a V_H186.2-DFL16.1-J_H2 rearrangement) were amplified by reverse-transcriptase–dependent polymerase chain reaction (RT-PCR). Primers specific for γ1 were used since μ to γ1 switching serves as an indicator of B cell participation in a germinal center reaction.

As described in chapter 3, a pronounced difference between B1-8i^a/*Igh*^{b} and B1-8iΔEμ^a/*Igh*^{b} mice was that in B cells from the former mouse strain,

Table 4.3 Reduced somatic hypermutation frequency in the absence of Eμ in splenic γ1 expressers.

Somatic hypermutation was analyzed in splenic γ1 expressing B cells from wild-type (*Igh*/*Igh*), B1-8i/*Igh* and B1-8iΔEμ/*Igh* mice. Detailed protocol is described in “Materials and Methods” (Chapter 2). V_H mutations were analyzed by V-QUEST program. For each indicated allele in B cells of the indicated genotype, the total number of independent clones, number of clones without mutations, the total number of point mutations identified, and the mutation frequency are shown. Data were pooled from the analyses of multiple animals of the same genotype.

Table 4.3 Reduced somatic hypermutation frequency in the absence of Eμ in splenic γ1 expressing B cells.

Region	V_H			
Genotype	*Igh*/*Igh*	B1-8i/*Igh*	B1-8iΔEμ/*Igh*	
Allele	*Igh*	B1-8i	B1-8iΔEμ	*Igh*
No. of sequences	51	47	93	39
No. of germline sequences	3	12***	38****	1
Total point mutations	315	250	161	193
Mutation frequency 1[a]	2.10%	1.81%	0.59%**	1.68%
Mutation frequency 2[b]	2.23%	2.43%	1%*	1.73%
[a] Mutation frequency 1 was calculated as follows: total number of mutations/total number of base pairs analyzed for all sequences scored				
[b] Mutation frequency 2 was calculated with only those sequences that contained at least one mutation				
* $p<0.001$ (unpaired two-tail t-test)				
** $p<0.0001$ (unpaired two-tail *t*-test)				
*** $p<0.01$ (*vs* *Igh*/*Igh*: *Igh*, χ^2 test)				
**** $p<0.0001$ (*vs* *Igh*/*Igh* : *Igh*, χ^2 test); $p<0.1$ (*vs* B1-8i/*Igh*: B1-8i, χ2 test);				

Figure 4.3 Distribution of clones with varying numbers of mutations in sequences cloned from splenic γ1 expressers

For the mutations shown in Table 4.3, the number of mutations in each cloned V_H sequence (294 bp) was counted. The proportions of clones with various numbers of mutations are presented in pie charts as described in Figure 4.1.

Figure 4.3 Distribution of clones with varying numbers of mutations in sequences cloned from splenic γ1 expressers

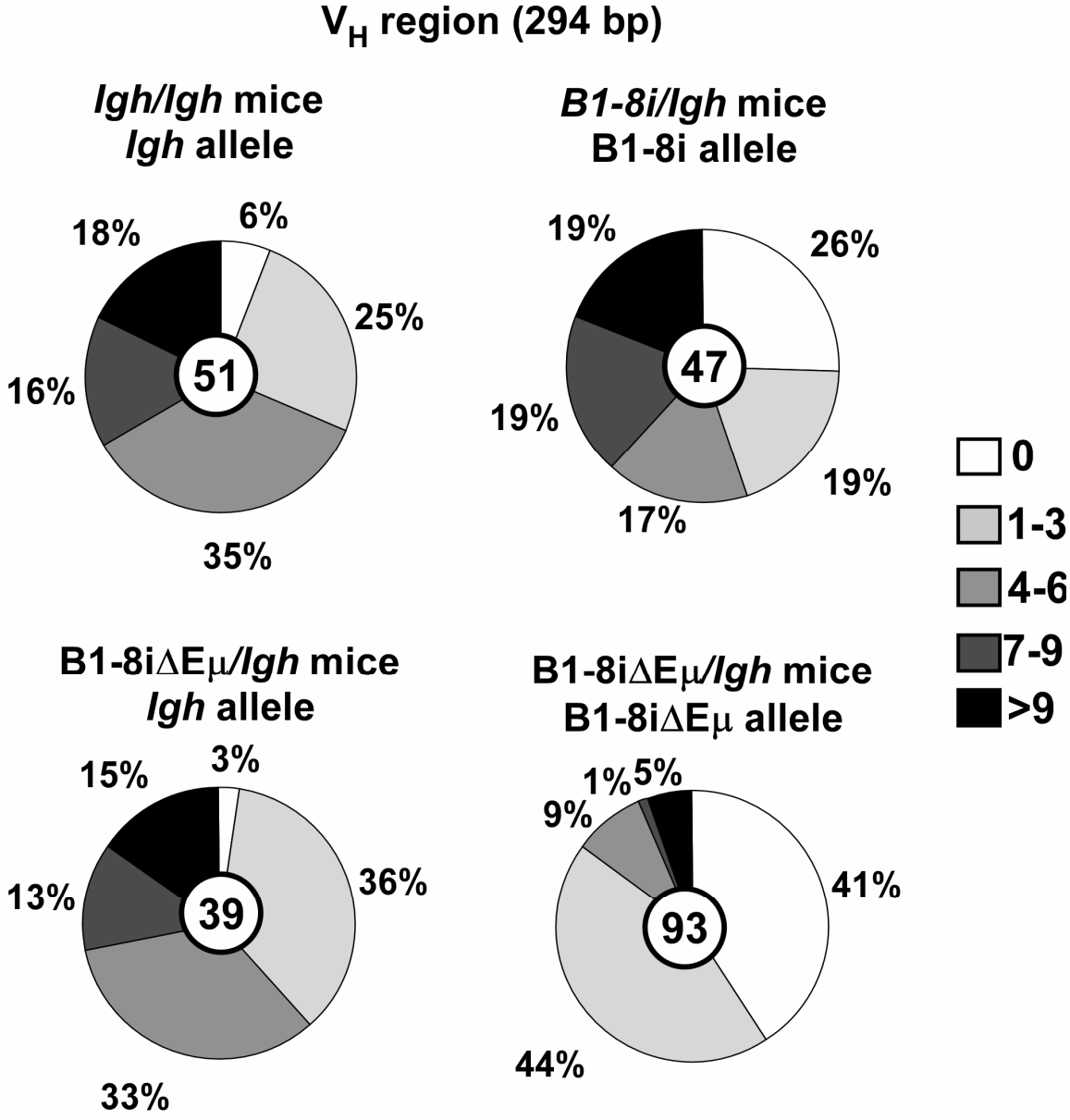

exclusion of the wild-type *Igh*^{b} allele was complete, while in B1-8iΔEμ^a/*Igh*^{b} mice, ~20% of B cells expressed the modified allele and a fully-assembled IgH gene on the wild-type *Igh*^{b} allele. For the present studies, this failure of allelic exclusion meant that we could measure SHM on two alleles expressed in the same B cells, one allele with and the other without Eμ *in cis*.

As summarized in Table 4.3, a total of 315 mutations were observed among 51 unique RT-PCR sequences cloned from wild-type mice, yielding an overall somatic hypermutation frequency of 2.10%. This is consistent with results from previous studies in wild-type mice, using a similar strategy (Zan H 2005). In B1-8i/*Igh*^{b} mice, 250 mutations were found among 47 clones, yielding a mutation frequency on the B1-8i allele (1.81%) that was similar to that of wild-type *Igh* alleles. Unique junction sequences and an engineered mutation in frame-work region 3 of the inserted V_HB1-8 gene served to unequivocally distinguish B1-8i and B1-8iΔEμ allele transcripts from *Igh*^{b}-allele transcripts.

When heterozygous B1-8iΔEμ^a/*Igh*^{b} mice were analyzed, 93 RT-PCR clones derived from B1-8iΔEμ γ1 transcripts yielded only 161 mutations (0.55% mutation frequency), representing a drop in mutation frequency to 1/3 that of the B1-8i allele (p=1.07^{-8}, F-test; p=5.75^{-5}, t-test) and wild-type alleles (Table 4.3). This striking decline in mutations suggested either that the somatic hypermutation machinery itself was aberrant in B1-8iΔEμ^a/*Igh*^{b} B cells, or, more likely, that targeting of the B1-8iΔEμ allele was made less efficient by Eμ's absence.

To distinguish between these possibilities, we focused on *Igh*^{b}-derived γ1 transcripts in the B1-8iΔEμ^a/*Igh*^{b} mice. These transcripts were generated in

double-producing, “allelically included” B cells and came from the *Igh*^{b} allele where Eμ was intact. 39 unique clones carrying V_H186.2 sequences were isolated and these carried a total of 193 mutations, yielding an overall mutation frequency of 1.68%, significantly higher than the mutation frequency of the B1-8iΔEμ allele from the same cells (p=3.84^{-7}, *t*-test) and comparable to the mutation frequency of the wild-type (p=0.29, *t*-test) and B1-8i alleles (p=0.94, *t*-test) (Table 4.3). Fifty-three unique clones that carried V_H sequences outside of the V_H186.2 family were also recovered from the wild-type allele of B1-8iΔEμ^a/*Igh*^{b} mice, and these had an overall mutation frequency of 1.62% (data not shown). These results, along with mutation rates found in sequences obtained from Peyer's patch B cells, confirm that the somatic hypermutation machinery is functional B1-8iΔEμ^a/*Igh*^{b} B cells. At the same time, the difference in mutation frequency on the B1-8iΔEμ and *Igh*^{b} alleles (0.5 vs 1.6) provides evidence that Eμ plays a significant role in determining the frequency of somatic hypermutation within the *Igh* locus.

Further analyses of the sequences obtained from splenic B cells revealed that 38 out of 93 (40.86%) B1-8iΔEμ clones were free of mutation while only 3 out of 51 *Igh*^{b} alleles (5.88%) from *Igh*^{b}/*Igh*^{b} wild-type mice were without mutations (Table 4.3 and Figure 4.3). Theoretically, the 38 un-mutated, B1-8iΔEμ clones could be derived from 38 independent B cells, or, alternatively, they could represent duplicates of RT-PCR products from a smaller number of B cells. Analysis of B1-8iΔEμ clones that carried mutations was not consistent, however, with the duplicate-clone hypothesis. Because of the mutations, it was possible to distinguish these mutated sequences from one another. Only one duplicate was

Table 4.4 Summary of the distribution and spectrum of mutations

Mutations shown in table 4.1, 4.2 and 4.3 were analyzed for their distribution relative to RGYW/WRCY hotspots, the frequency of mutations at AT, and the frequency of transitions.

Table 4.4 Summary of the distribution and spectrum of mutations

Mutations in germinal center B cells in Peyer's patch

Region	V_H		Intron		V_H		Intron	
Genotype	B1-8i /*Igh*	B1-8iΔEμ /*Igh*	B1-8i /*Igh*	B1-8iΔEμ /*Igh*	B1-8i/B1-8iΔEμ			
Allele	B1-8i	B1-8iΔEμ	B1-8i	B1-8iΔEμ	B1-8i	B1-8iΔEμ	B1-8i	B1-8iΔEμ
No. of sequences	46	53	46	53	49	42	49	42
Total point mutations	551	517	205	238	696	418	327	192
RGYW/WRCY mutations(%)	47.2	46.0	16.1	18.9	47.0	49.5	19.9	28.6
Mutations at AT (%)	45.1	38.9	56.5	65.2	42.4	45.0	55.4	58.9
Transition mutations (%)	58.5	57.1	52.7	50.0	61.0	57.4	53.9	53.6
Transition at AT (%)	47.5	44.2	42.3	45.1	50.0	51.6	45.8	52.1
Transition at CG (%)	67.7	65.2	66.2	59.0	69.1	62.2	63.9	55.7

Mutations in splenic γ1 expressers

Region	V_H			
Genotype	*Igh*/*Igh*	B1-8i/*Igh*	B1-8iΔEμ/*Igh*	
Allele	*Igh*	B1-8i	B1-8iΔEμ	*Igh*
No. of sequences	51	47	93	39
Total point mutations	315	250	161	193
RGYW/WRCY mutations(%)	50.2	44.8	50.3	38.9
Mutations at AT (%)	34.5	41.2	54.0	40.3
Transition mutations (%)	59.0	54.8	60.2	56.4
Transition at AT (%)	49.6	54.4	54.1	38.5
Transition at CG (%)	64.1	55.1	67.5	68.6

Table 4.5 Normal spectrum of somatic hypermutation in the absence of Eμ

Mutations shown in tables 4.1, 4.2 and 4.3 were analyzed for the detailed spectrum. For mutations in Peyer's patch germinal center (GC) B cells, mutations in the indicated region of the indicated allele were analyzed in sub-tables. For mutations in splenic γ1 expressers, mutations of the indicated allele in the indicated B cells were analyzed in sub-tables. The nucleotides shown in the first column of each sub-table are the nucleotides before mutation, and the nucleotides on the first row are the nucleotides after mutation. The numbers shown in this table were calculated as follow: (the number of mutations) / (the total number of mutations).

Table 4.5 Normal spectrum of somatic hypermutation in the absence of Eμ

Mutations in Peyer's patch GC B cells

B1-8i allele
V_H

from\to	A	C	G	T	Total
A		0.06	0.16	0.11	0.33
C	0.04		0.04	0.15	0.22
G	0.24	0.06		0.04	0.34
T	0.04	0.05	0.02		0.11

B1-8iΔEμ allele
V_H

from\to	A	C	G	T	Total
A		0.07	0.12	0.08	0.28
C	0.04		0.06	0.16	0.26
G	0.21	0.07		0.04	0.32
T	0.04	0.07	0.02		0.14

B1-8i allele
intron

from\to	A	C	G	T	Total
A		0.07	0.17	0.16	0.40
C	0.02		0.02	0.14	0.17
G	0.15	0.05		0.06	0.27
T	0.04	0.07	0.05		0.16

B1-8iΔEμ allele
intron

from\to	A	C	G	T	Total
A		0.07	0.20	0.14	0.42
C	0.01		0.06	0.10	0.17
G	0.11	0.05		0.04	0.20
T	0.05	0.10	0.06		0.21

Mutations in splenic γ1 expressers

***Igh/Igh* mice**
***Igh* allele**

from\to	A	C	G	T	Total
A		0.03	0.11	0.11	0.25
C	0.02		0.05	0.14	0.20
G	0.27	0.06		0.10	0.43
T	0.02	0.06	0.03		0.11

B1-8i/*Igh* mice
B1-8i allele

from\to	A	C	G	T	Total
A		0.04	0.18	0.12	0.34
C	0.07		0.03	0.15	0.25
G	0.17	0.08		0.07	0.31
T	0.01	0.04	0.04		0.09

B1-8iΔEμ/*Igh* mice
B1-8iΔEμ allele

from\to	A	C	G	T	Total
A		0.06	0.18	0.11	0.34
C	0.02		0.04	0.13	0.19
G	0.14	0.05		0.02	0.22
T	0.05	0.08	0.12		0.24

B1-8iΔEμ/*Igh* mice
***Igh* allele**

from\to	A	C	G	T	Total
A		0.04	0.09	0.15	0.29
C	0.00		0.04	0.16	0.21
G	0.23	0.08		0.04	0.35
T	0.04	0.05	0.05		0.15

found among all of the 55 mutated clones recovered (i.e. 56 clones recovered; 55 with unique sequences), supporting the notion that the clones without mutations were also independently-derived.

Interestingly, clones without mutation were also frequently recovered for the B1-8i allele, but to a lesser extent than the B1-8iΔEμ allele (25.53% vs 40.86%) (Figure 4.3). Even given this increase in clones without mutation (relative to wild-type *Igh*^{b} alleles), the frequency of highly-mutated clones ($\geqslant$7 Mutations) remained high (38%) for the B1-8i allele and substantially greater than that observed for the B1-8iΔEμ allele (6%).

5. Eμ deletion does not affect the distribution and spectrum of mutations

Two hallmarks of somatic hypermutation are its preference for RGYW/WRCY sequences (mutation "hotspots") and its bias toward transitions (~50% vs theoretical 33%) (reviewed in: Odegard and Schatz 2006; Di Noia and Neuberger 2007; Peled et al. 2008). As summarized in Table 4.4, mutations on all alleles analyzed (both from splenic γ1 producers and from Peyer's patch, germinal center B cells) were preferentially found within RGYW/WRCY sequences (40-50% mutations), and 50% or more were transition mutations. In a detailed analysis of mutation spectrum, no difference was noted (Table 4.5).

6. Class switch recombination is less efficient in the absence of Eμ

In order to study whether Eμ deletion affected class switch recombination, splenic B cells were stimulated *in vitro* with LPS in combination with T-cell-derived cytokines that promote IgH class-switching (IL-4, γ-interferon, or TGF). These experiments were carried out in collaboration with another Ph.D student in the lab, Yi Yan. As shown in 4.4, there was no statistically significant difference in the frequency of splenic B cells that had switched isotype between homozygous B1-8iΔEμ mice and homozygous B1-8i mice.

We took advantage of the phenomenon of "allelic inclusion" in B1-8iΔEμ^a/*Igh*^{b} heterozygous mice to more directly compare CSR on the B1-8iΔEμ^a allele with CSR on a wild-type (*Igh*^{b}) allele. "Double producers" from these mice ($\mu^{a+}\mu^{b+}$) were isolated by flow-cytometry and then stimulated to induce CSR. Purity of the sort was >96% with <2% single producers (Figure 4.4A, in contrast with single producers in 4.4B). Because there were no reliable allotype-specific antibodies for isotypes other than IgM, we focused on the loss of IgM surface expression as an indicator of CSR in these experiments. We reasoned that if the B1-8iΔEμ^a and wild-type *Igh*^{b} alleles switched at the same efficiency, we would recover one subset of cells from the switch-induced $\mu^{a+}\mu^{b+}$ culture that was negative for both μ allotypes (CSR on both alleles), and two subsets of roughly equal size that were $\mu^{a+}\mu^{b-}$ (CSR on *Igh*^{b} allele only) and $\mu^{a-}\mu^{b+}$ (CSR on B1-8iΔEμ^a allele only), respectively. As shown in Figure 4.5C and 4.5D,

Figure 4.4. Class switch recombination in homozygous B1-8iΔEμ B cells.

Homozygous wild-type (Igh/Igh), B1-8i, and B1-8iΔEμ(B1-8iDEm) splenic B cells were enriched by negative selection, and stimulated with LPS, LPS + IL4, LPS + γ-interferon, or LPS + TGF-β for 3-5 days. Stimulated B cells were analyzed for class switch recombination by flow cytometry, and the proportions of switched B cells to each isotype were summarized from analyses of three animals of each indicated genotype. Note, no significant difference was observed between B1-8i, and B1-8iΔEμ(B1-8iDEm) mice; the reading difference for IgG2b was not trusted since there was no clear distinction between IgG2b+ cells and IgG2b- cells in FACS analysis.

Figure 4.4. Class switch recombination in homozygous B1-8iΔEμ B cells.

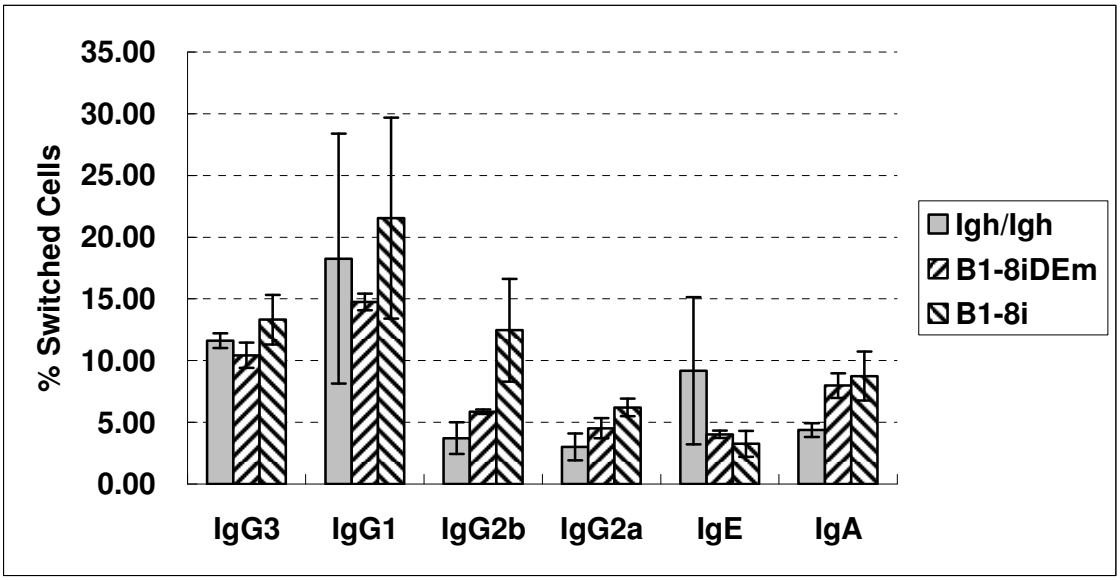

Figure 4.5 Class switch recombination in double expressing B cells from B1-8iΔEμ/*Igh* mice.

Splenic single expressing (IgM^{a+b-}) and double expressing (IgM^{a+b+}) B cells were sorted from pooled splenic B cells enriched by negative selection. The sorted double expressing had a purity of 98% (A), and they are distinct from the simultaneously sorted single expressing B cells (B). Sorted double expressers were stimulated with LPS + γ-interferon (C) and LPS + IL-4 (D) for 3 or 5 days respectively, and analyzed for class switch recombination by flow cytometry. Cells in the IgM^{a+b+} gate are cells that have not switched to anty of the downstream classes; Cells in the IgM^{a-b-} gate are cells that have switched both alleles; and Cells in the IgM^{a+b-} gate are cells that have switched their wild-type *Igh*^{b} alleles, but not the B1-8iΔEμ^a allele. (E) IgM^{a+b-} cells after stimulation of double producers, as shown in (C) and (D) were sorted, and analyzed for the amount of D-J rearrangements and V-DJ rearrangements as described in Figure 3.12 (These cells are referred to “sorted $\mu^{a+}\mu^{b-}$ cells from stimulated $\mu^{a+}\mu^{b+}$ cells”). Sorted splenic single expressing B cells (unstimulated $\mu^{a+}\mu^{b-}$ control) and double producers (unstimulated $\mu^{a+}\mu^{b+}$ control) were included for comparison.

Figure 4.5. Class switch recombination of B1-8iΔEμ/*Igh* double expressers

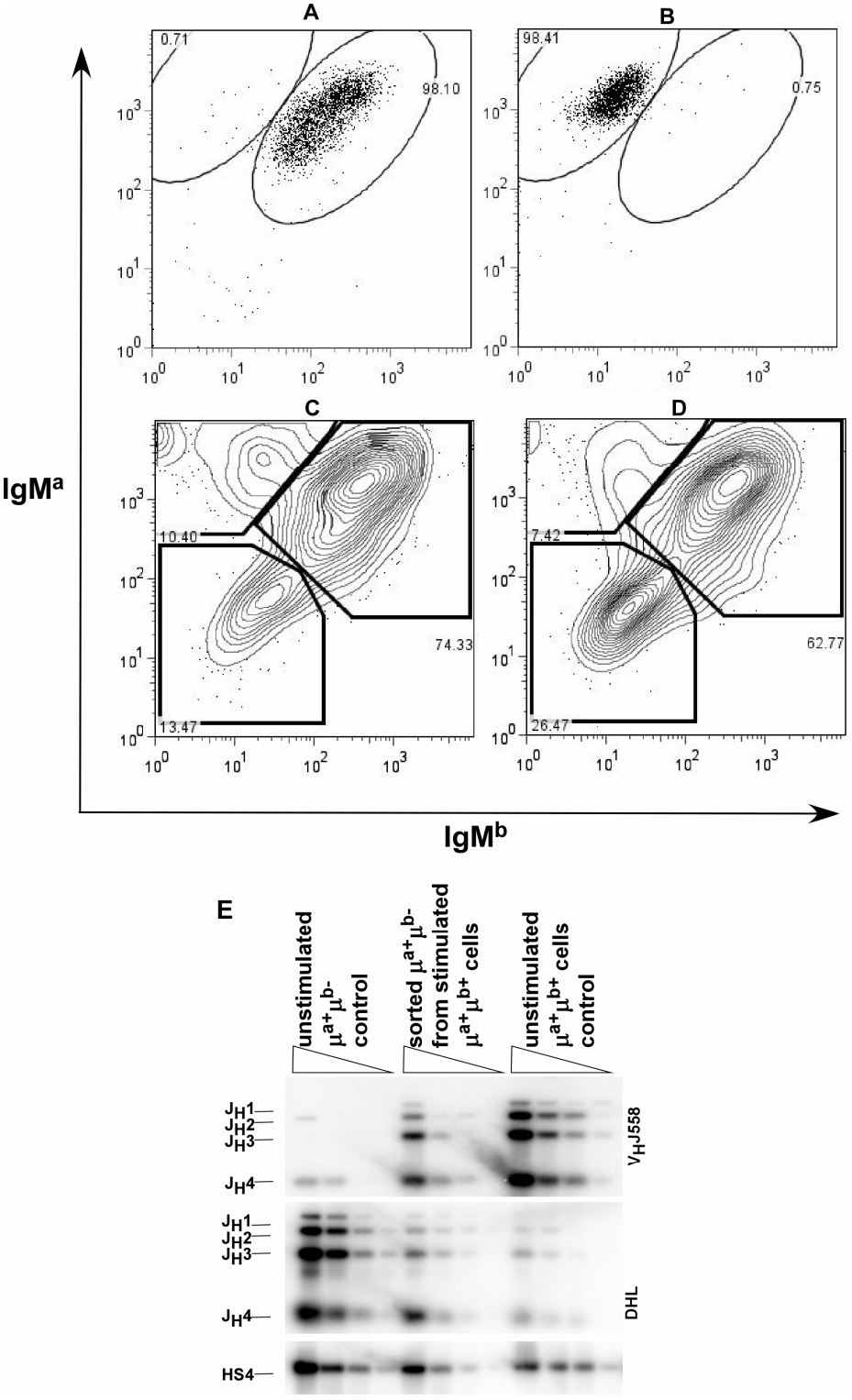

after stimulation, besides the double positive ($\mu^{a+}\mu^{b+}$; no CSR on either allele) and double negative populations ($\mu^{a-}\mu^{b-}$; CSR on both alleles), a third population ($\mu^{a+}\mu^{b-}$; CSR on *Igh*^{b} allele only) was always present. There was no matching, fourth population that was $\mu^{a-}\mu^{b+}$ (CSR on B1-8iΔEμ^{a} allele only). To rule out the possibility that the $\mu^{a+}\mu^{b-}$ cells arose from an expansion of contaminating $\mu^{a+}\mu^{b-}$ cells in the starting, sorted population of cells, we isolated the post-stimulation $\mu^{a+}\mu^{b-}$ cells and analyzed the VDJ rearrangement status of their *Igh*^{b} alleles. As shown in 4.5E, the sorted $\mu^{a+}\mu^{b-}$ cells from stimulated $\mu^{a+}\mu^{b+}$ precursors contained more V-DJ rearrangements and fewer D-J rearrangements than unstimulated $\mu^{a+}\mu^{b-}$ control cells, suggesting that at least some of these cells are double producers that have undergone CSR on the *Igh*^{b} allele but not the B1-8iΔEμ^{a} allele. We conclude that while class-switch recombination can proceed in Eμ's absence, an allele lacking this element is at a competitive disadvantage when in the presence of one that retains it.

7. μ mRNA level is not reduced in Eμ-deficient B cells

Somatic hypermutation frequency has been shown previously to positively correlate with transcription level (Fukita et al. 1998). In the Igκ locus, for example, deletion of the intronic enhancer (iEκ) had no effect on SHM frequency nor on transcription of assembled Igκ genes, but deletion of 3'Eκ decreased both (Inlay et al. 2006). By analogy, the observed decrease in somatic hypermutation frequency upon Eμ deletion might be due to a concomitant decrease in transcription. In order to investigate this possibility, we analyzed surface IgM

levels and/or μ mRNA levels in both resting and activated B cells. As showed in Figure 3.5B, surface IgM and μ mRNA levels in resting, splenic B cells were at least as high (or higher) in homozygous B1-8iΔEμ mice as in homozygous B1-8i mice. LPS stimulated homozygous B1-8iΔEμ B cells also had more μ mRNA than homozygous B1-8i B cells treated in the same way. Finally, germinal center B cells ($B220^{+}PNA^{high}CD95^{+}$) were isolated from Peyer's patch of B1-8i and B1-8iΔEμ homozygous mice, respectively. In this case, there was even a larger difference between cells from these two mouse strains, with the B1-8iΔEμ mice again showing higher μ mRNA levels. All of these data show that transcription of the Igμ gene created by B1-8iV_H insertion does not decrease upon Eμ deletion; rather, both resting and activated B cells produce more μ mRNA from the Eμ–deficient allele than from the allele with an intact Eμ.

Figure 4.6 Transcription of Eμ-deficient allele in activated B cells

Left: Homozygous splenic B cells of B1-8i and B1-8iΔEμ mice were negatively enriched and stimulated by LPS for 2 days. RNA was purified from stimulated B cells, and real-time RT-PCR was used to compare the VDJ-μ mRNA levels.

Right: Germinal center B cells were sorted from Peyer's patches pooled from six homozygous B1-8i and six B1-8iΔEμ mice, and VDJ-μ and VDJ-α mRNA levels were compared by real-time RT-PCR.

Figure 4.6 Transcription of Eμ-deficient allele in activated B cells

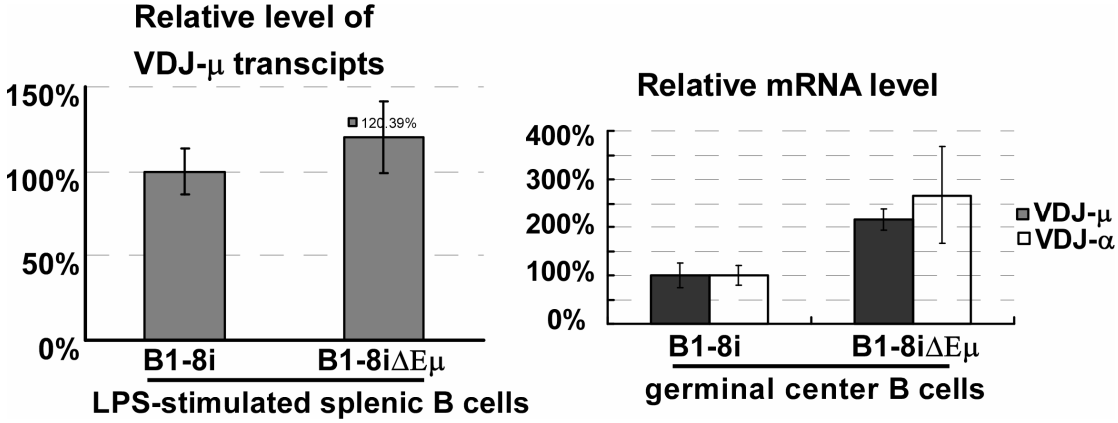

DISCUSSION

The finding that a rearranged κ transgene could be mutated initiated the extensive search for cis-control elements that recruit somatic hypermutation machinery to immunoglobulin gene loci (reviewed in: Odegard and Schatz 2006; Di Noia and Neuberger 2007; Peled et al. 2008). A serial studies defined the minimal requirements of efficient somatic hypermutation of a κ transgene, which included a Vκ promoter, the Jκ-Cκ intron that included Eκ and its MAR, and the κ 3' enhancer (Betz et al. 1994; Jolly et al. 1996; Goyenechea et al. 1997; Klix et al. 1998). In the *Igh* locus, Eμ was a focus of analysis from the very beginning of the search. Although mutations were not detected in a λ transgene under the control of a heavy chain promoter and Eμ, several transgenes (both Ig and non-Ig transgenes) driven by the immunoglobulin heavy chain promoter and Eμ were shown to mutate. Mutation was at a much lower frequency that endogenous assembled Ig variable region genes (Azuma et al. 1993; Sohn et al. 1993; Klotz and Storb 1996), however, suggesting that Eμ and the immunoglobulin heavy chain promoter (P_{VH}) can recruit the somatic hypermutation (SHM) machinery to the transgenes, that other control elements are required for boost SHM activity. Analysis of V_H transgenic (without constant region gene) mice showed that a V_H transgene driven by P_{VH} and Eμ was not mutated perhaps due to not because it was poorly transcribed, but the V_H transgenes that have recombined with the endogenous *Igh* locus, even when they retained as little as 150 bp of the natural 5' flanking sequence of the P_{VH} were well mutated (Giusti and Manser 1993). The authors of this study suggested that there were cis-control elements downstream

of Eμ, but not upstream of P_{VH} that were required for efficient SHM. Addition of the 3' RR element hs1,2 to μ transgenes failed to enhance SHM (Johnston et al. 1996; Tumas-Brundage et al. 1997). The minimal requirements for μ transgene SHM was finally defined as a μ transgene driven by a V_H promoter, Eμ/MAR and the 3' enhancers including hs1,2, hs3b and hs4 (Terauchi et al. 2001). This transgene was mutated at levels comparable to those observed in endogenous assembled V_H genes.

Interpretation of the IgH and IgL transgene studies were complicated by the fact that later studies of the endogenous IgH and Igκ loci with targeted deletion of cis-control elements did not confirm them. For instance, hs3b and hs4 was shown to be required for efficient somatic hypermutation in a μ transgene, but deletion of hs3b and hs4 from the endogenous *Igh* locus did not affect somatic hypermutation (Morvan et al. 2003). This finding suggested that cis-control elements necessary for efficient somatic hypermutation of transgenes might be compensated by others in the context of the endogenous locus. Therefore, it is important to study these cis-control elements in the context of the endogenous locus. Ronai et al (2005) exploited a tissue culture system and studied the effect of deletion of the entire Eμ or of cEμ and MARs individually on somatic hypermutation in the endogenous locus. Surprisingly, as long as the transcription was maintained, somatic hypermutation level was not reduced on the Eμ-deficient allele, but was reduced in the absence of either cEμ or MARs (Ronai et al. 2005). Although it is not clear in what way, this study suggested components in Eμ could dictate SHM, at least in this system. Soon after this report, Perlot et al (2005) reported normal somatic

hypermutation in cE$\mu^{\Delta/\Delta}$ mice, leaving some controversy surrounding the effect of cEμ on SHM. Notably, however, in Ronai *et al*'s study, the guanyl phophorybosyl transferase (gpt) gene was inserted between Cμ and Cδ to insulate the μ gene from 3'RR. And another reason the results of this study and that of Perlot et al might have differed is that it is not yet know how much the somatic hypermutation analysis in a tissue culture system (normally much lower mutation frequency) reflects the somatic hypermutation mechanism *in vivo.* On the other hand, the development of B cells in cE$\mu^{\Delta/\Delta}$ mice (Perlot et al's study) is impaired due to inefficient VDJ rearrangement and these mice produced only a limited number of B cells. It should be also noted that SHM was only analyzed in Peyer's patch in the latter study (Perlot et al 2005). In our model, B1-8iΔEμ mice, B cell development was rescued by knocking in a fully assembled VDJ, and the well populated B cells in spleen and Peyer's patch allowed us to analyze the effect of deletion of Eμ on somatic hypermutation *in vivo*.

Our analysis of V186.2-γ1 cDNA clearly showed that somatic hypermutation was impaired upon Eμ deletion (Table 4.3, and Figure 4.3).The overall mutation frequency of somatic hypermutation on the B1-8iΔEμ allele was reduced to 1/3 of wild-type levels, and this reduction was not likely due to any defect in the somatic hypermutation machinery process itself in B1-8iΔEμ^{a}/*Igh*^{b} mice for the following reasons: first, B cell development in B1-8iΔEμ^{a}/*Igh*^{b} mice was not impaired by Eμ deletion, and a good number of B lineage cells were present in both bone marrow and periphery; second, the observed mutations (in both V186.2-γ1 and Peyer's patch clones) had the characteristics of somatic hypermutation – mutations were

biased toward transitional mutations and were enriched in RGYW/WRCY hotspots, and the mutation spectrum is normal (Table 4.4 and 4.5); last and most importantly, some B1-8i$\Delta E\mu^a$/*Igh*^{b} B cells had undergone V-DJ rearrangements on their wild-type alleles, from which V186.2-γ1 cDNA clones were also analyzed, and the somatic hypermutation frequency on this wild-type allele was not reduced (Table 4.3, Figure 4.3).

It is intriguing that a much weaker effect of Eμ deletion on somatic hypermutation was observed when peyer's patch germinal center B cells ($B220^+PNA^{high}CD95^+$) were analyzed. Somatic hypermutation levels were essentially the same on the B1-8i^a and B1-8i$\Delta E\mu^a$ alleles, regardless of whether the V_H region or the following intron region was analyzed, in these cells isolated from B1-8i^a/*Igh*^{b} and B1-8i$\Delta E\mu^a$/*Igh*^{b} mice, respectively (Table 4.1). This is in contrast with the large decrease in somatic hypermutation frequency on the B1-8i$\Delta E\mu^a$ allele of V186.2-γ1 cDNA clones in spleen (Table 4.3 and Figure 4.3). The discrepancy in the two analyses was, however, not surprising. Since murine Peyer's patches have chronic germinal center reactions stimulated by antigens in the intestines (Griebel 1996), somatic mutations accumulate in murine Peyer's patch B cells and reach a plateau when the animals are about five months of age (Gonzalez-Fernandez and Milstein 1993; Gonzalez-Fernandez et al. 1994). These findings imply that mutated B cells undergo a cyclic re-entry into the hypermutation process. In contrast, the germinal center reaction in spleen was induced by immunization, and is expected to be present for only a short time. The age of heterozygous B1-8i^a/*Igh*^{b} and B1-8i$\Delta E\mu^a$/*Igh*^{b} mice used in both the spleen and

Peyer's patch analysis was about 3.5~5 months, which is close to the age when somatic mutation levels reach a plateau in Peyer's patch. Therefore, it appears that analysis of splenic V186.2-γ1 cDNA clones was a more sensitive means to in our system to study the effect of Eμ deletion on somatic hypermutation. This effect was masked in Peyer' patch germinal center, which was covered by analysis of peyer's patch germinal center B cells due to the accumulation of somatic mutations, especially when there was no competition from another rearranged allele. Consistent with this notion, a much higher mutation frequency was observed in the V_H region of Peyer's patch germinal center B cells relative to the V_H region of V186.2-γ1 cDNA clones (>4% *vs* ~2%). When allele competition was introduced, as in heterozygous B1-8i^a/B1-8iΔEμ^a germinal center B cells, the B1-8iΔEμ^a allele was less mutated than the B1-8i^a allele. The B1-8iΔEμ^a allele had a higher proportion of mutation-free clones and a significantly lower overall mutation frequency (Table 4.2 and Figure 4.1). Since every B cell had both B1-8i^a and B1-8iΔEμ^a alleles, this analysis is neither affected by the variation in the purity of sorted germinal center B cells, nor by the age or house-condition of the animal used in the analysis.

Interestingly, the transcription level of μ was not decreased upon Eμ deletion, as measured by mRNA level or by surface IgM level; instead, slight increase was observed. Splenic B cells of homozygous B1-8i^a and B1-8iΔEμ^a mice had the same surface IgM level, and the μ mRNA level was ~30% higher in the absence of Eμ (Figure 3.5B) .LPS stimulated B cells and sorted Peyer's patch germinal center B cells, which represent activated B cells *in vitro* and *in vivo*,

respectively, also showed an increase in immunoglobulin heavy chain mRNA level in the absence of Eμ (~20% increase in LPS stimulated B cells; ~200-300% increase in sorted peyer's patch germinal center B cells) (Figure 4.6). The sustained expression level of immunoglobulin heavy chain gene (μ or α) in the absence of Eμ is not surprising given the finding that 3' regulatory region become active since immature B cell stage (Yan et al 2007); but the increase of expression was not anticipated, suggesting that Eμ plays a negative role in splenic B cells and activated B cells. The large increase (from ~30% in splenic B cells and LPS stimulated B cells to 200-300% in peyer's patch B cells) in the extent of the increase of μ or α expression level in Peyer's patch germinal center B cells could result from the different regulatory effect of Eμ and the 3' regulatory region at different B cell stages. Another possibility is that it is related to the reduced somatic hypermutation level in the absence of Eμ. Lower levels of somatic hypermutation lead to less chance to generate non-sense mutations in the coding sequence of the variable region, maintaining the stability of μ or α mRNA.

Overall, our somatic hypermutation analyses suggest that Eμ it not required for somatic hypermutation in the *Igh* locus, but that Eμ increase the efficiency of this process without increasing μ transcription level, most likely, through directing the somatic hypermutation machinery to the *Igh* locus. It is not clear, however, whether deletion of cEμ or of MARs or of the combination is responsible for this effect. In Ronai *et al*'s study (2005), deletion of the entire Eμ did not affect somatic hypermutation, but individual deletion of cEμ or MARs leads to a decrease of

somatic hypermutation level without a decrease in transcription, suggesting complex influence of Eμ components on the process of somatic hypermutation (Ronai et al. 2005); In Perlot *et al*'s study (2005), cEμ deletion did not affect somatic hypermutation. However, Perlot *et al*'s published data actually show significantly more mutation-free clones isolated from $cE\mu^{\Delta/\Delta}$ peyer's patch germinal center B cells relative to wild-type germinal center B cells (31% for $cE\mu^{\Delta/\Delta}$ *vs*14% for wild-type), which is similar to our observation of an increased proportion of mutation-free clones for B1-8iΔEμ allele in B1-$8i^a$/B1-8iΔ$E\mu^a$ Peyer's patch germinal center B cells (Perlot et al. 2005). Therefore, it is possible that the effect we observed is due to the deletion of cEμ. On the other hand, the deletion of MARκ in the endogenous Igκ locus has been reported to reduce the somatic hypermutation frequency of somatic hypermutation without reduce transcription (Yi et al. 1999). Nevertheless, the deletion of entire Eκ (cEκ and MARκ) from endogenous Igκ locus had no effect on somatic hypermutation (Inlay et al. 2006). Further *in vivo* analyses of somatic hypermutation in mice with individual knock-outs of cEμ and MARs might clarify the contribution of these two regions make to somatic hypermutation.

Mechanistically, Eμ could direct somatic hypermutation to the *Igh* locus by recruiting components required for this process. Several protein binding motifs have been found in the cEμ region (reviewed in Ernst and Smale 1995), including five E-box motifs. Accidental introduction of two E-box motifs (CAGGTG) into somatic hypermutation substrate was found to enhance somatic hypermutation without increasing transcription (Michael et al. 2003). Reciprocally, inactivation of

E2A gene, which encodes the E-box binding proteins E47/E12, was reported to strongly reduce somatic hypermutation, and this reduction could be restored by expression of cDNA of either E47 or E12 (Schoetz et al. 2006)(Schoetz 2006). Liu *et al*'s search for non-Ig genes targeted by somatic hypermutation showed that genes containing evolutionarily conserved E-box motif CAG(G/C)TG within 2kb of the transcription start site were significantly enriched among AID targeted genes (Liu et al. 2008). And very recently, Kothapalli *et al* (2008) reported that a region containing 5 E-boxes in the 3' regulatory region of the chicken light chain locus is essential for targeting gene conversion to that locus (Kothapalli et al. 2008). E2A proteins might contribute to somatic hypermutation or gene conversion by maintaining histone acetylation (Kitao et al. 2008). In this context, the cEμ might be the primary contributor of Eμ to somatic hypermutation. However, in transgenic studies, the MARs surrounding cEμ have been shown to promote long-range chromatin accessibility and transcriptional activity of the Ig promoter by enhancing histone acetylation in transgenic studies (Forrester et al. 1994; Fernandez et al. 2001). There is also a possibility that subnuclear location, which might be determined by MARs, is involved in regulating somatic hypermutation.

Our model, for the first time, has provided for analysis for a large number of B cells that express IgH allele without Eμ. This not only allowed us to analyze somatic hypermutation, but also class switch recombination. Although B cells of homozygous B1-8iΔEμ^a mice can switch as frequently as homozygous B1-8i^a B cells after various *in vitro* stimulation, B1-8iΔEμ^a allele was less efficient when competing with the wild-type allele. These observations extend previous studies

that showed less efficient class-switch recombination in the absence of cEμ or Eμ, but the latter study were based mostly on the analysis of a non-productive Eμ deficient allele (Gu et al. 1993; Sakai et al. 1999a; Perlot et al. 2005). Analyses of B cells heterozygous for Eμ (or cEμ) deletion showed that the mutant allele was less efficient in class switch recombination as indicated by a recombination within Sμ region, and study of $cE\mu^{\Delta/\Delta}$ B cells also led to a similar result (Gu et al. 1993; Sakai et al. 1999a; Perlot et al. 2005). There is a possibility that the observed decrease in class switch recombination in these studies is secondary to the impaired VDJ rearrangement in the absence of Eμ. Since almost all Eμ(or cEμ)-deficient alleles analyzed in these studies did not undergo V-DJ rearrangement, no V_H promoter would be juxtaposed to the Sμ region to support the μ transcription through Sμ that is normally produced from an assembled *Igh* allele (aberrant or productive). Given the importance of transcription in class switch recombination and the normal (or even higher) μ transcription level of the knock-in allele without Eμ (Figure 3.5B and Figure 4.6), the previously reported effects of Eμ-deletion on class switch recombination are most likely due to a lack of V_H promoter. This notion is supported by the abundant class switch recombination observed on the expressed Eμ (or cEμ) –deficient alleles observed in Perlot et al's study and the present study (Figure 4.4). Class switch recombination analyses in naturally occurring B cells expressing both the wild-type and Eμ-deficient knock-in alleles provided evidence (Figure 4.5), for the first time, that the expressed Eμ-deficient allele is also less efficient in class switch recombination.

Chapter 5: Remaining Questions and Future Directions

In this project, a V_H knock-in, Eμ knock-out mouse system was exploited to study the potential regulatory functions of Eμ in the processes after immunoglobulin heavy chain variable region (V_H) gene assembly in B lineage lymphocytes. While this study has led to some previously unappreciated findings on the regulation of B cell development, it also raised new questions worthy of further study.

Previously, Eμ was found to be required for efficient VDJ rearrangement (Chen et al. 1993b; Serwe and Sablitzky 1993; Sakai et al. 1999b; Perlot et al. 2005; Afshar et al. 2006), and this function is related to its enhancer activity. Eμ enhances the μ0 transcription that is initiated from the promoter of the last D gene segment (Figure 1.2) and goes through the JH segments and Cμ. The μ0 transcript is an indication of an accessible DH-JH locus and correlates with VDJ recombination. The requirement for Eμ enhancer activity to drive μ0 transcription and VDJ recombination has been recently shown to be very stringent. Replacement of Eμ with a ubiquitous enhancer (SV40 enhancer) failed to support μ0 transcription and efficient VDJ recombination (Kuzin et al. 2008).

One major finding in this study is a role for Eμ in enforcing allelic exclusion. The V_H-knockin allele effectively inhibits V-DJ rearrangement on the wild-type

allele in both B1-8i^{a}/*Igh*^{b} and B1-8iΔEμ^{a}/*Igh*^{b} mice. This inhibition is, however, not absolute. In both mice, there are a small number of precursor B cells that successfully assembly V_H genes on their wild-type alleles. At the pre-B cell stage, these potential double expressers are present in both mice, but, at the immature B cell stage, double expressers are only evident in B1-8iΔEμ^{a}/*Igh*^{b} mice. These double expressers expand in the periphery, and they are preferentially selected into marginal zone and B-1 B cell pools. Based on decreased Igμ transcription in the absence of Eμ in pre-B cells and increased light-chain editing in B1-8iΔEμ^{a}/*Igh*^{b} mice, we hypothesized that emerging immature B cells that express only the B1-8iΔEμ^{a} allele are less likely to pass positive selection due to their low Igμ levels and therefore low tonic signaling levels. We further hypothesized that these cells can be rescued by either expressing a second *Igh* allele or editing their light chains. This hypothesis is supported by the observed expansion of double expressers in the periphery and the increased number of λ-expressers in B1-8iΔEμ^{a}/*Igh*^{b} mice. Therefore, we propose that Eμ enforces allelic exclusion by ensuring the positive selection of single producers at the pre-B/immature B cell transition. Another major finding in this study is that somatic hypermutation frequency decreases in the absence of Eμ, but this decrease is not due to a decrease in transcription, suggesting that Eμ has a role in recruiting the somatic hypermutation machinery to the assembled IgH locos.

1. What is driving the early expression in pre/pro B cells in the absence of Eμ?

One unexpected observation was the early expression of the Eμ-deficient knock-in allele in pro/pre-B cells. Nevertheless, in pre-B cells, Igμ transcription is reduced to 1/2 wild-type levels and the cytoplasmic μ protein level is also significantly decreased (Figure 3.18). While these data suggest that Eμ is the major enhancer supporting Igμ transcription in pro/pre-B cells, one remaining question is, in the absence of Eμ, what is the driving force for the remaining transcription.

One possibility is that the 3'RR is a weak enhancer for the V_H promoter in pro/pre-B cells. The enhancer activity of the 3'RR correlates with its physical interactions with its promoter target, as shown by chromosome conformation capture (3C) analyses (Ju et al. 2007). Therefore, 3C analysis can be used to test whether there are interactions between the VH promoter and the 3'RR in pro/pre-B cells.

Another possibility is the remaining transcription does not depend on the 3'RR, but is controlled by other elements in the same way as germline V_H transcriptions are regulated. Germline V_H transcriptions are initiated from the preceding V_H promoters of unrearranged V_H gene segments, and are believed to facilitate VDJ recombination in pro-B cells (reviewed in Jung et al. 2006). These transcripts seem to be independent of the 3'RR since an insertion of the neo^R gene into the endogenous Igh locus, which is believed to disrupt the interactions

between the VH promoters and the 3'RR in a number of studies (Cogne et al. 1994; Manis et al. 1998; Manis et al. 2003; Perlot et al. 2005), had no effect on these transcripts. If, in pro/pre-B cells, the low levels of Igμ transcription from the Eμ-deficient V_H knockin allele does not depend on the 3'RR, we would predict that a disruption of V_H-3'RR interactions by either a neo^R insertion or 3'RR-knockout would not affect B cell development in homozygous B1-8iΔEμ^a mice with such mutations until the immature B cell stage.

2. How to demonstrate that positive selection requires Eμ?

Our data suggest such a model in which emerging immature B cells with low Igμ levels (in absence of Eμ) result in low levels of tonic signaling transduced from the B cell receptor, and therefore reduce their chance to pass positive selection. Whether Igμ transcription levels or Eμ regulate positive selection is the central hypothesis in this model, and a direct demonstration of Eμ's role in positive selection is one of the goals of future studies.

According to our model, emerging immature B cells expressing only the Eμ-deficient V_H knockin allele (B1-8iΔEμ^a) can be rescued either by expressing a second allele, or by light-chain editing. If we block both rescue pathways, these emerging immature B cells will not be rescued and B cell development will be arrested. This can be tested by introducing a V_L knock-in into Rag-deficient B1-8iΔEμ^a/*Igh*^{b} mice. A large decrease in the number of immature and mature B

cells is predicted if the V_H/V_L combination cannot support positive selection due to low Igμ expression levels.

3. What is the basis of the rescue of positive selection by light chain editing?

We propose that light-chain editing can rescue the emerging immature B cells expressing low levels of Igμ, but it is not clear what the basis of this rescue is. In another words, what are the differences between the light chains that can support positive selection and those that cannot.

It has been shown that tonic signals transduced from B cell receptors do not depend on antigen binding (Bannish et al. 2001), but it remains possible that antigenic binding does, however, influence positive selection. Therefore, the first possibility would be that light-chain editing rescues emerging immature B cells that fail in positive selection by generating new light chains that are, perhaps, self-reactive. If this is true, single expressers in B1-8iΔEμ^a/*Igh*^{b} mice would be more self-reactive than single expressers in B1-8i^a/*Igh*^{b} mice, which could be tested by an analysis for self-reactivity.

On the other hand, some V_H/V_L combinations might have better signaling properties (independent of their specificity) than others because they are more suitable for each other. Good V_H/V_L combinations might compensate for a decrease in the number of B cell receptors in positive selection, while a large number of B cell receptors might compensate for bad V_H/V_L combinations. This model predicts that some V_Ls that can support positive selection in B1-8i^a/*Igh*^{b}

mice, but not in B1-8iΔEμ^a/*Igh*^{b} mice, will be absent in the emerging immature B cells that express only the B1-8iΔEμ^a allele. It also predicts that V_Ls with superior signaling capacities are used in B1-8iΔEμ^a/*Igh*^{b} single expressers more frequently, while V_Ls with poor signaling capacities are used in B1-8i^a/*Igh*^{b} single expressers more frequently. Both kinds of V_Ls can be identified by comparing the V_Ls used by the single expressers in the two kinds of mice. They can be tested for signaling capacities in cell line or mice.

4. How does Eμ contribute to somatic hypermutation?

Our data suggest that Eμ contributes to somatic hypermutation by recruiting the somatic hypermutation machinery to the assembled *Igh* locus. It predicts that these is a direct or indirect interaction between Eμ and some components of the somatic hypermutation machinery (such as AID), which could be analyzed by Chromatin immunoprecipitation (ChIP).

It is also necessary to identify the protein factors involved in this process to fully understand the targeting mechanism of somatic hypermutation. Several protein binding motifs have been found in Eμ, such as binding motifs for E2A, PU.1, and OctA-B (Ernst and Smale 1995) A tissue culture system might speed up the initial screen for the key protein factors. B1-8i^a/*Igh*^{b} and B1-8iΔEμ^a/*Igh*^{b} B cells could be immortalized by fusing them with B cell lines that support ongoing somatic hypermutation. Somatic hypermutation can be analyzed before and after the knockout or inhibition of the potential protein regulators. In this system, one prediction is that, after the knockout or inhibition of the key component that

underlies Eμ's regulatory function in somatic hypermutation, there will be decrease in somatic hypermutation on the B1-8i^{a} allele, but not on the B1-8iΔEμa allele. Studies of mice with conditional knock-out of Eμ-binding proteins in germinal center B cells would be more time- and cost-consuming, but also more informative.

The B1-8iΔEμ^{a}/*Igh*^{b} mouse system has proven to be a very useful model for study the Eμ function. It also contains large number of naturally occurring double expressers, therefore it might also be a useful model to study B cells that express two B cell receptors. The autoimmune risk associated with double producers, the selection of double expressers into different mature B cells pools, and their behaviors in the immune responses, are all potential subject for future studies.

Chapter 6: References

Afshar, R., Pierce, S., Bolland, D.J., Corcoran, A., and Oltz, E.M. 2006. Regulation of IgH gene assembly: role of the intronic enhancer and 5'DQ52 region in targeting DHJH recombination. *J Immunol* 176(4): 2439-2447.

Allman, D. and Pillai, S. 2008. Peripheral B cell subsets. *Curr Opin Immunol* 20(2): 149-157.

Alt, F.W., Yancopoulos, G.D., Blackwell, T.K., Wood, C., Thomas, E., Boss, M., Coffman, R., Rosenberg, N., Tonegawa, S., and Baltimore, D. 1984. Ordered rearrangement of immunoglobulin heavy chain variable region segments. *Embo* 3: 1209.

Arulampalam, V., Eckhardt, L., and Pettersson, S. 1997. The enhancer shift: a model to explain the developmental control of IgH gene expression in B-lineage cells. *Immunol Today* 18(11): 549-554.

Azuma, T., Motoyama, N., Fields, L.E., and Loh, D.Y. 1993. Mutations of the chloramphenicol acetyl transferase transgene driven by the immunoglobulin promoter and intron enhancer. *Int Immunol* 5(2): 121-130.

Banerji, J., Olson, L., and Schaffner, W. 1983. A lymphocyte-specific cellular enhancer is located downstream of the joining region in immunoglobulin heavy-chain genes. *Cell* 33: 729-740.

Bannish, G., Fuentes-Panana, E.M., Cambier, J.C., Pear, W.S., and Monroe, J.G. 2001. Ligand-independent signaling functions for the B lymphocyte antigen receptor and their role in positive selection during B lymphopoiesis. *J Exp Med* 194(11): 1583-1596.

Baumgarth, N., Choi, Y.S., Rothaeusler, K., Yang, Y., and Herzenberg, L.A. 2008. B cell lineage contributions to antiviral host responses. *Curr Top Microbiol Immunol* 319: 41-61.

Baumgarth, N., Tung, J.W., and Herzenberg, L.A. 2005. Inherent specificities in natural antibodies: a key to immune defense against pathogen invasion. *Springer Semin Immunopathol* 26(4): 347-362.

Betz, A.G., Milstein, C., Gonzalez-Fernandez, A., Pannell, R., Larson, T., and Neuberger, M.S. 1994. Elements regulating somatic hypermutation of an immunoglobulin kappa gene: critical role for the intron enhancer/matrix attachment region. *Cell* 77: 239-248.

Bothwell, A.L., Paskind, M., Reth, M., Imanishi-Kari, T., Rajewsky, K., and Baltimore, D. 1981. Heavy chain variable region contribution to the NPb family of antibodies: somatic mutation evident in a gamma 2a variable region. *Cell* 24(3): 625-637.

Bottaro, A., Young, F., Chen, J., Serwe, M., Sablitzky, F., and Alt, F.W. 1998. Deletion of the IgH intronic enhancer and associated matrix-attachment regions decreases, but does not abolish, class switching at the mu locus. *Int Immunol* 10(6): 799-806.

Brenner, S. and Milstein, C. 1966. Origin of antibody variation. *Nature* 211: 242-243.

Brochet, X., Lefranc, M.P., and Giudicelli, V. 2008. IMGT/V-QUEST: the highly customized and integrated system for IG and TR standardized V-J and V-D-J sequence analysis. *Nucleic Acids Res* 36(Web Server issue): W503-508.

Burnet, F.M. 1957. A Modification of Jerne's Theory of Antibody Production using the Concept of Clonal Selection. *Aust J Sci* 20(3): 67-69.

Busslinger, M. 2004. Transcriptional control of early B cell development. *Annu Rev Immunol* 22: 55-79.

Casellas, R., Zhang, Q., Zheng, N.Y., Mathias, M.D., Smith, K., and Wilson, P.C. 2007. Igkappa allelic inclusion is a consequence of receptor editing. *J Exp Med* 204(1): 153-160.

Chauveau, C., Pinaud, E., and Cogne, M. 1998. Synergies between regulatory elements of the immunoglobulin heavy chain locus and its palindromic 3' locus control region. *Eur J Immunol* 28: 3048-3056.

Chen, J., Young, F., Bottaro, A., Stewart, V., Smith, R.K., and Alt, F.W. 1993a. Mutations of the intronic IgH enhancer and its flanking sequences differentially affect accessibility of the JH locus. *Embo J* 12(12): 4635-4645.

-. 1993b. Mutations of the intronic IgH enhancer and its flanking sequences differentially affect accessibility of the JH locus. *EMBO J* 12: 4635-4645.

Clark, M.R., Cooper, A.B., Wang, L.D., and Aifantis, I. 2005. The pre-B cell receptor in B cell development: recent advances, persistent questions and conserved mechanisms. *Curr Top Microbiol Immunol* 290: 87-103.

Cockerill, P.N., Yuen, M.H., and Garrand, W.T. 1987. The enhancer of the immunoglobulin heavy chain locus is flanked by presumptive chromosomal loop anchroage element. *J Biol Chem* 262: 5394-5397.

Cogne, M., Lansford, R., Bottaro, A., Zheng, J., Gorman, J., Young, K.F., Cheng, H.L., and Alt, F.W. 1994. A class switch control region at the 3' end of the immunoglobulin heavy chain locus. *Cell* 77: 737-747.

Cohn, M., Mitchison, N.A., Paul, W.E., Silverstein, A.M., Talmage, D.W., and Weigert, M. 2007. Reflections on the clonal-selection theory. *Nat Rev Immunol* 7(10): 823-830.

Dariavach, P., Williams, G.T., Campbell, K., Pettersson, S., and Neuberger, M.S. 1991. The mouse IgH 3'-enhancer. *Eur J Immunol* 21: 1499-1504.

Delbos, F., Aoufouchi, S., Faili, A., Weill, J.C., and Reynaud, C.A. 2007. DNA polymerase eta is the sole contributor of A/T modifications during immunoglobulin gene hypermutation in the mouse. *J Exp Med* 204(1): 17-23.

Di Noia, J.M. and Neuberger, M.S. 2007. Molecular mechanisms of antibody somatic hypermutation. *Annu Rev Biochem* 76: 1-22.

Dunnick, W.A., Shi, J., Graves, K.A., and Collins, J.T. 2005. The 3' end of the heavy chain constant region locus enhances germline transcription

and switch recombination of the four gamma genes. *J Exp Med* 201(9): 1459-1466.

Eckhardt, L.A. and Birshtein, B.K. 1985. Independent immunoglobulin class-switch events occurring in a single myeloma cell line. *MolCell Biol* 5: 856-868.

Ernst, P. and Smale, S.T. 1995. Combinatorial regulation of transcription II: the immunoglobulin mu heavy chain gene. *Immunity* 2: 427-438.

Fernandez, L.A., Winkler, M., and Grosschedl, R. 2001. Matrix attachment region-dependent function of the immunoglobulin mu enhancer involves histone acetylation at a distance without changes in enhancer occupancy. *Mol Cell Biol* 21(1): 196-208.

Forrester, W.C., Fernandez, L.A., and Grosschedl, R. 1999. Nuclear matrix attachment regions antagonize methylation-dependent repression of long-range enhancer-promoter interactions. *Genes Dev* 13(22): 3003-3014.

Forrester, W.C., van Genderen, C., Jenuwein, T., and Grosschedl, R. 1994. Dependence of enhancer-mediated transcription of the immunoglobulin mu gene on nuclear matrix attachment regions. *Science* 265: 1221-1225.

Fukita, Y., Jacobs, H., and Rajewsky, K. 1998. Somatic hypermutation in the heavy chain locus correlates with transcription. *Immunity* 9(1): 105-114.

Fuxa, M., Skok, J., Souabni, A., Salvagiotto, G., Roldan, E., and Busslinger, M. 2004. Pax5 induces V-to-DJ rearrangements and locus contraction of the immunoglobulin heavy-chain gene. *Genes Dev* 18(4): 411-422.

Garrett, F.E., Emelyanov, A.V., Sepulveda, M.A., Flanagan, P., Volpi, S., Li, F., Loukinov, D., Eckhardt, L.A., Lobanenkov, V.V., and Birshtein, B.K. 2005. Chromatin architecture near a potential 3' end of the igh locus involves modular regulation of histone modifications during B-Cell development and in vivo occupancy at CTCF sites. *Mol Cell Biol* 25(4): 1511-1525.

Gilles, S.D. and Tonegawa, S. 1983. Expression of cloned immunoglobulin genes introduced into mouse L cells. *Nucl Acids Res* 11: 7981-7997.

Giusti, A.M. and Manser, T. 1993. Hypermutation is observed only in antibody H chain V region transgenes that have recombined with endogenous immunoglobulin H DNA: implications for the location of cis-acting elements required for somatic mutation. *J Exp Med* 177: 797-809.

Gonzalez-Fernandez, A., Gilmore, D., and Milstein, C. 1994. Age-related decrease in the proportion of germinal center B cells from mouse Peyer's patches is accompanied by an accumulation of somatic mutations in their immunoglobulin genes. *Eur J Immunol* 24(11): 2918-2921.

Gonzalez-Fernandez, A. and Milstein, C. 1993. Analysis of somatic hypermutation in mouse Peyer's patches using immunoglobulin

kappa light-chain transgenes. *Proc Natl Acad Sci U S A* 90(21): 9862-9866.

Gordon, M.S., Kanegai, C.M., Doerr, J.R., and Wall, R. 2003. Somatic hypermutation of the B cell receptor genes B29 (Igbeta, CD79b) and mb1 (Igalpha, CD79a). *Proc Natl Acad Sci U S A* 100(7): 4126-4131.

Goyenechea, B., Klix, N., Yelamos, J., Williams, G.T., Riddell, A., Neuberger, M.S., and Milstein, C. 1997. Cells strongly expressing Ig(kappa) transgenes show clonal recruitment of hypermutation: a role for both MAR and the enhancers. *Embo J* 16(13): 3987-3994.

Gregor, P.D. and Morrison, S.L. 1986. Myeloma mutant with a novel 3' flanking region: loss of normal sequence and insertion of repetitive elements leads to decreased transcription but normal processing of the alpha heavy-chain gene products. *Mol Cell Biol* 6: 1903-1916.

Griebel, P.J.H., W. N. 1996. Expanding the role of Peyer's patches in B-cell ontogeny. *Immunol Today* 17(1): 30-39.

Grosschedl, R., Weaver, D., Baltimore, D., and Constantini, F. 1984. Introduction of a mu immunoglobulin gene into the mouse germ line: specific expression in lymphoid cells and synthesis of functional antibody. *Cell* 38: 647-658.

Gu, H., Zou, Y.R., and Rajewsky, K. 1993. Independent control of immunoglobulin switch recombination at individual switch regions evidenced through Cre-loxP-mediated gene targeting. *Cell* 73: 1155-1164.

Hardy, R.R. 1991. CD5 B cells: a separate lineage at last? *Curr Biol* 1(5): 290-292.

Hardy, R.R. and Hayakawa, K. 1991. A developmental switch in B lymphopoiesis. *Proc Natl Acad Sci U S A* 88(24): 11550-11554.

-. 2005. Development of B cells producing natural autoantibodies to thymocytes and senescent erythrocytes. *Springer Semin Immunopathol* 26(4): 363-375.

Hardy, R.R., Kincade, P.W., and Dorshkind, K. 2007. The protean nature of cells in the B lymphocyte lineage. *Immunity* 26(6): 703-714.

Imler, J.L., Lemaire, C., Wasylyk, C., and Wasylyk, B. 1987. Negative regulation contributes to tissue specificity of the immunoglobulin heavy-chain enhancer. *Mol Cell Biol* 7: 2558-2567.

Inlay, M.A., Gao, H.H., Odegard, V.H., Lin, T., Schatz, D.G., and Xu, Y. 2006. Roles of the Ig kappa light chain intronic and 3' enhancers in Igk somatic hypermutation. *J Immunol* 177(2): 1146-1151.

Johnston, J.M., Ihyer, S.R., Smith, R.S., Tai, K.F., Farmer, T., Korsmeyer, S.J., Nadon, N.L., and Carroll, W.L. 1996. Analysis of hypermutation in immunoglobulin heavy chain passenger transgenes. *Eur J Immunol* 26(5): 1058-1062.

Jolly, C.J., Wagner, S.D., Rada, C., Klix, N., Milstein, C., and Neuberger, M.S. 1996. The targeting of somatic hypermutation. *Semin Immunol* 8(3): 159-168.

Ju, Z., Volpi, S.A., Hassan, R., Martinez, N., Giannini, S.L., Gold, T., and Birshtein, B.K. 2007. Evidence for physical interaction between the immunoglobulin heavy chain variable region and the 3' regulatory region. *J Biol Chem* 282(48): 35169-35178.

Jung, D., Giallourakis, C., Mostoslavsky, R., and Alt, F.W. 2006. Mechanism and control of V(D)J recombination at the immunoglobulin heavy chain locus. *Annu Rev Immunol* 24: 541-570.

Jung, S., Rajewsky, K., and Radbruch, A. 1993. Shutdown of class switch recombination by deletion of a switch region control element. *Science* 259: 984-987.

Kantor, A.B., Merrill, C.E., Herzenberg, L.A., and Hillson, J.L. 1997. An unbiased analysis of V(H)-D-J(H) sequences from B-1a, B-1b, and conventional B cells. *J Immunol* 158(3): 1175-1186.

Khamlichi, A.A., Pinaud, E., Decourt, C., Chauveau, C., and Cogne, M. 2000. The 3' IgH regulatory region: a complex structure in a search for a function. *Adv Immunol* 75: 317-345.

Kinoshita, K. and Honjo, T. 2001. Linking class-switch recombination with somatic hypermutation. *Nat Rev Mol Cell Biol* 2(7): 493-503.

Kinoshita, K., Tashiro, J., Tomita, S., Lee, C.G., and Honjo, T. 1998. Target specificity of immunoglobulin class switch recombination is not determined by nucleotide sequences of S regions. *Immunity* 9(6): 849-858.

Kitao, H., Kimura, M., Yamamoto, K., Seo, H., Namikoshi, K., Agata, Y., Ohta, K., and Takata, M. 2008. Regulation of histone H4 acetylation by transcription factor E2A in Ig gene conversion. *Int Immunol* 20(2): 277-284.

Klix, N., Jolly, C.J., Davies, S.L., Bruggemann, M., Williams, G.T., and Neuberger, M.S. 1998. Multiple sequences from downstream of the J kappa cluster can combine to recruit somatic hypermutation to a heterologous, upstream mutation domain. *Eur J Immunol* 28(1): 317-326.

Klotz, E.L. and Storb, U. 1996. Somatic hypermutation of a lambda 2 transgene under the control of the lambda enhancer or the heavy chain intron enhancer. *J Immunol* 157(10): 4458-4463.

Kotani, A., Kakazu, N., Tsuruyama, T., Okazaki, I.M., Muramatsu, M., Kinoshita, K., Nagaoka, H., Yabe, D., and Honjo, T. 2007. Activation-induced cytidine deaminase (AID) promotes B cell lymphomagenesis in Emu-cmyc transgenic mice. *Proc Natl Acad Sci U S A* 104(5): 1616-1620.

Kothapalli, N., Norton, D.D., and Fugmann, S.D. 2008. Cutting edge: a cis-acting DNA element targets AID-mediated sequence diversification to the chicken Ig light chain gene locus. *J Immunol* 180(4): 2019-2023.

Kuzin, II, Bagaeva, L., Young, F.M., and Bottaro, A. 2008. Requirement for enhancer specificity in immunoglobulin heavy chain locus regulation. *J Immunol* 180(11): 7443-7450.

Lakso, M., Pichel, J.G., Gorman, J.R., Sauer, B., Okamoto, Y., Lee, E., Alt, F.W., and Westphal, H. 1996. Efficient in vivo manipulation of mouse genomic sequences at the zygote stage. *Proc Natl Acad Sci U S A* 93(12): 5860-5865.

Lam, K.P. and Rajewsky, K. 1999. B cell antigen receptor specificity and surface density together determine B-1 versus B-2 cell development. *J Exp Med* 190(4): 471-477.

Li, Y.S., Hayakawa, K., and Hardy, R.R. 1993. The regulated expression of B lineage associated genes during B cell differentiation in bone marrow and fetal liver. *JExpMed* 178: 951-960.

Li, Z., Luo, Z., Ronai, D., Kuang, F.L., Peled, J.U., Iglesias-Ussel, M.D., and Scharff, M.D. 2007. Targeting AID to the Ig genes. *Adv Exp Med Biol* 596: 93-109.

Lieberson, R., Giannini, S.L., Birshtein, B.K., and Eckhardt, L.A. 1991. An enhancer at the 3'end of the mouse immunoglobulin heavy chain locus. *Nucleic Acids Res* 19: 933-937.

Lieberson, R., Ong, J., Shi, X., and Eckhardt, L.A. 1995. Transcription of an immunoglobulin gene ceases upon deletion of a distant enhancer. *EMBO J* 14: 6229-6238.

Liu, M., Duke, J.L., Richter, D.J., Vinuesa, C.G., Goodnow, C.C., Kleinstein, S.H., and Schatz, D.G. 2008. Two levels of protection for the B cell genome during somatic hypermutation. *Nature* 451(7180): 841-845.

Liu, S., Velez, M.G., Humann, J., Rowland, S., Conrad, F.J., Halverson, R., Torres, R.M., and Pelanda, R. 2005. Receptor editing can lead to allelic inclusion and development of B cells that retain antibodies reacting with high avidity autoantigens. *J Immunol* 175(8): 5067-5076.

Longo, N.S. and Lipsky, P.E. 2006. Why do B cells mutate their immunoglobulin receptors? *Trends Immunol* 27(8): 374-380.

Luby, T.M., Schrader, C.E., Stavnezer, J., and Selsing, E. 2001. The mu switch region tandem repeats are important, but not required, for antibody class switch recombination. *J Exp Med* 193(2): 159-168.

Madisen, L. and Groudine, M. 1994. Identification of a locus control region in the immunoglobulin heavy-chain locus that deregulates c-myc expression in plasmacytoma and Burkitt's lymphoma cells. *Genes Dev* 8: 2212-2226.

Manis, J.P., Michaelson, J.S., Birshtein, B.K., and Alt, F.W. 2003. Elucidation of a downstream boundary of the 3' IgH regulatory region. *Mol Immunol* 39(12): 753-760.

Manis, J.P., van der Stoep, N., Tian, M., Ferrini, R., Davidson, L., Bottaro, A., and Alt, F.W. 1998. Class switching in B cells lacking 3' immunoglobulin heavy chain enhancers. *J Exp Med* 188(8): 1421-1431.

Martensson, I.L., Keenan, R.A., and Licence, S. 2007. The pre-B-cell receptor. *Curr Opin Immunol* 19(2): 137-142.

Martin, F. and Kearney, J.F. 2002. Marginal-zone B cells. *Nat Rev Immunol* 2(5): 323-335.

Martomo, S.A., Yang, W.W., and Gearhart, P.J. 2004. A role for Msh6 but not Msh3 in somatic hypermutation and class switch recombination. *J Exp Med* 200(1): 61-68.

Matthias, P. and Baltimore, D. 1993. The immunoglobulin heavy chain locus contains another B-cell-specific 3' enhancer close to the alpha constant region. *Mol Cell Biol* 13: 1547-1553.

Michael, N., Shen, H.M., Longerich, S., Kim, N., Longacre, A., and Storb, U. 2003. The E box motif CAGGTG enhances somatic hypermutation without enhancing transcription. *Immunity* 19(2): 235-242.

Michaelson, J.S., Giannini, S.L., and Birshtein, B.K. 1995. Identification of 3'alpha-HS4, a novel Ig heavy chain enhancer element regulated at multiple stages of B cell differentiation. *Nucleic Acids Res* 23: 975-981.

Monroe, J.G. and Dorshkind, K. 2007. Fate decisions regulating bone marrow and peripheral B lymphocyte development. *Adv Immunol* 95: 1-50.

Morvan, C.L., Pinaud, E., Decourt, C., Cuvillier, A., and Cogne, M. 2003. The immunoglobulin heavy-chain locus hs3b and hs4 3' enhancers are

dispensable for VDJ assembly and somatic hypermutation. *Blood* 102(4): 1421-1427.

Mostoslavsky, R., Alt, F.W., and Rajewsky, K. 2004. The lingering enigma of the allelic exclusion mechanism. *Cell* 118(5): 539-544.

Muramatsu M, K.K., Fagarasan S, Yamada S, Shinkai Y, Honjo T. 2000. Class switch recombination and hypermutation require activation-induced cytidine deaminase (AID), a potential RNA editing enzyme. *Cell* 102(5): 553-563.

Muramatsu, M., Sankaranand, V.S., Anant, S., Sugai, M., Kinoshita, K., Davidson, N.O., and Honjo, T. 1999. Specific expression of activation-induced cytidine deaminase (AID), a novel member of the RNA-editing deaminase family in germinal center B cells. *J Biol Chem* 274(26): 18470-18476.

Muschen, M., Re, D., Jungnickel, B., Diehl, V., Rajewsky, K., and Kuppers, R. 2000. Somatic mutation of the CD95 gene in human B cells as a side-effect of the germinal center reaction. *J Exp Med* 192(12): 1833-1840.

Nemazee, D. 2006. Receptor editing in lymphocyte development and central tolerance. *Nat Rev Immunol* 6(10): 728-740.

Neuberger, M.S. 1983. Expression and regulation of immunoglobulin heavy chain genes transfected into lymphoid cells. *EMBO J* 2: 1373-1378.

Neuberger, M.S. and Calabi, F. 1983. Reciprocal chromosome translocation between c-myc and immunoglobulin gamma 2b genes. *Nature* 305(5931): 240-243.

Nussenzweig, M.C., Shaw, A.C., Sinn, E., Danner, D.B., Holmes, K.L., Morse, H.C., 3rd, and Leder, P. 1987. Allelic exclusion in transgenic mice that express the membrane form of immunoglobulin mu. *Science* 236(4803): 816-819.

Nutt, S.L., Heavey, B., Rolink, A.G., and Busslinger, M. 1999. Commitment to the B-lymphoid lineage depends on the transcription factor Pax5. *Nature* 401(6753): 556-562.

Oancea, A.E., Berru, M., and Shulman, M.J. 1997. Expression of the (recombinant) endogenous immunoglobulin heavy-chain locus requires the intronic matrix attachment regions. *Mol Cell Biol* 17(5): 2658-2668.

Odegard, V.H. and Schatz, D.G. 2006. Targeting of somatic hypermutation. *Nat Rev Immunol* 6(8): 573-583.

Okazaki, I.M., Kotani, A., and Honjo, T. 2007. Role of AID in tumorigenesis. *Adv Immunol* 94: 245-273.

Ong, J., Stevens, S., Roeder, R.G., and Eckhardt, L.A. 1998. 3' IgH enhancer elements shift synergistic interactions during B cell development. *J Immunol* 160: 4896-4903.

Papavasiliou, F., Jankovic, M., Gong, S., and Nussenzweig, M.C. 1997. Control of immunoglobulin gene rearrangements in developing B cells. *Curr Opin Immunol* 9(2): 233-238.

Pasqualucci, L., Migliazza, A., Fracchiolla, N., William, C., Neri, A., Baldini, L., Chaganti, R.S., Klein, U., Kuppers, R., Rajewsky, K., and Dalla-Favera, R. 1998. BCL-6 mutations in normal germinal center B cells: evidence of somatic hypermutation acting outside Ig loci. *Proc Natl Acad Sci U S A* 95(20): 11816-11821.

Peled, J.U., Kuang, F.L., Iglesias-Ussel, M.D., Roa, S., Kalis, S.L., Goodman, M.F., and Scharff, M.D. 2008. The biochemistry of somatic hypermutation. *Annu Rev Immunol* 26: 481-511.

Perlot, T., Alt, F.W., Bassing, C.H., Suh, H., and Pinaud, E. 2005. Elucidation of IgH intronic enhancer functions via germ-line deletion. *Proc Natl Acad Sci U S A* 102(40): 14362-14367.

Pettersson, S., Cook, G.P., Bruggemann, M., Williams, G.T., and Neuberger, M.S. 1990. A second B cell-specific enhancer 3' of the immunoglobulin heavy-chain locus. *Nature* 344: 165-168.

Pinaud, E., Khamlichi, A., Le Morvan, C., Drouet, M., Nalesso, V., Le Bert, M., and Cogne, M. 2001. Localization of the 3'IgH locus elements that effect long-distance regulation of class switch recombination. *Immunity* 15: 187-199.

Rada, C., Ehrenstein, M.R., Neuberger, M.S., and Milstein, C. 1998. Hot spot focusing of somatic hypermutation in MSH2-deficient mice suggests two stages of mutational targeting. *Immunity* 9(1): 135-141.

Rada, C. and Milstein, C. 2001. The intrinsic hypermutability of antibody heavy and light chain genes decays exponentially. *Embo J* 20(16): 4570-4576.

Rada, C., Williams, G.T., Nilsen, H., Barnes, D.E., Lindahl, T., and Neuberger, M.S. 2002. Immunoglobulin isotype switching is inhibited and somatic hypermutation perturbed in UNG-deficient mice. *Curr Biol* 12(20): 1748-1755.

Reth, M., Hammerling, G.J., and Rajewsky, K. 1978. Analysis of the repertoire of anti-NP antibodies in C57BL/6 mice by cell fusion. I. Characterization of antibody families in the primary and hyperimmune response. *Eur J Immunol* 8(6): 393-400.

Retter, I., Chevillard, C., Scharfe, M., Conrad, A., Hafner, M., Im, T.H., Ludewig, M., Nordsiek, G., Severitt, S., Thies, S., Mauhar, A., Blocker, H., Muller, W., and Riblet, R. 2007. Sequence and characterization of the Ig heavy chain constant and partial variable region of the mouse strain 129S1. *J Immunol* 179(4): 2419-2427.

Roldan, E., Fuxa, M., Chong, W., Martinez, D., Novatchkova, M., Busslinger, M., and Skok, J.A. 2005. Locus 'decontraction' and centromeric recruitment contribute to allelic exclusion of the immunoglobulin heavy-chain gene. *Nat Immunol* 6(1): 31-41.

Ronai, D., Iglesias-Ussel, M.D., Fan, M., Shulman, M.J., and Scharff, M.D. 2005. Complex regulation of somatic hypermutation by cis-acting sequences in the endogenous IgH gene in hybridoma cells. *Proc Natl Acad Sci U S A* 102(33): 11829-11834.

Rusconi, S. and Kohler, G. 1985. Transmission and expression of a specific pair of rearranged immunoglobulin mu and kappa genes in a transgenic mouse line. *Nature* 314(6009): 330-334.

Sakai, E., Bottaro, A., and Alt, F.W. 1999a. The Ig heavy chain intronic enhancer core region is necessary and sufficient to promote efficient class switch recombination. *Int Immunol* 11: 1709-1713.

Sakai, E., Bottaro, A., Davidson, L., Sleckman, B.P., and Alt, F.W. 1999b. Recombination and transcription of the endogenous Ig heavy chain locus is effected by the Ig heavy chain intronic enhancer core region in the absence of the matrix attachment regions. *Proc Natl Acad Sci USA* 96: 1526-1531.

Saleque, S., Singh, M., and Birshtein, B.K. 1999. Ig heavy chain expression and class switching in vitro from an allele lacking the 3' enhancers DNaseI-hypersensitive hs3A and hs1,2. *J Immunol* 162: 2791-2803.

Scheuermann, R.H. and Chen, U. 1989. A developmental-specific factor binds to suppressor sites flanking the immunoglobulin heavy-chain enhancer. *Genes and Dev* 3: 1255-1266.

Schlissel, M.S., Corcoran, L.M., and Baltimore, D. 1991. Virus-transformed pre-B cells show ordered activation but not inactivation of

immunoglobulin gene rearrangement and transcription. *J Exp Med* 173(3): 711-720.

Schoetz, U., Cervelli, M., Wang, Y.D., Fiedler, P., and Buerstedde, J.M. 2006. E2A expression stimulates Ig hypermutation. *J Immunol* 177(1): 395-400.

Seidl, K.J., Bottaro, A., Vo, A., Zhang, J., Davidson, L., and Alt, F.W. 1998. An expressed neo(r) cassette provides required functions of the 1gamma2b exon for class switching. *Int Immunol* 10(11): 1683-1692.

Serwe, M. and Sablitzky, F. 1993. V(D)J recombination in B cells is impaired but not blocked by targeted deletion of the immunoglobulin heavy chain intron enhancer. *EMBO J* 12: 2321-2327.

Shen, H.M., Peters, A., Baron, B., Zhu, X., and Storb, U. 1998. Mutation of BCL-6 gene in normal B cells by the process of somatic hypermutation of Ig genes. *Science* 280(5370): 1750-1752.

Shen, H.M., Tanaka, A., Bozek, G., Nicolae, D., and Storb, U. 2006. Somatic hypermutation and class switch recombination in Msh6(-/-)Ung(-/-) double-knockout mice. *J Immunol* 177(8): 5386-5392.

Shi, X. and Eckhardt, L.A. 2001. Deletional analyses reveal an essential role for the hs3b/hs4 IgH 3'enhancer pair in an Ig-secreting but not an earlier-stage B cell line. *Int Immunol* 13: 1003-1012.

Sohn, J., Gerstein, R.M., Hsieh, C.L., Lemer, M., and Selsing, E. 1993. Somatic hypermutation of an immunoglobulin mu heavy chain transgene. *J Exp Med* 177(2): 493-504.

Sonoda, E., Pewzner-Jung, Y., Schwers, S., Taki, S., Jung, S., Eilat, D., and Rajewsky, K. 1997. B cell development under the condition of allelic inclusion. *Immunity* 6: 225-233.

Stall, A.M., Kroese, F.G., Gadus, F.T., Sieckmann, D.G., Herzenberg, L.A., and Herzenberg, L.A. 1988. Rearrangement and expression of endogenous immunoglobulin genes occur in many murine B cells expressing transgenic membrane IgM. *Proc Natl Acad Sci U S A* 85(10): 3546-3550.

Storb, U. 1987. Transgenic mice with immunoglobulin genes. *AnnRevImmunol* 5: 151-174.

Storb, U., Pinkert, C., Arp, B., Engler, P., Gollahon, K., Manz, J., Brady, W., and Brinster, R.L. 1986. Transgenic mice with mu and kappa genes encoding antiphosphorylcholine antibodies. *J Exp Med* 164(2): 627-641.

ten Boekel, E., Melchers, F., and Rolink, A.G. 1998. Precursor B cells showing H chain allelic inclusion display allelic exclusion at the level of pre-B cell receptor surface expression. *Immunity* 8(2): 199-207.

Terauchi, A., Hayashi, K., Kitamura, D., Kozono, Y., Motoyama, N., and Azuma, T. 2001. A pivotal role for DNase I-sensitive regions 3b and/or 4 in the induction of somatic hypermutation of IgH genes. *J Immunol* 167(2): 811-820.

Tumas-Brundage, K.M., Vora, K.A., and Manser, T. 1997. Evaluation of the role of the 3'alpha heavy chain enhancer [3'alpha(hs1,2)] in Vh gene somatic hypermutation. *Mol Immunol* 34: 367-378.

van der Stoep, N., Gorman, J.R., and Alt, F.W. 1998. Reevaluation of 3'Ekappa function in stage- and lineage-specific rearrangement and somatic hypermutation. *Immunity* 8(6): 743-750.

Victor, K.D., Vu, K., and Feeney, A.J. 1994. Limited junctional diversity in kappa light chains. Junctional sequences from CD43+B220+ early B cell progenitors resemble those from peripheral B cells. *J Immunol* 152(7): 3467-3475.

Wabl, M. and Steinberg, C. 1982. A theory of allelic and isotypic exclusion for immunoglobulin genes. *Proc Natl Acad Sci U S A* 79(22): 6976-6978.

Wabl, M.R., Beck-Engeser, G.B., and Burrows, P.D. 1984. Allelic inclusion in the pre-B-cell line 18-81. *Proc Natl Acad Sci U S A* 81(3): 867-870.

Wardemann, H., Yurasov, S., Schaefer, A., Young, J.W., Meffre, E., and Nussenzweig, M.C. 2003. Predominant autoantibody production by early human B cell precursors. *Science* 301(5638): 1374-1377.

Watanabe, N., Nisitani, S., Ikuta, K., Suzuki, M., Chiba, T., and Honjo, T. 1999. Expression levels of B cell surface immunoglobulin regulate efficiency of allelic exclusion and size of autoreactive B-1 cell compartment. *J Exp Med* 190(4): 461-469.

Weaver, D., Costantini, F., Imanishi-Kari, T., and Baltimore, D. 1985. A transgenic immunoglobulin mu gene prevents rearrangement of endogenous genes. *Cell* 42(1): 117-127.

Wiesendanger, M., Kneitz, B., Edelmann, W., and Scharff, M.D. 2000. Somatic hypermutation in MutS homologue (MSH)3-, MSH6-, and MSH3/MSH6-deficient mice reveals a role for the MSH2-MSH6 heterodimer in modulating the base substitution pattern. *J Exp Med* 191(3): 579-584.

Wuerffel, R., Wang, L., Grigera, F., Manis, J., Selsing, E., Perlot, T., Alt, F.W., Cogne, M., Pinaud, E., and Kenter, A.L. 2007. S-S synapsis during class switch recombination is promoted by distantly located transcriptional elements and activation-induced deaminase. *Immunity* 27(5): 711-722.

Yan, Y., Park, S.S., Janz, S., and Eckhardt, L.A. 2007. In a model of immunoglobulin heavy-chain (IGH)/MYC translocation, the Igh 3' regulatory region induces MYC expression at the immature stage of B cell development. *Genes Chromosomes Cancer* 46(10): 950-959.

Yi, M., Wu, P., Trevorrow, K.W., Claflin, L., and Garrard, W.T. 1999. Evidence that the Igkappa gene MAR regulates the probability of premature V-J joining and somatic hypermutation. *J Immunol* 162: 6029-6039.

Zan, H., Shima, N., Xu, Z., Al-Qahtani, A., Evinger Iii, A.J., Zhong, Y., Schimenti, J.C., and Casali, P. 2005. The translesion DNA polymerase

theta plays a dominant role in immunoglobulin gene somatic hypermutation. *Embo J* 24(21): 3757-3769.

Zarrin, A.A., Del Vecchio, C., Tseng, E., Gleason, M., Zarin, P., Tian, M., and Alt, F.W. 2007. Antibody class switching mediated by yeast endonuclease-generated DNA breaks. *Science* 315(5810): 377-381.

Zeng, X., Winter, D.B., Kasmer, C., Kraemer, K.H., Lehmann, A.R., and Gearhart, P.J. 2001. DNA polymerase eta is an A-T mutator in somatic hypermutation of immunoglobulin variable genes. *Nat Immunol* 2(6): 537-541.

Zhang, B., Alaie-Petrillo, A., Kon, M., Li, F., and Eckhardt, L.A. 2007. Transcription of a productively rearranged Ig VDJC alpha does not require the presence of HS4 in the IgH 3' regulatory region. *J Immunol* 178(10): 6297-6306.

Zhang, J., Bottaro, A., Li, S., Stewart, V., and Alt, F.W. 1993. A selective defect in IgG2b switching as a result of targeted mutation of the I gamma 2b promoter and exon. *Embo J* 12(9): 3529-3537.

Zhou, J., Ashouian, N., Delepine, M., Matsuda, F., Chevillard, C., Riblet, R., Schildkraut, C.L., and Birshtein, B.K. 2002. The origin of a developmentally regulated Igh replicon is located near the border of regulatory domains for Igh replication and expression. *Proc Natl Acad Sci U S A* 99(21): 13693-13698.